Durham, A. L., Al Jaaly, E., Graham, R., Brook, P., Bae, J., Heesom, K. J., Postle, A., Lavender, P., Jazrawi, E., Reeves, B. C., Fiorentino, F., Mumby, S., Angelini, G. D., & Adcock, I. M. (2020). Multi-omic analysis of the effects of low frequency ventilation during cardiopulmonary bypass surgery. *International Journal of Cardiology*, *309*, 40-47. https://doi.org/10.1016/j.ijcard.2020.03.054

Multi-omic analysis of the effects of low frequency ventilation during cardiopulmonary bypass surgery.

Durham AL PhD[1], Al Jaaly E MD[2], Graham R MSc[1], Brook PO MSc[1], Bae JH BSc[1], Heesom KJ PhD[3], Postle AD PhD[4], Lavender P PhD[5], Jazrawi E BSc[1], Reeves B DPhil[2], Fiorentino F PhD[2], Mumby S PhD[1], Angelini GD MD[2,6]*, Adcock IM PhD[1].

*Author for correspondence

Professor Gianni Angelini

Bristol Heart Institute

Bristol Royal Infirmary

Upper Maudlin Street

Bristol

BS2 8HW

UK

Tel: +44 (0) 117 34 23165

email: g.d.angelini@bristol.ac.uk

1. Airways Disease Section, National Heart and Lung Institute, Imperial College London, Dovehouse Street, London SW3 6LY

2. Cardiothoracic Surgery, National Heart and Lung Institute, Imperial College London, Hammersmith Hospital, London, UK

3. University of Bristol Proteomics Facility, BioMedical Sciences Building, University Walk, Bristol, UK

4. Faculty of Medicine, University of Southampton, Building 85, Life Sciences Building, Highfield Campus, Southampton, UK

5. Department of Asthma, Allergy, and Respiratory Science, King's College London, London, UK

6. Bristol Heart Institute, University of Bristol, Bristol Royal Infirmary, Level 7, Marlborough Street, Bristol, UK

7. Immunobiology, Blizard Institute, Barts and the London School of Medicine and Dentistry, Queen Mary University of London, 4 Newark St, London, UK

Short Title.

Omic analysis of lungs ventilation during open heart surgery.

Total Word Count: 3725

Abstract

Background

Heart surgery with cardio-pulmonary bypass (CPB) is associated with lung ischemia leading to injury and inflammation. It has been suggested this is a result of the lungs being kept deflated throughout the duration of CPB. Low frequency ventilation (LFV) during CPB has been proposed to reduce lung dysfunction.

Methods

We used a semi-biased multi-omic approach to analyse lung biopsies taken before and after CPB from 37 patients undergoing coronary artery bypass surgery randomised to both lungs left collapsed or using LFV for the duration of CPB. We also examined inflammatory and oxidative stress markers from blood samples from the same patients.

Results

30 genes were induced when the lungs were left collapsed and 80 by LFV. Post-surgery 26 genes were significantly higher in the LFV vs. lungs left collapsed, including genes associated with inflammation (e.g. *IL6* and *IL8)* and hypoxia/ischemia (e.g. *HIF1A*, *IER3* and *FOS*). Relatively few changes in protein levels were detected, perhaps reflecting the early time point or the importance of post-translational modifications. However, pathway analysis of proteomic data indicated that LFV was associated with increased "cellular component morphogenesis" and a decrease in "blood circulation". Lipidomic analysis did not identify any lipids significantly altered by either intervention.

Discussion

Taken together these data indicate the keeping both lungs collapsed during CPB significantly induces lung damage, oxidative stress and inflammation. LFV during CPB increases these deleterious effects, potentially through prolonged surgery time, further decreasing blood flow to the lungs and enhancing hypoxia/ischemia.

Key Words:

Cardio-pulmonary bypass

Ventilation

Inflammation

Transcriptomics

Proteomics

1. Introduction

Cardiopulmonary bypass (CPB), which allows operation on a motionless and bloodless heart, is used in most heart surgery procedures. Recovery from cardiac surgery utilising CPB is generally good with a 30 day survival rate of 98.4% [1]. However, CPB is still associated with severe systemic inflammation and tissue damage with an accompanying mortality of 1.5% along with post-operative lung dysfunction of various degrees in up to 30% of patients [2]. The underlying mechanisms driving inflammation following CPB are yet to be fully elucidated and there are currently no strategies to effectively prevent it.

Institution of CPB is associated with significant physiological changes and insults to the lung. Ventilation is generally stopped, and lungs deflated to reduce mediastinal motions. Venous return is directed away from the right heart thereby pulmonary artery flow is dramatically reduced. Furthermore, bronchial blood flow is reduced due to haemodynamic and pulsatility changes during bypass and changes in vascular resistances. These atelectatic and ischemic changes may promote tissue hypoxia, oxidative stress and lung cellular damage [3–6]. Towards the end of CPB, full ventilation is recommenced and pulmonary blood flow is restored with potential injury by reperfusion including oxidative stress [7,8], and inflammatory cell infiltration [9]. Further oxidative stress could be triggered by free iron catalysed reactions [10,11] from iron released by haemolysis as the blood passes through the bypass circuit.

There have been various attempts made to protect the lung during CPB. Among these, it has been suggested that low frequency ventilation (LFV) during CPB may alleviate

hypoxia and ischemia of the lungs and thereby help to reduce inflammation. In contrast to previous animal trials [12], we have recently provided evidence that in patients undergoing elective coronary artery bypass grafting (CABG), the use of LFV during CPB when compared to both lungs left collapsed does not seem to reduce inflammation in lung biopsies and blood [13,14].

The low frequency ventilation technique reported in our study has been investigated previously by different groups with contrasting results. This study, for the first time, uses the simultaneous of human lung biopsy and blood samples to assess the effect of the technique. In order to establish a mechanistic link between the effects of both interventions on the lung we used a semi-biased multi-omics approach (transcriptomics, proteomics and lipidomics) to analyse lung biopsies taken at the start of surgery before CPB and at the end of surgery after lung reperfusion but before weaning from CPB from the above mentioned randomised study recently published [14]. We also analysed serial blood plasma taken before and after surgery.

2. Methods:

2.1 Study design

37 patients undergoing elective or urgent CABG with CPB and cold blood cardioplegic arrest at the Hammersmith Hospital, were recruited as part of a single-centre, parallel group, randomised, controlled trial investigating low frequency ventilation study recently published [14].

Venous blood samples were taken from the patients at induction, 10mins, 2, 6 and 24 hours post CPB.

Lung biopsies were taken both prior to and immediately after surgery. The pre-surgery biopsies were taken from the left upper lobe immediately after sternotomy with lungs ventilated for both groups. The post-surgery biopsy was taken from the left lower lobe at the end of the operation just before weaning from CPB.

This study was approved by the NRES committee London- Camden and Islington (Research Ethics Committee reference number 12/LO/0458) on 25/04/2012. Further approval was obtained from the research and development department of the Imperial College Healthcare NHS Trust. This research complied with the Helsinki Declaration. The trial is registered as ISRCTN No: 34428459. All patients involved in the study gave written and informed consent

2.2 Luminex:

Cytokines in human plasma samples, taken 24 hours post-surgery, were quantified using the Luminex Screening Human Magnetic Assay kit (R&D, Abingdon, UK).

2.3 Transcriptomics:

RNA was extracted and analysed by Affymetrix GeneChip Human Gene 1.0 ST Array (ThermoFisher) following the manufacturer's instructions.

RNA samples were also quantified using RT-qPCR. More details are available in the supplemental materials.

2.4 Proteomics:

Protein was extracted as described previously [14]. More details are available in the supplemental materials.

2.5 Heme assay:

Heme levels in the whole cell protein extracts were measured using the Heme colorimetric assay kit (BioVision, Milpitas, CA, USA) following manufacturer's instruction.

2.6 Lipidomics:

Lung tissue was processed as described previously [15,16].

More details are available in the supplemental materials.

2.7 Oxidative stress/ Anti-oxidant capacity:

We used the RedoxSys® to electrochemically measure the oxidant redox potential (ORP) and antioxidant capacity (AOC), following manufacturer's instructions (Aytu Biosciences, Englewood, CO, USA).

2.8 Statistics and Data analysis:

Gene arrays were analysed by Partek genomics Suite (Partek Inc). Gene and protein classification were tested using PANTHER Overrepresentation Test analysed against the Homo Sapiens reference list, using the PANTHER Go-SLIM Biological process annotation dataset [17]. Analysis included Bonferroni correction for multiple data.

The remaining data were analysed using Graphpad Prism 6 (Graphpad Software Inc, La Jolla, CA, USA) utilising Friedman and using Dunn's multiple comparison test unless otherwise stated. A probability value of <0.05 was considered significant.

3. Results:

Patient demographics and clinical characterisation are provided in detail in Fiorentino et al, 2019 [14].

3.1 Patient serum samples:

3.1.1 Luminex of serum cytokines:

Plasma IL-6, IL-8 and IL-10 levels increased significantly 24 hours post-surgery in both groups compared to the pre-surgery control samples. IL-6 levels increased 17-fold in lungs collapsed group and 25-fold in the LFV group (**Figure 1A**). IL-8 levels (**Figure 1B**) increased approximately 1.5-fold in both study groups, whilst IL-10 (**Figure 1C**) increased approximately 1.3x. In contrast, there was no significant change in inflammatory cytokines IL-1β and MCP-1 in the plasma of patients before CPB and 24hrs after CPB in both groups (**Figure 1D & E**).

3.1.2 Cell-Free heme:

The levels of cell free heme were measured in the blood plasma following surgery. Cell free heme was significantly higher in both groups at 10 minutes and 2 hours after surgery before returning to baseline. Cell-free heme levels in plasma were increased but not significantly in the LFV group (51.5μM vs 38.1μM, 2-way ANOVA $p=0.17$) (**Figure 2**).

3.1.3 Oxidative stress in blood:

Plasma ORP and AOC from all patients were measured following bypass. By 2-way ANOVA time after surgery was linked to significantly increased ORP ($p<0.0001$) and this was matched by a significant decline in AOC ($p<0.0001$). However, the ANOVA

did not identify any statistical significance related to intervention, indicating that CPB induced changes in ORP and AOC were not altered by LFV (p=0.44, p=0.16 respectively) (**Figure 2**).

Since LFV intervention did not effect plasma ORP or AOC we examined the combined data to increase statistical power and determine the effects of surgery. The combined data showed a significant increase in ORP within 10 minutes following surgery, which increased at all timepoints measured but appeared to plateau at 6 hours. Similarly, the decrease in AOC following surgery reached a nadir at 6 hours which was maintained (**Figure 2**).

3.2 Biopsy RNA gene expression data:

Full data set is available at https://figshare.com/articles/_/4772167. Principle component analysis (PCA) did not identify any significant outliers; therefore, no patient samples were excluded from the analysis (**Supplemental Figure 1**). There were no significant differences in gene expression between the two groups at baseline.

3.2.1 Transcriptional response to CPB with lungs collapsed:

Lungs left collapsed significantly increased the expression of 30 genes in the biopsy immediately after surgery (**Supplemental data: Table 1**). These genes include the inflammatory genes *CCL2* (encoding MCP-1) and *IL6*, which had the highest increase following surgery (6.7x and 6.6x higher than baseline respectively). Panther pathway analysis identified the "cholecystokinin receptor (CCKR) signalling map" (p=2.26E-08), the "Interleukin signalling pathway" (5.41E-05) and the "p53 pathway" (4.81E-

02) as significantly over-represented within the genes induced in the lung collapsed group (**Supplemental data: Table 2**).

3.2.2 Transcription response to CPB with LFV:

LFV significantly induced 80 genes in lung tissue after surgery (**Supplemental data: Table 3**). No genes were significantly suppressed. All CPB-induced genes were enhanced in the LFV group and up-regulated genes shared the same pathways as those induced by lungs collapsed CPB namely the "CCKR signalling map" (p= 2.14E-10), the "interleukin signaling pathway" (p=4.34E-03) and the "p53 pathway" (p=4.46E-02)(**Supplemental data: Table 4**). In addition, the "Inflammation mediated by chemokine and cytokine signaling pathway" and the "Gonadotropin-releasing hormone receptor pathway" were also enriched. Biological process analysis identified "endoderm development", "MAPK cascade", "cell death" and "response to stress" as significantly over-represented.

The 50 genes that were upregulated in the LFV group alone (i.e. not in CPB lungs collapsed group) included inflammatory genes such as *IL1B* and *CYR61*. Pathway and biological process analysis did not identify any specific pathways or processes as overrepresented in these 50 genes although raw, uncorrected p values indicated over-representation of the 'CCKR signalling map' and "Inflammation mediated by chemokine and cytokine signaling" pathways (p=2.01E-03).

3.2.3 Effect of low frequency ventilation:

Comparing gene expression biopsies from the LFV and lungs left collapsed groups taken after surgery identified statistically significant changes in 26 genes in patients

who underwent LFV compared to patients undergoing lungs collapsed CPB (**Supplemental data: Table 5**). *HLA-DRB5*, encoding the HLA class II histocompatibility antigen DRB5 was reduced in the LFV group whilst the remaining 25 genes were increased with LFV. The expression of HLA-DRB5 was not significantly altered following surgery in either groups compared to their respective pre-surgical controls.

The genes significantly increased by LFV intervention compared to lungs left collapsed included the inflammatory *IL6*, *CCL2* and *CCL8* (encoding IL-6, MCP1 and MCP2 respectively). Pathway analysis showed that LFV significantly activated the "Plasminogen activating cascade" (p=3.17E-02), "CCKR signaling map" (p=6.81E-03), and "Inflammation mediated by chemokine and cytokine signaling pathway" (p=3.30E-02)(**Supplemental data: Table 2**).

Combining both intervention groups to increase the analytical power of the effects of surgery identified 51 genes with significantly altered expression following surgery (**Supplemental data: Table 6**). Pathway analysis of this data identified the "Oxidative stress response" (p= 4.76E-02), "Interleukin signaling" (p= 5.10E-04), "CCKR signaling map" (p=9.53E-07) and "p53" (p= 8.22E-03) pathways as over-represented.

3.2.4 Validation of transcriptomic response:

We have previously examined the induction of *IL6*, *IL8* and *IL1B* gene expression in the lung biopsies by Taqman qPCR. The gene expression data following CPB showed the same increase in inflammatory gene expression in the LFV group compared to the

lungs collapsed group [14]. In addition, we demonstrated significant up-regulation of hypoxia inducible factor 1A (*HIF1A*) gene expression in the biopsies after lungs collapsed CBP, which was further enhanced in the biopsies from patients who underwent LFV (**Figure 3A**), compared to the pre-surgery control biopsies.

3.3 Biopsy Proteomic analysis:

Full data set is available at https://figshare.com/articles/_/4772167. Whole cell protein extracts from each biopsy were pooled into 4 groups: lungs left collapsed or LFV both pre and post-surgery. Tandem mass tagging (TMT) identified over 3000 distinct proteins in the pooled biopsy samples. There was minimal variation in the pre-surgery baseline levels of proteins detected. Two proteins were significantly elevated >2-fold in the lungs left collapsed group and 34 were elevated >2x in the LFV group (**Supplemental data: Table 7**) before surgery. Panther pathways analysis of these proteins did not identify any biological pathways or processes as overrepresented. Using a 1.5-fold cut-off, there were 4 significantly different proteins in the lungs collapsed group and 155 proteins more highly expressed in the LFV group. PANTHER analysis of these proteins identified "immune system process" as over-represented in the LFV group at baseline before surgery.

3.3.1 Proteomic response to CPB with lungs collapsed:

Lungs collapsed CBP resulted in 25 proteins having a >2-fold increase in expression post-surgery and 1 protein decreased >2-fold (**Supplemental data: Table 8**) relative to the same donors before surgery. The up-regulated proteins included the detoxifying enzyme glutathione S-transferase P (GSTP1), and eosinophil peroxidase. The decreased protein was identified as "cDNA FLJ50754, highly similar to voltage-

dependent L-type calcium channel subunit alpha-1D". Reducing the cut-off ratio to 1.5-fold change increased the number of differentially expressed proteins to 109 with enhanced expression and 8 proteins that were decreased. These did not reflect any pathways or processes although at the unadjusted p value level the "CCKR signalling map" and "intergrin signalling pathways" were identified as over-represented (p=4.91E-2 and p=1.33E-02 respectively).

3.3.2 Proteomic response to CPB with LFV:

CBP in the presence of LFV resulted in >2-fold upregulation of 7 proteins with keratin, both type I and II, making up 6 out of 7 of these proteins (**Supplemental data: Table 8**). Keratin is a common contaminant of proteomic experiments, so these changes may simply be an artefact, however keratin expression in the lungs has previously been reported, including its upregulation during lung repair [18] and by shear forces.[19,20] The remaining protein was "cDNA FLJ50754, highly similar to Voltage-dependent L-type calcium channel subunit alpha-1D". Whilst no pathways were identified as changed the keratin proteins were all linked to the process of "cellular component organisation or biogenesis" ($p=2.8x10^{-6}$). 15 proteins were decreased >2-fold following surgery with LFV, including 5 haemoglobin subunits (HBA2, HBB, HBD). Analysis of biological processes identified "blood circulation" as overrepresented (p>0.001).

19 proteins were increased following LFV using a 1.5-fold cut off, 7 of which were linked to the "cellular component morphogenesis" process (p>0.001). 47 proteins were decreased following surgery. The analysis did not identify any pathways

significantly altered by LFV at the protein level, however, cellular process analysis again identified "blood circulation" as overrepresented (p=0.001).

3.3.3 Comparison of LFV with lungs left collapsed:

Direct comparison of the post-bypass samples identified 4 proteins that were increased in the lungs collapsed group with >2-fold change and 9 proteins that were increased in the LFV group (**Supplemental data: Table 5**). Biological pathway and process analysis did not identify any significantly over-represented pathways/processes between these groups. 16 proteins were identified as >1.5-fold higher in lungs collapsed compared to LFV, of which 3 were also higher at baseline and therefore excluded from the analysis. Proteins increased in the lungs collapsed group included haemoglobin alpha, beta and delta. These proteins were not associated with any significant changes in biological pathways but were identified with the processes of blood circulation (p=2.27E-04) and transport (p=3.14E-05).

11 proteins were higher in the LFV group compared to lungs collapsed post-surgery but not pre-surgery. No processes or pathways were identified as significant.

3.4 Confirmation of reduced haemoglobin in biopsies following LFV:

Due to the proteomics identification of haemoglobin as downregulated in the LFV group the level of heme was measured in the protein isolated from each lung biopsy (**Figure 3B**). The amount of heme in the biopsies did not significantly change following CPB with lungs collapsed, however, it was significantly reduced following surgery with LFV.

3.5 Lipidomics:

Full data set is available at https://figshare.com/articles/_/4772167. There were no significant differences in lipid class or species between groups either before or after surgery regardless of intervention. (Data is shown in **Supplemental Figure 2**.)

4 Discussion:

Surgery with CPB is associated with acute systemic and pulmonary inflammation and can lead to pulmonary dysfunction in a significant number of patients. We confirmed previous data showing enhanced levels of inflammatory cytokines, oxidative stress, cell free heme and decreased plasma anti-oxidant capacity with CPB. We also provided evidence for the first time in transcriptomic analysis of lung biopsy in patients undergoing CABG, that CPB triggers a significant increase in hypoxic and inflammatory responses and a decrease in genes associated with blood flow. These effects were amplified in patients undergoing CPB with LFV when compared with CPB with lungs collapsed. These data provide a mechanistic link to the adverse clinical effects seen with the addition of LFV to CPB in patients undergoing CABG (14).

Analysis of the patients' plasma showed that following CPB with lungs collapsed there was a significant increase in the levels of inflammatory cytokines, oxidative stress, cell free heme and a decrease in plasma anti-oxidant capacity corresponding to the effects of CPB surgery previously reported [21]. These systemic effects were not significantly altered by CPB with LFV intervention.

LFV may increase the deleterious effects of CPB by three main mechanisms: increased surgical time, direct oxygenation of the lungs or ventilator-associated injury. The movement of the lungs during CPB with LFV may increase surgery time. The LFV group had a higher levels of cell free heme in the blood following CPB, a reflection of the longer CPB time compared to the lungs left collapsed CPB group

(87.5 minutes median (range 68-97) vs 69 minutes median (range 54-79)) (p=0.03) [14].

The increased oxygenation of the lungs during LFV may also enhance lung injury. Without the hypoxic response to reduce metabolic rates, LFV may cause a more rapid use of metabolic substrates and the build-up of by-products causing increased lung damage. Hyperoxia during surgery showed similar inflammation and stress following CPB as normoxia, although hyperoxia led to oxygen-mediated myocardial, hepatic and cerebral injury [22]. This hypothesis is unlikely as the LFV group showed increased *HIF1A* gene expression in blood indicating that the lungs were less, not more, oxygenated during LFV. However, intermittent hypoxia has been shown to be more potent at activating HIF-1α and FOS/AP-1 than continuous hypoxia [23].

Finally, LFV may cause biotrauma to the lung by repetitive alveolar collapse and hyperinflation [24].

Our data are unique because of the use of lung biopsies taken during the surgery in the on-going debate regarding relative contributions of ischaemia and reperfusion to tissue injury. The data indicate that the practice of lungs left collapsed during CPB prior to reperfusion, can trigger gene expression, inflammation and stress in the lungs. These could be the consequence of atelectasis, direct effect of lung hypoperfusion and ischemia superimposed by perfusion with activated inflammatory cells due to their activation by the CPB machine and circuit. There has been considerable debate as to the relative importance of these mechanisms in driving lung inflammation [3,4,25] but the strong correlation between increased stress, hypoxia and inflammation in the lungs

support the hypothesis that ischemia alone is enough to drive inflammation. Ischemia during surgery is associated with significant changes in inflammation (interleukin signalling pathway) and stress (CCKR and p53 pathways) in the lung.

In addition, the principle driver of increased inflammation in the LFV group appears to be increased surgery time, and hence ischemic, time, whilst reperfusion remained unchanged. As our lung biopsies were collected immediately after reperfusion it is unlikely that systemic inflammation or reperfusion injury would have been able to influence gene expression, but rather that ischemia alone is capable of significantly damaging the lungs.

Whilst the proteomic analysis of CPB identified several proteins that changed expression in the pooled samples, this did not identify any specific pathways as activated by routine CPB with lungs left collapsed. Proteomic analysis is hampered by the short timeframes in which the surgery occurs and (to overcome resource constraints) the pooling of samples from all patients in each treatment group. Whilst pooling the samples loses the ability to discern individual patient variation, this approach reduces biological variation and thereby increases the power to detect treatment differences [26]. Nevertheless, CCKR signalling and integrin signalling pathways were significantly over-represented by proteins up-regulated by CPB when assessed using a raw p value <0.05. As stated above, the CCKR signalling may be induced by hypoxic conditions and up-regulated protein levels correlated well with gene expression. The integrin signalling proteins consisted of collagen alpha-1 (I) chain, the collagen alpha-1 (XIV) chain, the adapter molecule Crk and Crk-like (CrkL) proteins. Crk and CrkL have been shown to play a key role in the activation

and transformation of fibroblasts, which are the principle produces of extracellular matrix, including collagen in response to injury. These data indicate that fibroblast activation, in response to lung injury, occurs at an early stage in CPB. This study provides valuable insight into the underlying mechanisms that drive lung inflammation during CPB. This increased understanding may lead to more effective interventions in the future.

Proteomic analysis of the LFV group showed a significant decrease in proteins representing blood circulation, such as haemoglobin, which was confirmed in the biopsy samples. These data indicate that LFV may have increased vascular resistance and further reduced pulmonary blood flow during surgery, which may increase the level of ischemia and the level of pulmonary inflammation [27]. Patients undergoing LFV did show an increase in requiring haemodynamic support following surgery compared to those undergoing CPB with lungs left collapsed, so alternatively this may reflect a reduction in blood pressure [14].

Whilst changes in lipids have been reported in response to oxidative stress, such as the accumulation of pro-inflammatory isoprostanes and oxylipins in smokers and in patients with cardiovascular disease, no significant changes in lipidomics were detected following CPB, indicating that either the timeframe of the study was too short for these changes to occur or CPB has little effect on the lipid composition of the lung. The lack of change in the proteomics and lipidomic profiles detected may also reflect the important role that post-translational modifications play in regulating

protein and lipid function. Unfortunately, examination of post-translational modifications was beyond the scope of this study.

A major limitation of the study is the timing of the sample collection. The initial pilot study was not designed to identify differences between ischemia and reperfusion and ideally lung biopsies should have been taken immediately before and after reperfusion occurred. Additionally the timing may be suboptimal for detecting changes which drive lung injury following CPB. A study by Hepponstall examining the plasma proteome following CPB found changes in C-reactive protein and hepatoglobin peaked at 12-24 hours following surgery [28]. This is reflected in the differences in results between the Luminex measure of cytokines in the plasma and the lung biopsy proteomics. In the biopsies collected immediately post-surgery there was no significant increases in the levels of inflammatory cytokines detected, which contrasted with the significant increases in the plasma samples collected 24 hours later, reflecting the several hours of transcription, translation and post-translational modification required for fully mature cytokines to be produced. However, as shown by our previous publication on LFV and CPB inflammatory signals, such as NF-κB were significantly higher immediately after surgery in the lung biopsies [14]. However, for practical reasons, later timepoints could not be directly measured in the lung.

Summary

LFV increased pulmonary, but not systemic inflammation, following CPB. Semi-biased transcriptomic and proteomic analysis of lung biopsies suggest that ischemia is the principle driver of pulmonary inflammation following CPB and that LFV,

possibly through reduced blood flow through the bronchial artery and increased surgery time, further enhances pulmonary ischemia and inflammation.

Sources of Funding

The work was supported by a project grant by the British Heart Foundation (BHF) Grant PG/13/9/29990 and the National Institute for Health Research [NIHR] Biomedical Research Centre at University Hospitals Bristol NHS Foundation Trust and the University of Bristol. The views expressed in this publication are those of the author(s) and not necessarily those of the NHS, the National Institute for Health Research or the Department of Health and Social Care.

Acknowledgements

The authors would like to thank Nandor Marczin for their help finalising the manuscript and co-supervision of JHB.

Statement of the contribution

Substantial contributions to the conception or design of the work; or the acquisition, analysis, or interpretation of data for the work: ALD, EAJ, RG, POB, JHB, KJH, ADP, PL, EJ, BR

Drafting the work or revising it critically for important intellectual content: ALD, EAJ, KJH, ADP, PL, FF, GDA, SM, IMA

Final approval of the version to be published: ALD, EAJ, FF, GDA, IMA

Agreement to be accountable for all aspects of the work in ensuring that questions related to the accuracy or integrity of any part of the work are appropriately investigated and resolved: ALD, EAJ, FF, GDA, IMA

Conflicts of interest

None declared

1

2

References:

[1] B. Bridgewater, B. Keogh, R. Kinsman, P. Walton, SCTS 6th National Adult Cardiac Surgical Database Report 2008, 2008. https://doi.org/10.1016/j.healun.2014.04.010.

[2] R.A. Bronicki, M. Hall, Cardiopulmonary Bypass-Induced Inflammatory Response: Pathophysiology and Treatment., Pediatr. Crit. Care Med. 17 (2016) S272-8. https://doi.org/10.1097/PCC.0000000000000759.

[3] C. Schlensak, T. Doenst, S. Preusser, M. Wunderlich, M. Kleinschmidt, F. Beyersdorf, Cardiopulmonary bypass reduction of bronchial blood flow: a potential mechanism for lung injury in a neonatal pig model., J. Thorac. Cardiovasc. Surg. 123 (2002) 1199–1205.

[4] C. Schlensak, T. Doenst, S. Preusser, M. Wunderlich, M. Kleinschmidt, F. Beyersdorf, Bronchial artery perfusion during cardiopulmonary bypass does not prevent ischemia of the lung in piglets: assessment of bronchial artery blood flow with fluorescent microspheres., Eur. J. Cardiothorac. Surg. 19 (2001) 322–326.

[5] P.J. Chai, J.A. Williamson, A.J. Lodge, C.W. Daggett, J.E. Scarborough, J.N. Meliones, I.M. Cheifetz, J.J. Jaggers, R.M. Ungerleider, Effects of ischemia on pulmonary dysfunction after cardiopulmonary bypass., Ann. Thorac. Surg. 67 (1999) 731–735.

[6] J.M. Dodd-o, L.E. Welsh, J.D. Salazar, P.L. Walinsky, E.A. Peck, J.G. Shake, D.J. Caparrelli, B.T. Bethea, S.M. Cattaneo, W.A. Baumgartner, D.B. Pearse, Effect of bronchial artery blood flow on cardiopulmonary bypass-induced lung injury., Am. J. Physiol. Heart Circ. Physiol. 286 (2004) H693-700.

https://doi.org/10.1152/ajpheart.00888.2003.

[7] F. Bagheri, V. Khori, A.M. Alizadeh, S. Khalighfard, S. Khodayari, H. Khodayari, Reactive oxygen species-mediated cardiac-reperfusion injury: Mechanisms and therapies., Life Sci. 165 (2016) 43–55. https://doi.org/10.1016/j.lfs.2016.09.013.

[8] E. Pantazi, M. Bejaoui, E. Folch-Puy, R. Adam, J. Rosello-Catafau, Advances in treatment strategies for ischemia reperfusion injury., Expert Opin. Pharmacother. 17 (2016) 169–179. https://doi.org/10.1517/14656566.2016.1115015.

[9] B.P. Van Putte, J. Kesecioglu, J.M.H. Hendriks, V.P. Persy, E. van Marck, P.E.Y. Van Schil, M.E. De Broe, Cellular infiltrates and injury evaluation in a rat model of warm pulmonary ischemia-reperfusion., Crit. Care. 9 (2005) R1-8. https://doi.org/10.1186/cc2992.

[10] P.B. Anning, Y. Chen, N.J. Lamb, S. Mumby, G.J. Quinlan, T.W. Evans, J.M. Gutteridge, Iron overload upregulates haem oxygenase 1 in the lung more rapidly than in other tissues., FEBS Lett. 447 (1999) 111–114.

[11] S. Mumby, T.W. Koh, J.R. Pepper, J.M. Gutteridge, Risk of iron overload is decreased in beating heart coronary artery surgery compared to conventional bypass., Biochim. Biophys. Acta. 1537 (2001) 204–210.

[12] H. Imura, M. Caputo, K. Lim, M. Ochi, M.S. Suleiman, K. Shimizu, G.D. Angelini, Pulmonary injury after cardiopulmonary bypass: Beneficial effects of low-frequency mechanical ventilation, J. Thorac. Cardiovasc. Surg. 137 (2009) 1530–1537. https://doi.org/10.1016/j.jtcvs.2008.11.014.

[13] A.B. Durukan, H.A. Gurbuz, N. Salman, E.U. Unal, H.I. Ucar, C.E.M. Yorgancioglu, Ventilation during cardiopulmonary bypass did not attenuate

inflammatory response or affect postoperative outcomes., Cardiovasc. J. Afr. 24 (2013) 224–230. https://doi.org/10.5830/CVJA-2013-041.

[14] F. Fiorentino, E. Al Jaaly, A. Durham, I. Adcock, G. Lockwood, E. Jazrawi, C. Rogers, R. Ascione, B. Reeves, G. Angelini, Low frequency ventilation during cardiopulmonary bypass for lung protection: A randomised controlled trial, J. Card. Surg. (2019). https://doi.org/10.1111/jocs.14044.

[15] E.G. Bligh, W.J. Dyer, A Rapid Method Of Total Lipid Extraction And Purification, Can. J. Biochem. Physiol. 37 (1959) 911–917. https://doi.org/10.1139/o59-099.

[16] A.D. Postle, D.C. Wilton, A.N. Hunt, G.S. Attard, Probing phospholipid dynamics by electrospray ionisation mass spectrometry, Prog. Lipid Res. 46 (2007) 200—224. https://doi.org/10.1016/j.plipres.2007.04.001.

[17] H. Mi, S. Poudel, A. Muruganujan, J.T. Casagrande, P.D. Thomas, PANTHER version 10: expanded protein families and functions, and analysis tools., Nucleic Acids Res. 44 (2016) D336-42. https://doi.org/10.1093/nar/gkv1194.

[18] M. Ficial, C. Antonaglia, M. Chilosi, M. Santagiuliana, A.-O. Tahseen, D. Confalonieri, L. Zandona, R. Bussani, M. Confalonieri, Keratin-14 expression in pneumocytes as a marker of lung regeneration/repair during diffuse alveolar damage., Am. J. Respir. Crit. Care Med. 189 (2014) 1142–1145. https://doi.org/10.1164/rccm.201312-2134LE.

[19] K.M. Ridge, L. Linz, F.W. Flitney, E.R. Kuczmarski, Y.-H. Chou, M.B. Omary, J.I. Sznajder, R.D. Goldman, Keratin 8 phosphorylation by protein kinase C delta regulates shear stress-mediated disassembly of keratin intermediate filaments in alveolar epithelial cells., J. Biol. Chem. 280 (2005) 30400–30405. https://doi.org/10.1074/jbc.M504239200.

[20] S. Sivaramakrishnan, J. V DeGiulio, L. Lorand, R.D. Goldman, K.M. Ridge, Micromechanical properties of keratin intermediate filament networks, Proc. Natl. Acad. Sci. 105 (2008) 889–894. https://doi.org/10.1073/pnas.0710728105.

[21] D. Paparella, T.M. Yau, E. Young, Cardiopulmonary bypass induced inflammation: pathophysiology and treatment. An update., Eur. J. Cardiothorac. Surg. 21 (2002) 232–244.

[22] M. Caputo, A. Mokhtari, C.A. Rogers, N. Panayiotou, Q. Chen, M.T. Ghorbel, G.D. Angelini, A.J. Parry, C. M., M. A., R. C.A., P. N., C. Q., G. M.T., A. G.D., P. A.J., The effects of normoxic versus hyperoxic cardiopulmonary bypass on oxidative stress and inflammatory response in cyanotic pediatric patients undergoing open cardiac surgery : A randomized controlled trial, J. Thorac. Cardiovasc. Surg. 138 (2010) 206–214. https://doi.org/10.1016/j.jtcvs.2008.12.028.The.

[23] J. Nanduri, G. Yuan, G.K. Kumar, G.L. Semenza, N.R. Prabhakar, Transcriptional responses to intermittent hypoxia., Respir. Physiol. Neurobiol. 164 (2008) 277–281. https://doi.org/10.1016/j.resp.2008.07.006.

[24] A.S. Slutsky, R. V Marco, Ventilator-Induced Lung Injury, N. Engl. J. Med. 369 (2013) 2126–2136. https://doi.org/10.1056/NEJMra1208707.

[25] C. Schlensak, F. Beyersdorf, Lung injury during CPB: pathomechanisms and clinical relevance, Interact. Cardiovasc. Thorac. Surg. . 4 (2005) 381–382. https://doi.org/10.1510/icvts.2005.117853.

[26] A.P. Diz, M. Truebano, D.O.F. Skibinski, The consequences of sample pooling in proteomics: an empirical study., Electrophoresis. 30 (2009) 2967–2975. https://doi.org/10.1002/elps.200900210.

[27] K.A. Dora, C.P. Stanley, E. Al Jaaly, F. Fiorentino, R. Ascione, B.C. Reeves, G.D. Angelini, Isolated Human Pulmonary Artery Structure and Function Pre- and Post-Cardiopulmonary Bypass Surgery, J. Am. Hear. Assoc. Cardiovasc. Cerebrovasc. Dis. 5 (2016) e002822. https://doi.org/10.1161/JAHA.115.002822.

[28] M. Hepponstall, V. Ignjatovic, S. Binos, C. Attard, V. Karlaftis, Y. d'Udekem, P. Monagle, I.E. Konstantinov, Cardiopulmonary bypass changes the plasma proteome in children undergoing tetralogy of Fallot repair, Perfusion. 30 (2015) 556–564. https://doi.org/10.1177/0267659114566065.

Figure Legends:

Figure 1. Cytokine levels following surgery.

Plasma was extracted from the blood of patients collected after anaesthetic induction but before the cardio-pulmonary bypass (CPB) procedure (pre-CPB), and at 24hrs post-operation (post-CPB). Patients who underwent CPB with lungs left collapsed shown in black (n=18). Patients shown in grey (n=18) received CPB with low frequency ventilation (LFV). Concentrations of **(A)** IL-6, **(B)** IL-8, **(C)** IL-10, **(D)** IL-1β and **(E)** MCP-1 in the plasma were quantified with a multiplex assay. Data was analysed Freidman Test statistical analysis with Dunn's multiple comparison post-test; **p<0.01, ***p<0.001, ****p<0.0001.

Figure 2. Measurements in blood plasma following surgery.

Plasma samples were measured at various timepoints following surgery, **(A)** cell free heme in the patients undergoing CPB with lungs left collapsed (n=18), **(B)** heme in patients undergoing CPB with LFV (n=18) **(C)** oxidation reduction potential (ORP) **(D)** anti-oxidant capacity (AOC). The control group is shown in black and the LFV group in grey. Data from both patient groups were combined to examine the effects of the CPB circuit on **(E)** ORP and **(F)** AOC. Data were analysed using Freidman Test statistical analysis with Dunn's multiple comparison post-test *p<0.05, **p<0.01, ***p<0.001, ****p<0.0001.

Figure 3. Measurements in lung biopsies following surgery.

(A) Hypoxia inducible factor 1 alpha (*HIF1A*) gene expression in lung biopsies pre- and post-surgery using either CPB with lungs left collapsed or with LFV. *HIF1A* gene expression (normalised to 18S) was significantly increased (the median gene expression doubled) in lung tissue following CPB, with (n=18) or without LFV (n=18). LFV biopsies had significantly higher levels of *HIF1A* gene expression compared to biopsies from patients who underwent CPB with lungs left collapsed. Lung biopsies were taken prior to bypass (Pre) and after surgery, immediately before reperfusion (Post). n=18 in each group of patients *$p<0.05$, **$p<0.01$ comparing groups post-surgery, Wilcoxon matched-pairs signed rank test.

(B) Total Heme in lung biopsy samples from both groups, both pre- and post-surgery. Whilst heme levels were not significantly altered in the biopsies from patients undergoing CPB with lungs left collapsed they were significantly reduced in the biopsies from patients undergoing CPB with LFV following surgery. n=18 in each group of patients *$p<0.05$, **$p<0.01$ comparing groups post-surgery, Wilcoxon matched-pairs signed rank test.

Figures:
Figure 1.

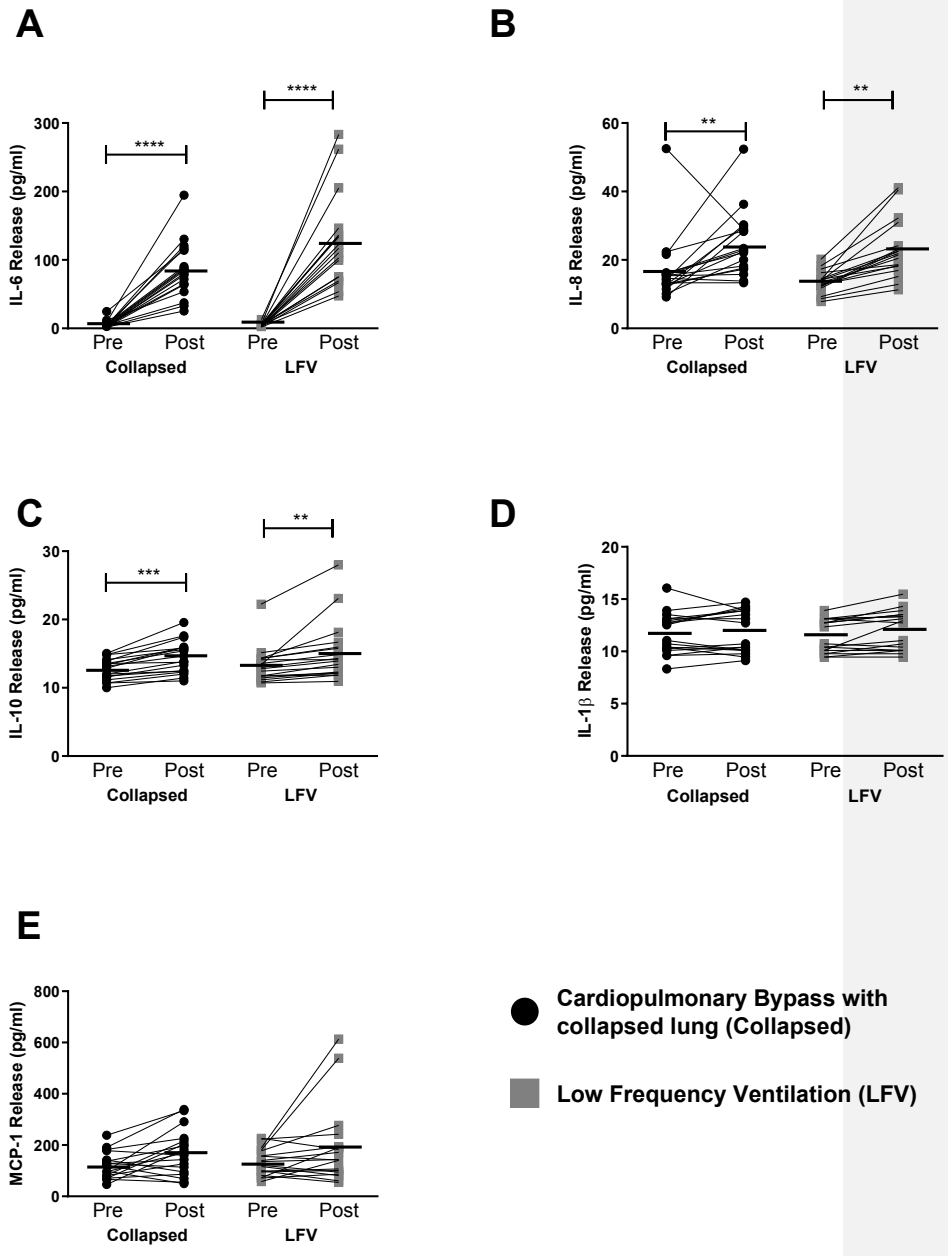

Commented [1]: Figure order updated

Figure 2.

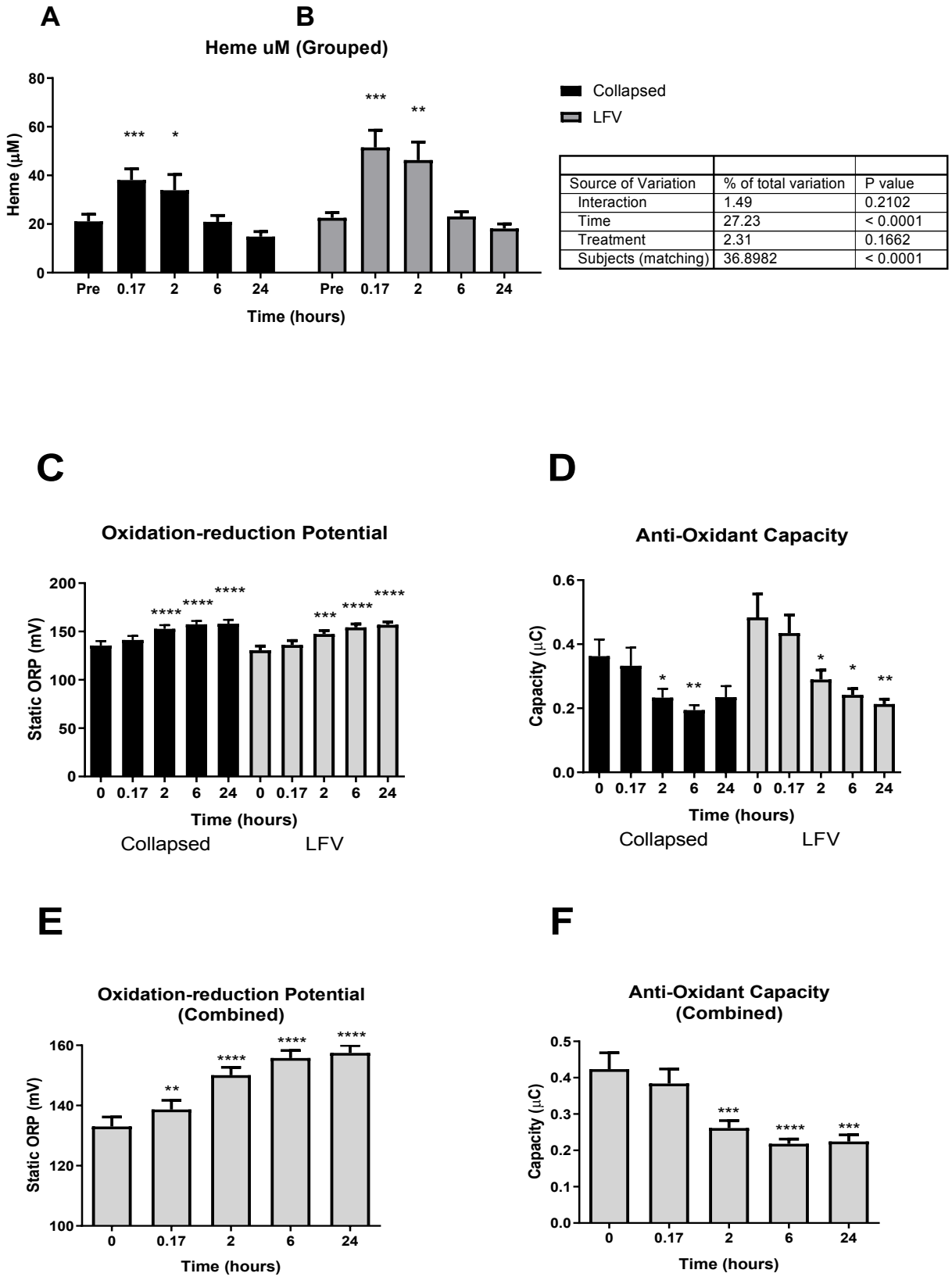

Source of Variation	% of total variation	P value
Interaction	1.49	0.2102
Time	27.23	< 0.0001
Treatment	2.31	0.1662
Subjects (matching)	36.8982	< 0.0001

Figure 3.

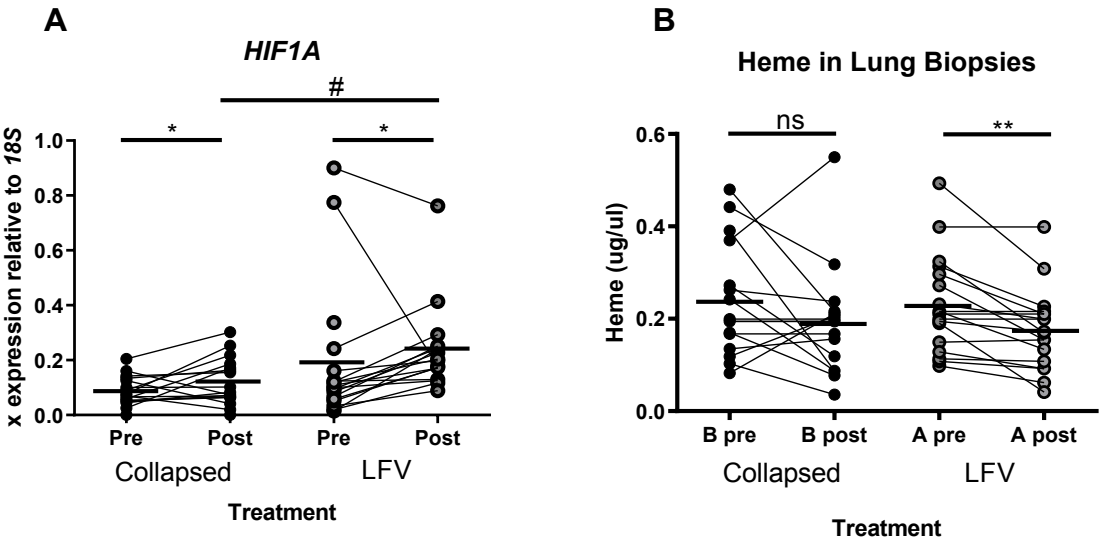
A
HIF1A
#
*
*
x expression relative to 18S
1.0
0.8
0.6
0.4
0.2
0.0
Pre
Post
Pre
Post
Collapsed
LFV
Treatment
B
Heme in Lung Biopsies
ns
**
Heme (ug/ul)
0.6
0.4
0.2
0.0
B pre
B post
A pre
A post
Collapsed
LFV
Treatment

Supplemental Data:

Multi-omic analysis of the effects of low frequency ventilation during cardiopulmonary bypass surgery.

Durham AL PhD[1], Al Jaaly E MD[2], Graham R MSc[1], Brook PO MSc[1], Bae JH BSc[1], Heesom KJ PhD[3], Postle AD PhD[4], Lavender P PhD[5], Jazrawi E BSc[1], Reeves B DPhil[2], Fiorentino F PhD[2], Mumby S PhD[1], Angelini GD MD[2,6], Adcock IM PhD[1].

Supplemental methods:

Transcriptomics:

For RNA extraction biopsies were placed in in RLT buffer (Qiagen) and homogenized using Precellys® ceramic beads (Cayman Chemicals, Cambridge, UK). Subsequently RNA was extracted using RNeasy extraction kit following manufacturer's instructions (Qiagen, Manchester, UK).

RNA was quantified by NanoDrop spectrophotometer (ThermoFisher, Waltham, MA, USA) and quality was checked by LabChip® spectrophotometer (Perkin Elmer). Subsequently RNA was amplified, converted to cDNA using the cDNA Ovation Pico WTA System (NuGen, San Carlos, CA, USA) and biotin labelled, using the Encore BiotinIL Module (Nugen), following the manufacturer's instructions. The cDNA was quantified and qualified, as above, and gene expression was measured using the Affymetrix GeneChip Human Gene 1.0 ST Array (ThermoFisher) following the manufacturer's instructions. Microarray data was

analysed using Partek Genomics Suite 6.6 (Partek GS, St. Louis, MI, USA) software and PANTHER gene ontology.[1]

RNA samples were also quantified using RT-qPCR. In brief the RNA concentration was determined using a NanoDrop 2000c spectrophotometer and standardised to 50ng/μL. Reverse transcription to create single stranded cDNA was performed using a high-capacity cDNA kit (Applied Biosystems, Foster City, CA, USA), following the manufacturer's instructions. qPCR was performed using a Rotor-Gene 3000 PCR machine (Corbett Research, Cambridge, UK) using a QuantiTect SYBR Green PCR kit and normalised to *18S* rRNA.

Proteomics:

Protein was extracted as described previously. In brief samples were homogenized in RIPA buffer (Sigma Aldrich, Poole, UK) containing HALT protease and phosphatase inhibitors (ThermoFisher, Paisley, UK) using Precellys® ceramic beads (Cayman Chemicals). After 30 minutes incubation at 4°C the samples were centrifuged (13,000g, 5 minutes, 4°C).

Supernatants from each group were quantified against a standard curve using the bininchoninic acid (BCA) assay (Sigma Aldrich) and equal amounts from each sample were pooled and changes in protein expression analysed using tandem mass tagging (TMT), as described previously.[2]

TMT Labelling and cation exchange chromatography

Aliquots of 100µg of each sample were digested with trypsin (2.5µg trypsin per 100µg protein; 37°C, overnight) and labelled with Tandem Mass Tag (TMT) sixplex reagents according to the manufacturer's protocol (Thermo Fisher Scientific, Loughborough, LE11 5RG, UK). After labelling, samples were pooled and a 50µg aliquot evaporated to dryness and resuspended in Buffer A (10mM KH2PO4, 25%MeCN pH3) prior to fractionation by strong cation exchange using an Ettan LC system (GE Healthcare). In brief, the sample was loaded onto a PolysulphoethylA column (100 x 2.1mm, 5µm, 200A; PolyLC Inc.) in buffer A and peptides eluted with an increasing gradient of buffer B (10mM KH2PO4, 25%MeCN 1M KCl pH3) from 0-100% over 30 minutes. The resulting fractions were evaporated to dryness, resuspended in 5% formic acid and then desalted using SepPak cartridges according to the manufacturer's instructions (Waters, Milford, Massachusetts, USA)). Eluate from the SepPak cartridge was again evaporated to dryness and resuspended in 1% formic acid prior to analysis by nano-LC MSMS using an LTQ-Orbitrap Velos Mass Spectrometer.

Nano-LC Mass Spectromerty

Cation exchange fractions were further fractionated using an Ultimate 3000 nanoHPLC system in line with an LTQ-Orbitrap Velos mass spectrometer (Thermo Scientific). In brief, peptides in 1% (vol/vol) formic acid were injected onto an Acclaim PepMap C18 nano-trap column (Thermo Scientific). After washing with 0.5% (vol/vol) acetonitrile 0.1% (vol/vol) formic acid peptides were resolved on a 250 mm × 75 µm Acclaim PepMap C18 reverse phase analytical column (Thermo Scientific) over a 150 min. organic gradient, using 7 gradient segments (1-6% solvent B over 1min., 6-15% B over 58min., 15-32%B

over 58min., 32-40%B over 5min., 40-90%B over 1min., held at 90%B for 6min and then reduced to 1%B over 1min.) with a flow rate of 300 nl min^{-1}. Solvent A was 0.1% formic acid and Solvent B was aqueous 80% acetonitrile in 0.1% formic acid. Peptides were ionized by nano-electrospray ionization at 2.0kV using a stainless-steel emitter with an internal diameter of 30 μm (Thermo Scientific) and a capillary temperature of 250°C. Tandem mass spectra were acquired using an LTQ- Orbitrap Velos mass spectrometer controlled by Xcalibur 2.1 software (Thermo Scientific) and operated in data-dependent acquisition mode. The Orbitrap was set to analyze the survey scans at 60,000 resolution (at m/z 400) in the mass range m/z 300 to 1800 and the top ten multiply charged ions in each duty cycle selected for MS/MS fragmentation using higher-energy collisional dissociation (HCD) with normalized collision energy of 45%, activation time of 0.1 ms and at a resolution of 7500 within the Orbitrap. Charge state filtering, where unassigned precursor ions were not selected for fragmentation, and dynamic exclusion (repeat count, 1; repeat duration, 30s; exclusion list size, 500) were used.

Data Analysis

The raw data files were processed and quantified using Proteome Discoverer software v1.2 (Thermo Scientific) and searched against the UniProt Human database using the SEQUEST algorithm. Peptide precursor mass tolerance was set at 10ppm, and MS/MS tolerance was set at 20mmu. Search criteria included oxidation of methionine (+15.9949) as a variable modification and carbamidomethylation of cysteine (+57.0214) and the addition of the TMT 6Plex mass tag (+229.163) to peptide N-termini and lysine as fixed modifications.

Searches were performed with full tryptic digestion and a maximum of 1 missed cleavage was allowed. The reverse database search option was enabled and all peptide data was filtered to satisfy false discovery rate (FDR) of 5%.

Lipidomics:

Lung tissue was weighed and homogenised on ice in 1.6ml of 0.9% saline together with 20µl of the anti-oxidant butylated hydroxyl toluene (BHT) (20 mg/ml in methanol), using a Heidolph Silent Crusher S. The homogenised lung samples were stored at -80^{o}C for subsequent lipid extraction. An aliquot of lung homogenate (800 µl) was lipid extracted with dichloromethane and methanol[3] after addition of internal quantification standards (PC14:0/14:0 10nmol, PE14:0/14:0 4nmol, TAG14:0/14:0/14:0 10nmol, PG14:0/14:0 2nmol, PS14:0/14:0 2nmol, PS14:0/14:0 2nmole, CE17:0 1nmol, CL14:0/14:0/14:0/14:0/14:0 1nmol) in 100µl methanol. The dichloromethane fraction was dried under nitrogen gas and the resultant extract was analysed using a Waters Xevo TQ mass spectrometer (Waters, Wythenshaw, UK). Samples were introduced to the mass spectrometer by syringe-driven direct infusion and the various lipid classes analysed by a comprehensive platform of diagnostic precursor and neutral loss scans as described previously.[4] Mass spectrometry results were initially processed by MassLynx software and subsequently quantified by dedicated Excel macro programmes.

Supplemental references:

[1] H. Mi, S. Poudel, A. Muruganujan, J.T. Casagrande, P.D. Thomas, PANTHER version 10: expanded protein families and functions, and analysis tools., Nucleic Acids Res. 44 (2016) D336-42. https://doi.org/10.1093/nar/gkv1194.

[2] S. Abdul-Ghani, K.J. Heesom, G.D. Angelini, M.-S. Suleiman, Cardiac phosphoproteomics during remote ischemic preconditioning: a role for the sarcomeric Z-disk proteins., Biomed Res. Int. 2014 (2014) 767812. https://doi.org/10.1155/2014/767812.

[3] E.G. Bligh, W.J. Dyer, A Rapid Method Of Total Lipid Extraction And Purification, Can. J. Biochem. Physiol. 37 (1959) 911–917. https://doi.org/10.1139/o59-099.

[4] A.D. Postle, D.C. Wilton, A.N. Hunt, G.S. Attard, Probing phospholipid dynamics by electrospray ionisation mass spectrometry, Prog. Lipid Res. 46 (2007) 200—224. https://doi.org/10.1016/j.plipres.2007.04.001.

Supplemental Tables:

Table 1. Differentially expressed genes in lung following CBP with lungs left collapsed.

Gene expression was measured in lung biopsies taken immediately following induction of bypass and immediately prior to the commencement of reperfusion. Data are organised by ratio of gene expression of the post: pre-surgery samples from patients undergoing CPB with lungs left collapsed.

Gene Name	*p-value*	*Ratio (Post vs. pre surgery)*
CCL2	1.56E-17	6.7442
IL6	2.66E-13	6.59224
THBS1	2.69E-10	4.99284
IER3	3.45E-14	4.95907
EGR1	1.19E-11	4.85421
ADAMTS1	9.20E-13	4.52339
NAMPT	7.02E-14	4.38552
ZFP36	8.06E-13	4.24673
MT2A	9.45E-11	4.18274
AXUD1	6.87E-12	3.93191
PTGS2	1.89E-10	3.63922
GADD45B	7.16E-11	3.41388
CDKN1A	7.22E-13	3.39603
NFIL3	4.68E-14	3.38138
MYC	6.46E-13	3.37585

IL8	2.29E-09	3.11566
PIM1	1.77E-11	3.07144
RGS2	1.27E-09	3.05557
NR4A2	4.01E-10	3.03127
SIK1	4.11E-11	2.88863
CXCL2	1.13E-10	2.87649
FOSB	1.59E-05	2.85606
RNF122	3.23E-10	2.74991
BHLHB2	7.16E-10	2.69932
DUSP5	2.27E-10	2.61988
EGR3	6.07E-11	2.59004
NR4A3	4.53E-11	2.57595
SLC2A3	8.13E-09	2.44753
MIDN	7.50E-07	2.31974
FOS	1.52E-05	2.16802

Table 2. Altered transcriptomic pathways and processes altered by lungs left collapsed and LFV.

Table showing the pathways and biological processes activated during cardio-pulmonary bypass with lungs left collapsed (collapsed) or with low-frequency ventilation (LFV) during surgery. Data shows the fold enrichment compared to the expected gene number in the sample size. P values include Bonferroni correction for multiple comparisons.

	Collapsed		LFV		LFV vs. Collapsed		Combined Collapsed and LFV groups post vs. pre surgery	
Pathway	Fold-change	Adj P value	Fold-change	Adj P value	Fold-change	Adj P value	Fold-change	Adj P value
CCKR signalling map	+ 31.28	2.26E-08	+ 19.66	2.14E-10	+ 20.20	6.81E-03	+ 20.20	9.53E-07
Interleukin signaling pathway	+ 34.52	5.41E-05	+ 14.46	4.34E-03			+ 22.29	5.10E-04
p53 pathway	+ 23.06	4.81E-02	+ 12.88	4.46E-02			+ 19.86	8.22E-03
Inflammation mediated by chemokine and cytokine signaling pathway			+ 8.69	6.60E-04	13.39	3.30E-02		

Gonadotropin-releasing hormone receptor pathway			+ 8.44	3.27E-03				
Plasminogen activating cascade					+ 97.09	3.17E-02		
Oxidative Stress Response							+ 23.41	4.76E-02
Process								
Endoderm development			+ >100	3.66E-02			+ >100	1.53E-02
MAPK cascade			+ 7.75	3.16E-02			+ 11.95	4.62E-04
Cell death			+ 65.40	3.30E-02	+ >100	2.53E-02		
Response to stress			+ 4.28	2.23E-03			5.08	5.05E-03
Localization							+ 14.21	4.52E-02

Table 3. Differentially expressed genes in lung samples in the LFV group. The expression of the same genes in the lungs left collapsed (Collapsed) group is shown for comparison (where also significantly changed).

The data shows the genes that were significantly changed post-surgery comparing the pre- and post-surgery samples from the LFV group. Data are organised by ratio of gene expression of the post: pre-surgery samples. Also shown are the p-values and ratios for the same genes in the CPB group pre- and post-surgery.

Gene	*p-value (Post LFV post vs. pre LFV)*	*Ratio (Post LFV post vs. pre LFV)*	*p-value (Collapsed post vs. Collapsed pre)*	*Ratio (Collapsed post vs. Collapsed pre)*
EGR1	1.52E-10	4.31211	1.19E-11	4.85421
CCL2	3.14E-11	3.7367	1.56E-17	6.7442
ZFP36	2.33E-10	3.39726	8.06E-13	4.24673
IER3	5.24E-10	3.36618	3.45E-14	4.95907
FOSB	1.97E-06	3.23688	1.59E-05	2.85606
IL6	4.20E-07	3.20897	2.66E-13	6.59224
AXUD1	7.36E-09	2.97975	6.87E-12	3.93191
GADD45B	8.53E-09	2.84233	7.16E-11	3.41388
RGS2	9.57E-09	2.82692	1.27E-09	3.05557
PTGS2	2.02E-07	2.71364	1.89E-10	3.63922
NAMPT	2.76E-08	2.69011	7.02E-14	4.38552

ADAMTS1	3.20E-07	2.65546	9.20E-13	4.52339
THBS1	4.31E-05	2.58619	2.69E-10	4.99284
CDKN1A	2.66E-09	2.58471	7.22E-13	3.39603
NR4A2	4.81E-08	2.54051	4.01E-10	3.03127
MT2A	1.58E-05	2.3859	9.45E-11	4.18274
MYC	3.80E-08	2.34622	6.46E-13	3.37585
SIK1	2.79E-08	2.33506	4.11E-11	2.88863
DUSP5	1.37E-08	2.3046	2.27E-10	2.61988
CYR61	0.000139197	2.28028		
BHLHB2	1.21E-07	2.26944	7.16E-10	2.69932
MT1A	0.00023541	2.21719		
FOS	9.31E-06	2.21653	1.52E-05	2.16802
SLC2A3	1.90E-07	2.20188	8.13E-09	2.44753
NFIL3	5.29E-08	2.19547	4.68E-14	3.38138
IL8	1.23E-05	2.17884	2.29E-09	3.11566
PIM1	4.81E-07	2.172	1.77E-11	3.07144
CXCL2	7.34E-07	2.13394	1.13E-10	2.87649
DUSP1	0.000566532	2.12812		
CRISPLD2	0.000119155	2.12754		
MIDN	1.03E-05	2.087	7.50E-07	2.31974
NR4A3	1.67E-07	2.02404	4.53E-11	2.57595
EGR3	2.96E-07	2.00958	6.07E-11	2.59004
SGK	0.000488729	2.00601		
RNF122	3.46E-06	2.00402	3.23E-10	2.74991
TRIB1	0.000175232	2.0034		

MTE	0.000367452	1.91892		
CHSY1	7.99E-05	1.8969		
CEBPD	9.24E-06	1.89357		
LDLR	0.00117263	1.86047		
NR4A1	1.09E-07	1.85738		
GADD45A	9.63E-08	1.82664		
ERRFI1	0.000199363	1.82399		
RASD1	0.00262772	1.81266		
LOC441019	3.63E-05	1.80627		
ELL2	0.000212275	1.80179		
FOSL2	1.06E-06	1.79105		
MIR21	0.000263131	1.76523		
JUNB	9.80E-08	1.7545		
ATP1B3	0.000288746	1.74548		
MAT2A	0.0012663	1.73094		
SLC20A1	8.56E-05	1.72167		
MT1E	3.74E-05	1.71535		
B4GALT1	0.00558024	1.69002		
NFKBIZ	1.00E-05	1.68699		
ALDH1A3	0.00342271	1.68698		
OBFC2A	0.000204148	1.65775		
SPSB1	0.0011272	1.65691		
LOC387763	1.66E-05	1.64433		
NFKBIA	0.00184104	1.63908		
IL1B	4.37E-05	1.62737		

CXCR7	0.00129761	1.62714		
RHOU	6.78E-05	1.62591		
CCL8	0.000337713	1.62543		
APOLD1	0.000140595	1.61926		
SYT4	0.0240593	1.58715		
PLAU	9.09E-05	1.56036		
UAP1	3.77E-05	1.55889		
SOD2	0.00203168	1.51347		
MT1X	0.00693741	1.50511		
C2CD4B	0.000338994	1.49971		
NNMT	0.00555558	1.49559		
SERPINB2	0.00229441	1.45598		
TIMP1	0.0251605	1.42749		
RDH10	0.000361211	1.42187		
C13orf33	0.000883785	1.3788		
TRK1	0.0259384	1.32595		
TRQ1	0.00924457	1.3179		
PTX3	0.0140338	1.29593		

Table 4. Differentially expressed proteins identified by TMT, comparing CPB with lungs left collapsed and LFV.

The proteins highlighted in bold were not changed at baseline between the two groups.

Accession	# AAs	MW [kDa]	calc. pI	Collapsed /LFV	Description
Q15423	64	7.1	8.18	3.700	Serum amyloid A protein (Fragment)
B4DIF5	**345**	**39.2**	**8.92**	**2.478**	**cDNA FLJ55687, highly similar to Cell cycle control protein 50A**
P20851	**252**	**28.3**	**5.14**	**2.283**	**C4b-binding protein beta chain**
Q8IUL9	**105**	**11.5**	**6.05**	**2.251**	**Hemoglobin beta chain variant Hb.Sinai-Bel Air (Fragment)**
Q6VFQ6	**42**	**4.5**	**8.24**	**1.766**	**Hemoglobin beta chain (Fragment)**
Q92531	**187**	**19.7**	**6.32**	**1.712**	**P35-related protein (Fragment)**
Q3MIB5	**262**	**28.7**	**5.27**	**1.617**	**INMT protein (Fragment)**
P02774	**474**	**52.9**	**5.54**	**1.608**	**Vitamin D-binding protein**
B4DWJ7	155	17.5	8.37	1.597	cDNA FLJ54968
P11686	**197**	**21.0**	**6.65**	**1.583**	**Pulmonary surfactant-associated protein C**
Q5T619	**568**	**62.3**	**8.62**	**1.573**	**Zinc finger protein 648**
E5RGQ7	**148**	**16.8**	**8.88**	**1.563**	**Dematin (Fragment)**
S6BGD6	235	24.8	7.24	1.557	IgG L chain
Q6J1Z9	**90**	**9.6**	**9.50**	**1.540**	**Hemoglobin alpha 1 (Fragment)**

P02042	**147**	**16.0**	**8.05**	**1.522**	**Hemoglobin subunit delta**
Q6J1Z8	**42**	**4.5**	**9.38**	**1.507**	**Hemoglobin beta (Fragment)**
D3DTX7	885	84.7	6.24	0.664	Collagen, type I, alpha 1, isoform CRA_a
M0QZ50	**93**	**9.8**	**4.48**	**0.663**	**Microtubule-associated protein 1S**
P01861	327	35.9	7.36	0.662	Ig gamma-4 chain C region
A0A087WTA8	**1364**	**129.1**	**9.01**	**0.658**	**Collagen alpha-2(I) chain**
O76041	**1014**	**116.4**	**7.99**	**0.654**	**Nebulette**
P08519	4548	501.0	5.88	0.652	Apolipoprotein(a)
C9JNE5	191	21.7	9.61	0.648	Myeloid leukemia factor 1 (Fragment)
H3BRW3	109	11.7	9.96	0.636	FAD-linked sulfhydryl oxidase ALR
P27701	**267**	**29.6**	**5.24**	**0.636**	**CD82 antigen**
Q9NZ09	**502**	**55.0**	**5.11**	**0.635**	**Ubiquitin-associated protein 1**
A4FU00	317	35.6	5.81	0.634	SYT2 protein (Fragment)
B4DMJ5	242	27.3	4.50	0.634	cDNA FLJ53012, highly similar to Tubulin beta-7 chain
P07451	**260**	**29.5**	**7.34**	**0.633**	**Carbonic anhydrase 3**
Q6PII6	533	58.3	4.77	0.610	TMF1 protein (Fragment)
P35908	**639**	**65.4**	**8.00**	**0.603**	**Keratin, type II cytoskeletal 2 epidermal**
P01880	384	42.2	7.93	0.591	Ig delta chain C region
A2J1N5	94	10.4	9.13	0.590	Rheumatoid factor RF-ET6 (Fragment)
P81605	110	11.3	6.54	0.586	Dermcidin
Q7Z6I6	**1101**	**118.5**	**4.81**	**0.567**	**Rho GTPase-activating protein 30 SV=3**

P13761	266	29.8	7.44	0.562	HLA class II histocompatibility antigen, DRB1-7 beta chain
A8K9A9	638	71.3	8.22	0.521	cDNA FLJ77744, highly similar to Homo sapiens kallikrein B, plasma (Fletcher factor) 1 (KLKB1), mRNA
Q96Q06	**1357**	**134.3**	**8.73**	**0.519**	**Perilipin-4**
B3KMX3	270	28.5	4.73	0.497	cDNA FLJ12857 fis, clone NT2RP2003513, highly similar to Homo sapiens paralemmin (PALM),
Q15323	416	47.2	4.88	0.436	Keratin, type I cuticular Ha1
Q30167	266	30.0	7.75	0.373	HLA class II histocompatibility antigen, DRB1-10 beta chain
B7Z269	351	40.3	7.24	0.299	cDNA FLJ50754, highly similar to Voltage-dependent L-type calcium channel subunit alpha-1D
A0JNT2	**447**	**49.6**	**5.39**	**0.240**	**KRT83 protein**
A0A087X2I6	**404**	**46.1**	**4.84**	**0.206**	**Keratin, type I cuticular Ha3-II**
O76013	467	52.2	4.94	0.144	Keratin, type I cuticular Ha6
Q701L7	513	56.6	6.74	0.073	Type II hair keratin 2
Q9BYT5	123	12.9	7.81	0.072	Keratin-associated protein 2-2

Table 5. Differentially expressed genes in lung biopsies post CBP with collapsed lungs (Collapsed) versus post CBP+LFV (LFV).

The data shows the genes that were significantly changed post-surgery comparing the LFV and CPB with lungs collapsed groups. Data are organised by ratio of gene expression in the CPB:LFV groups. Also shown are the p-values and ratios for the same genes in the CPB and LFV groups pre- and post-surgery.

Gene	*p-value Collapsed vs. LFV)*	*Ratio (Collapsed vs. LFV)*	*p-value (Collapsed post vs. Collapsed pre)*	*Ratio (Collapsed post vs. Collapsed pre)*	*p-value (LFV post vs. LFV pre)*	*Ratio (LFV post vs. LFV pre)*
HLA-DRB5	0.0311729	1.69779				
MIR21	0.00716334	0.664162	0.00026313	1.76523	3.13E-08	2.5143
PLAU	0.00027089	0.663153	9.09E-05	1.56036	3.92E-10	2.18467
NAMPT	0.00887185	0.653954	2.76E-08	2.69011	7.02E-14	4.38552
CRISPLD2	0.0245826	0.65374	0.00011915	2.12754	2.77E-08	3.19182
SPSB1	0.00543046	0.652837	0.0011272	1.65691	3.46E-08	2.51871
PIM1	0.00237397	0.643988	4.81E-07	2.172	1.77E-11	3.07144
MT2A	0.0212365	0.64331	1.58E-05	2.3859	9.45E-11	4.18274
CYR61	0.0334855	0.642119	0.00013919	2.28028	1.35E-05	2.60616
PTX3	3.35E-05	0.633302	0.0140338	1.29593	3.50E-09	2.00809
NFIL3	0.00061884	0.630321	5.29E-08	2.19547	4.68E-14	3.38138
C13ORF33	4.01E-06	0.629229	0.00088378	1.3788	9.54E-13	2.24342

PTGS2	0.00877579	0.627638	2.02E-07	2.71364	1.89E-10	3.63922
OBFC2A	0.00039958	0.619068	0.00020414	1.65775	1.34E-09	2.46718
SERPINB2	6.89E-05	0.604865	0.00229441	1.45598	4.19E-10	2.37424
FST	3.24E-07	0.604399	0.0263664	1.22358	1.07E-09	1.87432
TRK1	9.80E-05	0.598732	0.0259384	1.32595	3.25E-08	2.16599
NNMT	0.00050317	0.598371	0.00555558	1.49559	2.12E-10	2.85178
IER3	0.00213579	0.585514	5.24E-10	3.36618	3.45E-14	4.95907
TRQ1	1.05E-06	0.575413	0.00924457	1.3179	3.91E-10	2.12356
ADAMTS1	0.00128987	0.560691	3.20E-07	2.65546	9.20E-13	4.52339
CCL2	0.00088664	0.560328	3.14E-11	3.7367	1.56E-17	6.7442
CCL8	8.14E-06	0.537271	0.00033771	1.62543	2.39E-12	2.99664
ALDH1A3	0.00014072	0.498751	0.00342271	1.68698	3.40E-09	3.22296
IL6	0.00081229	0.481974	4.20E-07	3.20897	2.66E-13	6.59224
THBS1	0.00091702	0.470781	4.31E-05	2.58619	2.69E-10	4.99284

Table 6:

Genes significantly altered in the combined CPB with collapsed lungs and LFV dataset (all patients) comparing biopsies taken before and immediately post-surgery (prior to reperfusion).

Probeset ID	p-value	Fold-Change (Post vs. Pre)	Fold-Change (Post vs. Pre)
ADAMTS1	2.29E-14	3.46579	Post up vs Pre
ALDH1A3	2.06E-08	2.33175	Post up vs Pre
AXUD1	7.62E-16	3.42288	Post up vs Pre
BHLHB2	1.27E-13	2.47507	Post up vs Pre
CCL2	5.10E-20	5.02006	Post up vs Pre
CCL8	9.21E-11	2.20699	Post up vs Pre
CDKN1A	2.13E-16	2.96273	Post up vs Pre
CEBPD	1.48E-12	2.29829	Post up vs Pre
CHSY1	2.26E-09	2.15588	Post up vs Pre
CRISPLD2	6.38E-10	2.6059	Post up vs Pre
CXCL2	3.47E-13	2.47755	Post up vs Pre
CYR61	9.06E-08	2.43778	Post up vs Pre
DUSP1	7.63E-07	2.21634	Post up vs Pre
DUSP5	1.01E-14	2.45719	Post up vs Pre
EGR1	6.78E-17	4.57514	Post up vs Pre
EGR3	1.29E-13	2.28143	Post up vs Pre
ELL2	9.39E-10	2.13515	Post up vs Pre
ERRFI1	7.92E-10	2.21222	Post up vs Pre
FOS	3.79E-09	2.19214	Post up vs Pre
FOSB	9.80E-10	3.04051	Post up vs Pre
FOSL2	1.28E-13	2.11261	Post up vs Pre

GADD45A	1.46E-14	2.10184	Post up vs Pre
GADD45B	4.21E-15	3.11502	Post up vs Pre
IER3	3.18E-17	4.08572	Post up vs Pre
IL6	1.54E-14	4.59938	Post up vs Pre
IL8	1.49E-11	2.60548	Post up vs Pre
LOC441019	4.99E-12	2.27893	Post up vs Pre
MIDN	5.01E-10	2.20029	Post up vs Pre
MIR21	2.24E-09	2.10673	Post up vs Pre
MT1A	4.47E-10	2.90963	Post up vs Pre
MT2A	2.60E-12	3.15905	Post up vs Pre
MTE	1.97E-09	2.35834	Post up vs Pre
MYC	1.82E-15	2.81434	Post up vs Pre
NAMPT	2.56E-16	3.43475	Post up vs Pre
NFIL3	1.39E-15	2.72465	Post up vs Pre
NNMT	3.81E-09	2.06521	Post up vs Pre
NR4A2	3.74E-14	2.77506	Post up vs Pre
NR4A3	5.09E-14	2.28338	Post up vs Pre
OBFC2A	7.07E-10	2.02236	Post up vs Pre
PIM1	1.76E-13	2.58286	Post up vs Pre
PTGS2	2.79E-13	3.14254	Post up vs Pre
RASD1	5.52E-07	2.12328	Post up vs Pre
RGS2	2.93E-14	2.93902	Post up vs Pre
RNF122	3.02E-12	2.34752	Post up vs Pre
SGK	9.65E-07	2.07768	Post up vs Pre
SIK1	4.42E-15	2.59714	Post up vs Pre
SLC2A3	8.98E-13	2.32146	Post up vs Pre
SPSB1	9.27E-09	2.04286	Post up vs Pre

THBS1	4.71E-11	3.59339	Post up vs Pre
TRIB1	3.44E-08	2.15623	Post up vs Pre
ZFP36	1.56E-17	3.79832	Post up vs Pre

Table 7:

Data showing the proteins changed between the pooled control CPB with collapsed lung and LFV groups immediately prior to surgery, with a 1.5x change cutoff. Only 2 proteins had a greater than 2x increase in the CPB group and 34 were 2x higher in the LFV group (shown in bold).

Accession	# AAs	MW [kDa]	calc. pI	Collapsed (Pre)/ LFV (Pre)	Description
Q15423	**64**	**7.1**	**8.18**	**4.664**	**Serum amyloid A protein (Fragment) OS=Homo sapiens PE=2 SV=1 - [Q15423_HUMAN]**
B7Z269	**351**	**40.3**	**7.24**	**3.939**	**cDNA FLJ50754, highly similar to Voltage-dependent L-type calcium channel subunit alpha-1D OS=Homo sapiens PE=2 SV=1 - [B7Z269_HUMAN]**
Q6P4A8	553	63.2	9.06	1.677	Phospholipase B-like 1 OS=Homo sapiens GN=PLBD1 PE=1 SV=2 - [PLBL1_HUMAN]
O96009	420	45.4	6.61	1.507	Napsin-A OS=Homo sapiens GN=NAPSA PE=1 SV=1 - [NAPSA_HUMAN]
F2X0V0	23	2.8	7.78	0.666	Truncated CD61 (Fragment) OS=Homo sapiens GN=ITGB3 PE=4 SV=1 - [F2X0V0_HUMAN]
Q96T46	76	8.4	7.14	0.666	Hemoglobin alpha 2 (Fragment) OS=Homo sapiens GN=HBA2 PE=3 SV=1 - [Q96T46_HUMAN]
Q96P70	1041	115.9	4.81	0.665	Importin-9 OS=Homo sapiens GN=IPO9 PE=1 SV=3 - [IPO9_HUMAN]
Q86Z07	374	41.7	9.14	0.664	Guanine nucleotide binding protein-like 1 OS=Homo sapiens GN=HSR1 PE=4 SV=1 - [Q86Z07_HUMAN]
Q9NWH4	148	16.9	11.09	0.664	cDNA FLJ10024 fis, clone HEMBA1000636 OS=Homo sapiens PE=2 SV=1 - [Q9NWH4_HUMAN]
Q7Z379	478	51.6	6.52	0.664	Putative uncharacterized protein DKFZp686K04218 (Fragment) OS=Homo sapiens GN=DKFZp686K04218 PE=1 SV=1 - [Q7Z379_HUMAN]
B4E0V3	947	107.2	6.11	0.663	cDNA FLJ61519, highly similar to Leukocyte common antigen (EC 3.1.3.48) OS=Homo sapiens PE=2 SV=1 - [B4E0V3_HUMAN]
P32456	591	67.2	5.71	0.661	Interferon-induced guanylate-binding protein 2 OS=Homo sapiens GN=GBP2 PE=1 SV=3 - [GBP2_HUMAN]
Q0PNF2	2570	275.3	6.49	0.661	FEX1 OS=Homo sapiens PE=2 SV=1 - [Q0PNF2_HUMAN]

Q5VW33	215	24.2	7.09	0.660	BRO1 domain-containing protein BROX (Fragment) OS=Homo sapiens GN=BROX PE=1 SV=1 - [Q5VW33_HUMAN]
A2MYC8	104	11.0	7.28	0.659	V5-2 protein (Fragment) OS=Homo sapiens GN=V5-2 PE=1 SV=1 - [A2MYC8_HUMAN]
F8WD82	762	88.1	6.95	0.659	Sodium channel protein type 7 subunit alpha OS=Homo sapiens GN=SCN7A PE=4 SV=1 - [F8WD82_HUMAN]
B2R4C9	102	11.2	9.52	0.659	cDNA, FLJ92044, highly similar to Homo sapiens death-associated protein (DAP), mRNA OS=Homo sapiens PE=2 SV=1 - [B2R4C9_HUMAN]
A8K6V3	1217	135.5	5.21	0.659	cDNA FLJ78677, highly similar to Homo sapiens splicing factor 3b, subunit 3, 130kDa (SF3B3), mRNA OS=Homo sapiens PE=2 SV=1 - [A8K6V3_HUMAN]
S6B2A1	184	20.4	5.52	0.658	IgG L chain OS=Homo sapiens PE=2 SV=1 - [S6B2A1_HUMAN]
Q9H3P7	528	60.6	5.06	0.658	Golgi resident protein GCP60 OS=Homo sapiens GN=ACBD3 PE=1 SV=4 - [GCP60_HUMAN]
C9JIN6	264	29.8	7.84	0.657	Transporter (Fragment) OS=Homo sapiens GN=SLC6A20 PE=3 SV=1 - [C9JIN6_HUMAN]
E5RHW5	125	13.1	5.39	0.657	Pulmonary surfactant-associated protein C (Fragment) OS=Homo sapiens GN=SFTPC PE=4 SV=3 - [E5RHW5_HUMAN]
F8WAW4	140	15.6	9.13	0.656	Enoyl-CoA delta isomerase 2, mitochondrial OS=Homo sapiens GN=ECI2 PE=1 SV=1 - [F8WAW4_HUMAN]
B8ZZ75	194	21.5	6.93	0.655	Aldose 1-epimerase OS=Homo sapiens GN=GALM PE=1 SV=1 - [B8ZZ75_HUMAN]
H3BML9	118	13.1	5.68	0.655	Myosin regulatory light chain 2, skeletal muscle isoform (Fragment) OS=Homo sapiens GN=MYLPF PE=4 SV=1 - [H3BML9_HUMAN]
P16157	1881	206.1	6.01	0.655	Ankyrin-1 OS=Homo sapiens GN=ANK1 PE=1 SV=3 - [ANK1_HUMAN]
A0A087WXZ6	250	28.9	9.00	0.655	High affinity immunoglobulin gamma Fc receptor IB (Fragment) OS=Homo sapiens GN=FCGR1B PE=4 SV=1 - [A0A087WXZ6_HUMAN]
P31942	346	36.9	6.87	0.654	Heterogeneous nuclear ribonucleoprotein H3 OS=Homo sapiens GN=HNRNPH3 PE=1 SV=2 - [HNRH3_HUMAN]
P40261	264	29.6	5.74	0.654	Nicotinamide N-methyltransferase OS=Homo sapiens GN=NNMT PE=1 SV=1 - [NNMT_HUMAN]
P15529	392	43.7	6.74	0.654	Membrane cofactor protein OS=Homo sapiens GN=CD46 PE=1 SV=3 - [MCP_HUMAN]
G3XAJ6	542	58.7	5.34	0.653	Raft-linking protein, isoform CRA_c OS=Homo sapiens GN=RFTN1 PE=1 SV=1 - [G3XAJ6_HUMAN]
H7BZW6	143	16.0	9.13	0.652	Histone deacetylase complex subunit SAP18 (Fragment) OS=Homo sapiens

					GN=SAP18 PE=1 SV=2 - [H7BZW6_HUMAN]
P19397	219	24.3	7.52	0.652	Leukocyte surface antigen CD53 OS=Homo sapiens GN=CD53 PE=1 SV=1 - [CD53_HUMAN]
Q9C055	306	35.6	7.50	0.652	Inositol polyphosphate-5-phosphatase (Fragment) OS=Homo sapiens GN=INPP5A PE=4 SV=1 - [Q9C055_HUMAN]
P16402	221	22.3	11.02	0.651	Histone H1.3 OS=Homo sapiens GN=HIST1H1D PE=1 SV=2 - [H13_HUMAN]
P01023	1474	163.2	6.46	0.650	Alpha-2-macroglobulin OS=Homo sapiens GN=A2M PE=1 SV=3 - [A2MG_HUMAN]
Q19UK3	33	3.7	8.09	0.648	Truncated coagulation factor IX (Fragment) OS=Homo sapiens GN=F9 PE=4 SV=1 - [Q19UK3_HUMAN]
Q59FC4	687	75.9	6.51	0.648	Presynaptic protein SAP97 variant (Fragment) OS=Homo sapiens PE=4 SV=1 - [Q59FC4_HUMAN]
Q15661	275	30.5	7.11	0.647	Tryptase alpha/beta-1 OS=Homo sapiens GN=TPSAB1 PE=1 SV=1 - [TRYB1_HUMAN]
D3JV43	68	7.4	8.78	0.646	C-X-C motif chemokine (Fragment) OS=Homo sapiens PE=3 SV=1 - [D3JV43_HUMAN]
H0YH87	916	98.1	9.41	0.639	Ataxin-2 (Fragment) OS=Homo sapiens GN=ATXN2 PE=1 SV=1 - [H0YH87_HUMAN]
B7Z7P4	547	59.9	5.59	0.639	cDNA FLJ53627, highly similar to Antigen peptide transporter 1 OS=Homo sapiens PE=2 SV=1 - [B7Z7P4_HUMAN]
P13761	266	29.8	7.44	0.638	HLA class II histocompatibility antigen, DRB1-7 beta chain OS=Homo sapiens GN=HLA-DRB1 PE=1 SV=1 - [2B17_HUMAN]
B7Z539	645	72.1	7.68	0.637	cDNA FLJ56954, highly similar to Inter-alpha-trypsin inhibitor heavy chain H1 OS=Homo sapiens PE=2 SV=1 - [B7Z539_HUMAN]
H7C034	173	19.3	4.88	0.636	AP-1 complex subunit beta-1 (Fragment) OS=Homo sapiens GN=AP1B1 PE=1 SV=1 - [H7C034_HUMAN]
A8K2T4	843	93.3	6.51	0.636	cDNA FLJ78207, highly similar to Human complement protein component C7 mRNA OS=Homo sapiens PE=2 SV=1 - [A8K2T4_HUMAN]
Q9UL88	131	14.1	9.63	0.636	Myosin-reactive immunoglobulin heavy chain variable region (Fragment) OS=Homo sapiens PE=2 SV=1 - [Q9UL88_HUMAN]
P23381	471	53.1	6.23	0.636	Tryptophan--tRNA ligase, cytoplasmic OS=Homo sapiens GN=WARS PE=1 SV=2 - [SYWC_HUMAN]
E9PC44	393	43.9	6.15	0.635	Protein transport protein Sec24D OS=Homo sapiens GN=SEC24D PE=1 SV=2 - [E9PC44_HUMAN]
O76013	467	52.2	4.94	0.634	Keratin, type I cuticular Ha6 OS=Homo sapiens GN=KRT36 PE=1 SV=1 -

					[KRT36_HUMAN]
B4DM28	634	72.1	9.67	0.633	cDNA FLJ50575, highly similar to U4/U6 small nuclear ribonucleoprotein Prp3 OS=Homo sapiens PE=2 SV=1 - [B4DM28_HUMAN]
M0R088	681	78.1	12.06	0.633	Serine/arginine repetitive matrix protein 1 (Fragment) OS=Homo sapiens GN=SRRM1 PE=1 SV=1 - [M0R088_HUMAN]
E3Q1J2	273	31.6	5.97	0.633	MHC class I antigen (Fragment) OS=Homo sapiens GN=HLA-B PE=3 SV=1 - [E3Q1J2_HUMAN]
Q5JTB5	87	9.3	7.09	0.631	Placenta-specific protein 9 OS=Homo sapiens GN=PLAC9 PE=4 SV=1 - [Q5JTB5_HUMAN]
Q5CZ93	159	19.2	9.88	0.630	Putative uncharacterized protein DKFZp686A0568 OS=Homo sapiens GN=DKFZp686A0568 PE=2 SV=1 - [Q5CZ93_HUMAN]
P33764	101	11.7	4.78	0.628	Protein S100-A3 OS=Homo sapiens GN=S100A3 PE=1 SV=1 - [S10A3_HUMAN]
Q6GMX6	465	51.1	8.69	0.628	IGH@ protein OS=Homo sapiens GN=IGH@ PE=1 SV=1 - [Q6GMX6_HUMAN]
Q9P2B2	879	98.5	6.61	0.628	Prostaglandin F2 receptor negative regulator OS=Homo sapiens GN=PTGFRN PE=1 SV=2 - [FPRP_HUMAN]
Q15323	416	47.2	4.88	0.627	Keratin, type I cuticular Ha1 OS=Homo sapiens GN=KRT31 PE=2 SV=3 - [K1H1_HUMAN]
H0YA93	1400	158.1	5.82	0.625	NEDD4-binding protein 2 (Fragment) OS=Homo sapiens GN=N4BP2 PE=1 SV=1 - [H0YA93_HUMAN]
A5Z217	470	53.6	5.27	0.623	Mutant desmin OS=Homo sapiens PE=2 SV=1 - [A5Z217_HUMAN]
K7EMQ9	140	16.3	6.89	0.622	Eukaryotic translation initiation factor 3 subunit K (Fragment) OS=Homo sapiens GN=EIF3K PE=1 SV=1 - [K7EMQ9_HUMAN]
A0A024RAL1	2409	264.9	4.54	0.620	Chondroitin sulfate proteoglycan 2 (Versican), isoform CRA_c OS=Homo sapiens GN=CSPG2 PE=4 SV=1 - [A0A024RAL1_HUMAN]
H3BPF7	236	25.5	8.46	0.618	Lon protease homolog 2, peroxisomal (Fragment) OS=Homo sapiens GN=LONP2 PE=4 SV=3 - [H3BPF7_HUMAN]
A0A087WUP0	265	30.0	5.34	0.617	Annexin A8-like protein 1 OS=Homo sapiens GN=ANXA8L1 PE=4 SV=1 - [A0A087WUP0_HUMAN]
A0A068LKQ0	120	13.3	5.99	0.617	Ig heavy chain variable region (Fragment) OS=Homo sapiens PE=4 SV=1 - [A0A068LKQ0_HUMAN]
Q86YQ1	91	9.7	9.25	0.614	Hemoglobin alpha-2 (Fragment) OS=Homo sapiens GN=HBA2 PE=3 SV=1 - [Q86YQ1_HUMAN]
B5MBZ8	274	31.3	4.63	0.610	Protein phosphatase 1 regulatory subunit 7 OS=Homo sapiens GN=PPP1R7 PE=1 SV=1 - [B5MBZ8_HUMAN]

Q8N1G4	583	63.4	8.28	0.609	Leucine-rich repeat-containing protein 47 OS=Homo sapiens GN=LRRC47 PE=1 SV=1 - [LRC47_HUMAN]
O15078	2479	290.2	5.95	0.609	Centrosomal protein of 290 kDa OS=Homo sapiens GN=CEP290 PE=1 SV=2 - [CE290_HUMAN]
Q9BXN1	380	43.4	7.08	0.608	Asporin OS=Homo sapiens GN=ASPN PE=1 SV=2 - [ASPN_HUMAN]
C0IMJ3	781	87.2	7.94	0.604	Periostin isoform thy6 OS=Homo sapiens PE=2 SV=1 - [C0IMJ3_HUMAN]
B7ZMG8	83	9.1	4.59	0.602	Uncharacterized protein OS=Homo sapiens PE=2 SV=1 - [B7ZMG8_HUMAN]
E9PQ22	191	22.9	9.45	0.602	Uncharacterized protein C11orf65 (Fragment) OS=Homo sapiens GN=C11orf65 PE=4 SV=3 - [E9PQ22_HUMAN]
Q5CZB5	1157	125.0	4.49	0.601	Putative uncharacterized protein DKFZp686M0430 OS=Homo sapiens GN=DKFZp686M0430 PE=2 SV=1 - [Q5CZB5_HUMAN]
E9PQI8	164	17.5	11.17	0.600	U4/U6.U5 tri-snRNP-associated protein 1 OS=Homo sapiens GN=SART1 PE=1 SV=1 - [E9PQI8_HUMAN]
P19075	237	26.0	5.60	0.600	Tetraspanin-8 OS=Homo sapiens GN=TSPAN8 PE=1 SV=1 - [TSN8_HUMAN]
B4DSW4	157	16.4	12.25	0.598	cDNA FLJ51541, moderately similar to Transcription factor Sp8 OS=Homo sapiens PE=2 SV=1 - [B4DSW4_HUMAN]
P31146	461	51.0	6.68	0.597	Coronin-1A OS=Homo sapiens GN=CORO1A PE=1 SV=4 - [COR1A_HUMAN]
Q0KKI6	219	24.0	8.06	0.593	Immunoblobulin light chain (Fragment) OS=Homo sapiens PE=1 SV=1 - [Q0KKI6_HUMAN]
P01623	109	11.7	8.91	0.593	Ig kappa chain V-III region WOL OS=Homo sapiens PE=1 SV=1 - [KV305_HUMAN]
P08311	255	28.8	11.19	0.593	Cathepsin G OS=Homo sapiens GN=CTSG PE=1 SV=2 - [CATG_HUMAN]
P01598	108	11.8	8.44	0.592	Ig kappa chain V-I region EU OS=Homo sapiens PE=1 SV=1 - [KV106_HUMAN]
Q6P3R8	708	81.4	8.87	0.592	Serine/threonine-protein kinase Nek5 OS=Homo sapiens GN=NEK5 PE=1 SV=1 - [NEK5_HUMAN]
Q4QZC0	273	31.8	6.09	0.592	MHC class I antigen (Fragment) OS=Homo sapiens GN=HLA-A PE=3 SV=1 - [Q4QZC0_HUMAN]
C9JW69	372	39.6	8.37	0.591	Regulator of chromosome condensation (Fragment) OS=Homo sapiens GN=RCC1 PE=1 SV=1 - [C9JW69_HUMAN]
P10109	184	19.4	5.83	0.591	Adrenodoxin, mitochondrial OS=Homo sapiens GN=FDX1 PE=1 SV=1 - [ADX_HUMAN]
A0A075B785	1018	112.7	5.49	0.591	LisH domain and HEAT repeat-containing protein KIAA1468 OS=Homo sapiens GN=KIAA1468 PE=1 SV=2 - [A0A075B785_HUMAN]
K7ERI9	77	8.6	6.71	0.590	Truncated apolipoprotein C-I (Fragment) OS=Homo sapiens GN=APOC1 PE=4

					SV=1 - [K7ERI9_HUMAN]
P01833	764	83.2	5.74	0.589	Polymeric immunoglobulin receptor OS=Homo sapiens GN=PIGR PE=1 SV=4 - [PIGR_HUMAN]
P62854	115	13.0	11.00	0.587	40S ribosomal protein S26 OS=Homo sapiens GN=RPS26 PE=1 SV=3 - [RS26_HUMAN]
B4E1L5	555	63.8	6.37	0.585	cDNA FLJ51601, highly similar to Interferon-induced guanylate-binding protein 1 OS=Homo sapiens PE=2 SV=1 - [B4E1L5_HUMAN]
Q9HCM7	1045	110.8	9.67	0.585	Fibrosin-1-like protein OS=Homo sapiens GN=FBRSL1 PE=1 SV=4 - [FBSL_HUMAN]
P01611	108	11.6	7.28	0.581	Ig kappa chain V-I region Wes OS=Homo sapiens PE=1 SV=1 - [KV119_HUMAN]
B4DRW1	474	51.7	6.81	0.576	cDNA FLJ55805, highly similar to Keratin, type II cytoskeletal 4 OS=Homo sapiens PE=2 SV=1 - [B4DRW1_HUMAN]
J3KPM9	714	83.3	6.42	0.574	Signal transducer and activator of transcription OS=Homo sapiens GN=STAT1 PE=1 SV=1 - [J3KPM9_HUMAN]
Q8N1W1	1705	191.8	6.04	0.573	Rho guanine nucleotide exchange factor 28 OS=Homo sapiens GN=ARHGEF28 PE=1 SV=3 - [ARG28_HUMAN]
P23946	247	27.3	9.29	0.573	Chymase OS=Homo sapiens GN=CMA1 PE=1 SV=1 - [CMA1_HUMAN]
Q7L0Q8	258	28.2	8.06	0.572	Rho-related GTP-binding protein RhoU OS=Homo sapiens GN=RHOU PE=1 SV=1 - [RHOU_HUMAN]
O75443	2155	239.4	5.40	0.569	Alpha-tectorin OS=Homo sapiens GN=TECTA PE=1 SV=3 - [TECTA_HUMAN]
A0A087WZW8	233	25.6	6.01	0.569	Protein IGKV3-11 OS=Homo sapiens GN=IGKV3-11 PE=4 SV=1 - [A0A087WZW8_HUMAN]
A0A087WX11	918	103.3	5.12	0.565	Folliculin-interacting protein 1 OS=Homo sapiens GN=FNIP1 PE=4 SV=1 - [A0A087WX11_HUMAN]
Q9H029	130	14.8	5.30	0.564	GTP-binding protein SAR1b OS=Homo sapiens GN=DKFZp434B2017 PE=1 SV=1 - [Q9H029_HUMAN]
H0YD72	237	26.1	9.39	0.563	Liprin-alpha-1 (Fragment) OS=Homo sapiens GN=PPFIA1 PE=1 SV=1 - [H0YD72_HUMAN]
Q5NV82	104	11.1	7.97	0.562	V4-2 protein (Fragment) OS=Homo sapiens GN=V4-2 PE=1 SV=1 - [Q5NV82_HUMAN]
H3BRW3	109	11.7	9.96	0.562	FAD-linked sulfhydryl oxidase ALR OS=Homo sapiens GN=GFER PE=1 SV=1 - [H3BRW3_HUMAN]
P02452	1464	138.9	5.80	0.555	Collagen alpha-1(I) chain OS=Homo sapiens GN=COL1A1 PE=1 SV=5 - [CO1A1_HUMAN]

B2R9B9	120	13.0	6.37	0.551	cDNA, FLJ94321, highly similar to Homo sapiens eukaryotic translation initiation factor 4E binding protein 2 (EIF4EBP2), mRNA OS=Homo sapiens PE=2 SV=1 - [B2R9B9_HUMAN]
Q9UK54	128	14.0	6.95	0.547	Hemoglobin beta subunit variant (Fragment) OS=Homo sapiens GN=HBB PE=2 SV=1 - [Q9UK54_HUMAN]
P81605	110	11.3	6.54	0.547	Dermcidin OS=Homo sapiens GN=DCD PE=1 SV=2 - [DCD_HUMAN]
Q05707	1796	193.4	5.30	0.547	Collagen alpha-1(XIV) chain OS=Homo sapiens GN=COL14A1 PE=1 SV=3 - [COEA1_HUMAN]
C9JA05	70	8.2	8.56	0.547	Immunoglobulin J chain (Fragment) OS=Homo sapiens GN=IGJ PE=1 SV=1 - [C9JA05_HUMAN]
S6C4R7	212	22.5	8.24	0.546	IgG L chain OS=Homo sapiens PE=2 SV=1 - [S6C4R7_HUMAN]
P01861	327	35.9	7.36	0.541	Ig gamma-4 chain C region OS=Homo sapiens GN=IGHG4 PE=1 SV=1 - [IGHG4_HUMAN]
B2R7Z6	484	52.5	7.55	0.539	cDNA, FLJ93674 OS=Homo sapiens PE=2 SV=1 - [B2R7Z6_HUMAN]
Q9NZ09	502	55.0	5.11	0.532	Ubiquitin-associated protein 1 OS=Homo sapiens GN=UBAP1 PE=1 SV=1 - [UBAP1_HUMAN]
Q64FY1	1364	146.2	6.60	0.530	AKNA transcript B1 (Fragment) OS=Homo sapiens GN=AKNA PE=2 SV=1 - [Q64FY1_HUMAN]
M0QZ50	93	9.8	4.48	0.526	Microtubule-associated protein 1S OS=Homo sapiens GN=MAP1S PE=1 SV=1 - [M0QZ50_HUMAN]
B4DQY2	711	78.9	7.06	0.525	cDNA FLJ59388, highly similar to Mitochondrial inner membrane protein OS=Homo sapiens PE=2 SV=1 - [B4DQY2_HUMAN]
B4DEH8	168	19.0	9.23	0.516	Polyadenylate-binding protein 2 OS=Homo sapiens GN=PABPN1 PE=1 SV=1 - [B4DEH8_HUMAN]
D6RC64	136	15.6	10.14	0.513	SH3 domain-binding protein 2 (Fragment) OS=Homo sapiens GN=SH3BP2 PE=4 SV=1 - [D6RC64_HUMAN]
Q6N095	475	52.3	8.57	0.511	Putative uncharacterized protein DKFZp686K03196 OS=Homo sapiens GN=DKFZp686K03196 PE=1 SV=1 - [Q6N095_HUMAN]
B4DLF9	342	39.4	8.68	0.510	cDNA FLJ56988, highly similar to cGMP-dependent protein kinase 2 (EC 2.7.11.12) OS=Homo sapiens PE=2 SV=1 - [B4DLF9_HUMAN]
H0Y892	688	79.3	9.14	0.508	Zinc finger protein 782 (Fragment) OS=Homo sapiens GN=ZNF782 PE=4 SV=1 - [H0Y892_HUMAN]
Q4ZGM8	100	10.8	9.04	0.502	Hemoglobin alpha-2 globin mutant (Fragment) OS=Homo sapiens PE=3 SV=1 - [Q4ZGM8_HUMAN]
Q6N093	**417**	**46.0**	**7.59**	**0.497**	**Putative uncharacterized protein DKFZp686I04196 (Fragment) OS=Homo**

					sapiens GN=DKFZp686I04196 PE=1 SV=1 - [Q6N093_HUMAN]
A0A075B6L1	106	11.3	8.29	0.496	Ig lambda-7 chain C region (Fragment) OS=Homo sapiens GN=IGLC7 PE=4 SV=2 - [A0A075B6L1_HUMAN]
B2R941	417	48.7	9.00	0.495	cDNA, FLJ94198, highly similar to Homo sapiens carboxypeptidase A3 (mast cell) (CPA3), mRNA OS=Homo sapiens PE=2 SV=1 - [B2R941_HUMAN]
P14555	144	16.1	9.23	0.492	Phospholipase A2, membrane associated OS=Homo sapiens GN=PLA2G2A PE=1 SV=2 - [PA2GA_HUMAN]
C9JNE5	191	21.7	9.61	0.481	Myeloid leukemia factor 1 (Fragment) OS=Homo sapiens GN=MLF1 PE=4 SV=1 - [C9JNE5_HUMAN]
Q7Z3E2	898	103.6	6.27	0.478	Coiled-coil domain-containing protein 186 OS=Homo sapiens GN=CCDC186 PE=1 SV=2 - [CC186_HUMAN]
P08519	4548	501.0	5.88	0.474	Apolipoprotein(a) OS=Homo sapiens GN=LPA PE=1 SV=1 - [APOA_HUMAN]
Q7L7X3	1001	116.0	7.65	0.468	Serine/threonine-protein kinase TAO1 OS=Homo sapiens GN=TAOK1 PE=1 SV=1 - [TAOK1_HUMAN]
B2R8C8	140	15.1	5.26	0.461	Ubiquitin-like protein ATG12 OS=Homo sapiens PE=2 SV=1 - [B2R8C8_HUMAN]
B7Z962	190	19.9	10.84	0.461	cDNA FLJ52231 OS=Homo sapiens PE=2 SV=1 - [B7Z962_HUMAN]
F8W9J4	7461	847.4	5.25	0.457	Dystonin OS=Homo sapiens GN=DST PE=1 SV=1 - [F8W9J4_HUMAN]
Q5T4S7	5183	573.5	6.04	0.450	E3 ubiquitin-protein ligase UBR4 OS=Homo sapiens GN=UBR4 PE=1 SV=1 - [UBR4_HUMAN]
B0QYR0	100	11.1	5.36	0.447	BTB/POZ domain-containing protein 3 (Fragment) OS=Homo sapiens GN=BTBD3 PE=4 SV=3 - [B0QYR0_HUMAN]
Q3MI39	167	16.7	9.70	0.447	HNRPA1 protein (Fragment) OS=Homo sapiens GN=HNRPA1 PE=2 SV=1 - [Q3MI39_HUMAN]
Q701L7	513	56.6	6.74	0.430	Type II hair keratin 2 OS=Homo sapiens GN=KRTHB2 PE=2 SV=1 - [Q701L7_HUMAN]
P01880	384	42.2	7.93	0.404	Ig delta chain C region OS=Homo sapiens GN=IGHD PE=1 SV=2 - [IGHD_HUMAN]
B3KMX3	270	28.5	4.73	0.398	cDNA FLJ12857 fis, clone NT2RP2003513, highly similar to Homo sapiens paralemmin (PALM), transcript variant 2, mRNA OS=Homo sapiens PE=2 SV=1 - [B3KMX3_HUMAN]
Q9BYT5	123	12.9	7.81	0.397	Keratin-associated protein 2-2 OS=Homo sapiens GN=KRTAP2-2 PE=2 SV=3 - [KRA22_HUMAN]
P46109	303	33.8	6.74	0.388	Crk-like protein OS=Homo sapiens GN=CRKL PE=1 SV=1 - [CRKL_HUMAN]
H7BZ55	2252	248.2	5.83	0.386	Putative ciliary rootlet coiled-coil protein-like 3 protein OS=Homo sapiens PE=5

					SV=2 - [CROL3_HUMAN]
Q5RHS7	95	11.0	9.28	0.379	Protein S100-A2 OS=Homo sapiens GN=S100A2 PE=1 SV=2 - [Q5RHS7_HUMAN]
Q05D28	370	41.8	5.44	0.377	CCDC91 protein (Fragment) OS=Homo sapiens GN=CCDC91 PE=2 SV=1 - [Q05D28_HUMAN]
B3KS56	594	68.5	5.45	0.376	cDNA FLJ35559 fis, clone SPLEN2005009, highly similar to GRIP and coiled-coil domain-containing protein 1 OS=Homo sapiens PE=2 SV=1 - [B3KS56_HUMAN]
H0UI60	536	60.7	5.17	0.369	Taxilin beta, isoform CRA_a OS=Homo sapiens GN=TXLNB PE=4 SV=1 - [H0UI60_HUMAN]
Q30167	266	30.0	7.75	0.357	HLA class II histocompatibility antigen, DRB1-10 beta chain OS=Homo sapiens GN=HLA-DRB1 PE=1 SV=2 - [2B1A_HUMAN]
A4FU00	317	35.6	5.81	0.351	SYT2 protein (Fragment) OS=Homo sapiens GN=SYT2 PE=2 SV=1 - [A4FU00_HUMAN]
B4E1L4	668	71.6	5.63	0.347	cDNA FLJ59081, highly similar to Mucin-5B OS=Homo sapiens PE=2 SV=1 - [B4E1L4_HUMAN]
Q69YL0	99	10.9	12.00	0.337	Uncharacterized protein NCBP2-AS2 OS=Homo sapiens GN=NCBP2-AS2 PE=4 SV=1 - [NCAS2_HUMAN]
A8K9A9	638	71.3	8.22	0.334	cDNA FLJ77744, highly similar to Homo sapiens kallikrein B, plasma (Fletcher factor) 1 (KLKB1), mRNA OS=Homo sapiens PE=2 SV=1 - [A8K9A9_HUMAN]
A2J1N5	94	10.4	9.13	0.306	Rheumatoid factor RF-ET6 (Fragment) OS=Homo sapiens PE=2 SV=1 - [A2J1N5_HUMAN]
Q6PII6	533	58.3	4.77	0.288	TMF1 protein (Fragment) OS=Homo sapiens GN=TMF1 PE=2 SV=1 - [Q6PII6_HUMAN]
A0A087X243	69	7.4	7.08	0.286	Glutathione S-transferase P (Fragment) OS=Homo sapiens GN=GSTP1 PE=4 SV=1 - [A0A087X243_HUMAN]
O76041	1014	116.4	7.99	0.275	Nebulette OS=Homo sapiens GN=NEBL PE=1 SV=1 - [NEBL_HUMAN]
B4DMJ5	242	27.3	4.50	0.118	cDNA FLJ53012, highly similar to Tubulin beta-7 chain OS=Homo sapiens PE=2 SV=1 - [B4DMJ5_HUMAN]

Table 8:

Proteins changed post surgery in the control CPB with collapsed lung group, with a 1.5x cutoff. Proteins with a >2x change following surgery are in bold.

Accession	# AAs	MW [kDa]	calc. pI	Collapsed (Post)/ Collapsed (Pre)	Description
B4DMJ5	242	27.3	4.50	8.276	cDNA FLJ53012, highly similar to Tubulin beta-7 chain OS=Homo sapiens PE=2 SV=1 - [B4DMJ5_HUMAN]
A0A087X243	69	7.4	7.08	3.627	Glutathione S-transferase P (Fragment) OS=Homo sapiens GN=GSTP1 PE=4 SV=1 - [A0A087X243_HUMAN]
Q69YL0	99	10.9	12.00	3.266	Uncharacterized protein NCBP2-AS2 OS=Homo sapiens GN=NCBP2-AS2 PE=4 SV=1 - [NCAS2_HUMAN]
A4FU00	317	35.6	5.81	2.985	SYT2 protein (Fragment) OS=Homo sapiens GN=SYT2 PE=2 SV=1 - [A4FU00_HUMAN]
B4DIF5	345	39.2	8.92	2.960	cDNA FLJ55687, highly similar to Cell cycle control protein 50A OS=Homo sapiens PE=2 SV=1 - [B4DIF5_HUMAN]
H0UI60	536	60.7	5.17	2.740	Taxilin beta, isoform CRA_a OS=Homo sapiens GN=TXLNB PE=4 SV=1 - [H0UI60_HUMAN]
Q9BYT5	123	12.9	7.81	2.683	Keratin-associated protein 2-2 OS=Homo sapiens GN=KRTAP2-2 PE=2 SV=3 - [KRA22_HUMAN]
O76041	1014	116.4	7.99	2.555	Nebulette OS=Homo sapiens GN=NEBL PE=1 SV=1 - [NEBL_HUMAN]
F8W9J4	7461	847.4	5.25	2.521	Dystonin OS=Homo sapiens GN=DST PE=1 SV=1 - [F8W9J4_HUMAN]
Q701L7	513	56.6	6.74	2.519	Type II hair keratin 2 OS=Homo sapiens GN=KRTHB2 PE=2 SV=1 - [Q701L7_HUMAN]
Q6PII6	533	58.3	4.77	2.512	TMF1 protein (Fragment) OS=Homo sapiens GN=TMF1 PE=2 SV=1 - [Q6PII6_HUMAN]
A2J1N5	94	10.4	9.13	2.497	Rheumatoid factor RF-ET6 (Fragment) OS=Homo sapiens PE=2 SV=1 - [A2J1N5_HUMAN]
B7Z962	190	19.9	10.84	2.430	cDNA FLJ52231 OS=Homo sapiens PE=2 SV=1 - [B7Z962_HUMAN]
Q05D28	370	41.8	5.44	2.342	CCDC91 protein (Fragment) OS=Homo sapiens GN=CCDC91 PE=2 SV=1 - [Q05D28_HUMAN]
B3KS56	594	68.5	5.45	2.327	cDNA FLJ35559 fis, clone SPLEN2005009, highly similar to GRIP and coiled-

					coil domain-containing protein 1 OS=Homo sapiens PE=2 SV=1 - [B3KS56_HUMAN]
Q92531	187	19.7	6.32	2.313	P35-related protein (Fragment) OS=Homo sapiens GN=FCN1 PE=4 SV=1 - [Q92531_HUMAN]
H0Y892	688	79.3	9.14	2.291	Zinc finger protein 782 (Fragment) OS=Homo sapiens GN=ZNF782 PE=4 SV=1 - [H0Y892_HUMAN]
Q3MI39	167	16.7	9.70	2.287	HNRPA1 protein (Fragment) OS=Homo sapiens GN=HNRPA1 PE=2 SV=1 - [Q3MI39_HUMAN]
B2R8C8	140	15.1	5.26	2.263	Ubiquitin-like protein ATG12 OS=Homo sapiens PE=2 SV=1 - [B2R8C8_HUMAN]
Q7L7X3	1001	116.0	7.65	2.241	Serine/threonine-protein kinase TAO1 OS=Homo sapiens GN=TAOK1 PE=1 SV=1 - [TAOK1_HUMAN]
B3KMU4	481	54.5	5.08	2.107	cDNA FLJ12640 fis, clone NT2RM4001940, highly similar to Timeless homolog OS=Homo sapiens PE=2 SV=1 - [B3KMU4_HUMAN]
P14555	144	16.1	9.23	2.101	Phospholipase A2, membrane associated OS=Homo sapiens GN=PLA2G2A PE=1 SV=2 - [PA2GA_HUMAN]
B0QYR0	100	11.1	5.36	2.088	BTB/POZ domain-containing protein 3 (Fragment) OS=Homo sapiens GN=BTBD3 PE=4 SV=3 - [B0QYR0_HUMAN]
P11678	715	81.0	10.29	2.012	Eosinophil peroxidase OS=Homo sapiens GN=EPX PE=1 SV=2 - [PERE_HUMAN]
P46109	303	33.8	6.74	2.003	Crk-like protein OS=Homo sapiens GN=CRKL PE=1 SV=1 - [CRKL_HUMAN]
Q8NEY1	1877	202.3	8.07	1.998	Neuron navigator 1 OS=Homo sapiens GN=NAV1 PE=1 SV=2 - [NAV1_HUMAN]
Q0PNF2	2570	275.3	6.49	1.979	FEX1 OS=Homo sapiens PE=2 SV=1 - [Q0PNF2_HUMAN]
H0YF46	255	28.3	5.82	1.977	SPOC domain-containing protein 1 (Fragment) OS=Homo sapiens GN=SPOCD1 PE=4 SV=1 - [H0YF46_HUMAN]
Q8TBP3	101	11.8	9.92	1.941	TOP1MT protein (Fragment) OS=Homo sapiens GN=TOP1MT PE=2 SV=1 - [Q8TBP3_HUMAN]
Q05707	1796	193.4	5.30	1.917	Collagen alpha-1(XIV) chain OS=Homo sapiens GN=COL14A1 PE=1 SV=3 - [COEA1_HUMAN]
M0QZ50	93	9.8	4.48	1.907	Microtubule-associated protein 1S OS=Homo sapiens GN=MAP1S PE=1 SV=1 - [M0QZ50_HUMAN]
H7BZ55	2252	248.2	5.83	1.883	Putative ciliary rootlet coiled-coil protein-like 3 protein OS=Homo sapiens PE=5 SV=2 - [CROL3_HUMAN]
Q8N1W1	1705	191.8	6.04	1.874	Rho guanine nucleotide exchange factor 28 OS=Homo sapiens

					GN=ARHGEF28 PE=1 SV=3 - [ARG28_HUMAN]
P20851	252	28.3	5.14	1.835	C4b-binding protein beta chain OS=Homo sapiens GN=C4BPB PE=1 SV=1 - [C4BPB_HUMAN]
Q8N1G4	583	63.4	8.28	1.830	Leucine-rich repeat-containing protein 47 OS=Homo sapiens GN=LRRC47 PE=1 SV=1 - [LRC47_HUMAN]
D6RC64	136	15.6	10.14	1.819	SH3 domain-binding protein 2 (Fragment) OS=Homo sapiens GN=SH3BP2 PE=4 SV=1 - [D6RC64_HUMAN]
Q7L0Q8	258	28.2	8.06	1.811	Rho-related GTP-binding protein RhoU OS=Homo sapiens GN=RHOU PE=1 SV=1 - [RHOU_HUMAN]
H0YCG2	258	28.2	6.52	1.809	Lysosome-associated membrane glycoprotein 2 (Fragment) OS=Homo sapiens GN=LAMP2 PE=1 SV=1 - [H0YCG2_HUMAN]
Q05315	142	16.4	7.37	1.809	Galectin-10 OS=Homo sapiens GN=CLC PE=1 SV=3 - [LEG10_HUMAN]
Q6P3R8	708	81.4	8.87	1.805	Serine/threonine-protein kinase Nek5 OS=Homo sapiens GN=NEK5 PE=1 SV=1 - [NEK5_HUMAN]
Q5T4S7	5183	573.5	6.04	1.799	E3 ubiquitin-protein ligase UBR4 OS=Homo sapiens GN=UBR4 PE=1 SV=1 - [UBR4_HUMAN]
Q7Z3E2	898	103.6	6.27	1.778	Coiled-coil domain-containing protein 186 OS=Homo sapiens GN=CCDC186 PE=1 SV=2 - [CC186_HUMAN]
B4DLF9	342	39.4	8.68	1.768	cDNA FLJ56988, highly similar to cGMP-dependent protein kinase 2 (EC 2.7.11.12) OS=Homo sapiens PE=2 SV=1 - [B4DLF9_HUMAN]
P62854	115	13.0	11.00	1.742	40S ribosomal protein S26 OS=Homo sapiens GN=RPS26 PE=1 SV=3 - [RS26_HUMAN]
A0A024R637	1298	146.5	7.01	1.737	TBC1 domain family, member 4, isoform CRA_b OS=Homo sapiens GN=TBC1D4 PE=4 SV=1 - [A0A024R637_HUMAN]
Q9H029	130	14.8	5.30	1.735	GTP-binding protein SAR1b OS=Homo sapiens GN=DKFZp434B2017 PE=1 SV=1 - [Q9H029_HUMAN]
S6BGD6	235	24.8	7.24	1.733	IgG L chain OS=Homo sapiens PE=1 SV=1 - [S6BGD6_HUMAN]
Q30058	257	29.1	6.54	1.728	HLA-DP protein OS=Homo sapiens GN=HLA-DP PE=2 SV=1 - [Q30058_HUMAN]
H3BMN5	158	18.5	4.82	1.727	Calretinin (Fragment) OS=Homo sapiens GN=CALB2 PE=4 SV=2 - [H3BMN5_HUMAN]
P02452	1464	138.9	5.80	1.710	Collagen alpha-1(I) chain OS=Homo sapiens GN=COL1A1 PE=1 SV=5 - [CO1A1_HUMAN]
B2R9B9	120	13.0	6.37	1.705	cDNA, FLJ94321, highly similar to Homo sapiens eukaryotic translation initiation factor 4E binding protein 2 (EIF4EBP2), mRNA OS=Homo sapiens

					PE=2 SV=1 - [B2R9B9_HUMAN]
B4DVF1	785	87.3	6.96	1.702	cDNA FLJ51111, highly similar to Aldehyde oxidase (EC 1.2.3.1) (Fragment) OS=Homo sapiens PE=2 SV=1 - [B4DVF1_HUMAN]
P12724	160	18.4	10.02	1.692	Eosinophil cationic protein OS=Homo sapiens GN=RNASE3 PE=1 SV=2 - [ECP_HUMAN]
Q9BXN1	380	43.4	7.08	1.691	Asporin OS=Homo sapiens GN=ASPN PE=1 SV=2 - [ASPN_HUMAN]
Q9HCM7	1045	110.8	9.67	1.667	Fibrosin-1-like protein OS=Homo sapiens GN=FBRSL1 PE=1 SV=4 - [FBSL_HUMAN]
Q86UX7	667	75.9	6.98	1.660	Fermitin family homolog 3 OS=Homo sapiens GN=FERMT3 PE=1 SV=1 - [URP2_HUMAN]
Q4QZC0	273	31.8	6.09	1.654	MHC class I antigen (Fragment) OS=Homo sapiens GN=HLA-A PE=3 SV=1 - [Q4QZC0_HUMAN]
B2R6V9	732	83.2	6.00	1.638	cDNA, FLJ93141, highly similar to Homo sapiens coagulation factor XIII, A1 polypeptide (F13A1), mRNA OS=Homo sapiens PE=2 SV=1 - [B2R6V9_HUMAN]
P15529	392	43.7	6.74	1.634	Membrane cofactor protein OS=Homo sapiens GN=CD46 PE=1 SV=3 - [MCP_HUMAN]
H0YH87	916	98.1	9.41	1.633	Ataxin-2 (Fragment) OS=Homo sapiens GN=ATXN2 PE=1 SV=1 - [H0YH87_HUMAN]
P27487	766	88.2	6.04	1.628	Dipeptidyl peptidase 4 OS=Homo sapiens GN=DPP4 PE=1 SV=2 - [DPP4_HUMAN]
P08311	255	28.8	11.19	1.624	Cathepsin G OS=Homo sapiens GN=CTSG PE=1 SV=2 - [CATG_HUMAN]
O76013	467	52.2	4.94	1.624	Keratin, type I cuticular Ha6 OS=Homo sapiens GN=KRT36 PE=1 SV=1 - [KRT36_HUMAN]
A0A075B785	1018	112.7	5.49	1.610	LisH domain and HEAT repeat-containing protein KIAA1468 OS=Homo sapiens GN=KIAA1468 PE=1 SV=2 - [A0A075B785_HUMAN]
P31146	461	51.0	6.68	1.607	Coronin-1A OS=Homo sapiens GN=CORO1A PE=1 SV=4 - [COR1A_HUMAN]
P10109	184	19.4	5.83	1.604	Adrenodoxin, mitochondrial OS=Homo sapiens GN=FDX1 PE=1 SV=1 - [ADX_HUMAN]
O15078	2479	290.2	5.95	1.604	Centrosomal protein of 290 kDa OS=Homo sapiens GN=CEP290 PE=1 SV=2 - [CE290_HUMAN]
B2R4M6	114	13.2	6.13	1.604	Protein S100 OS=Homo sapiens PE=2 SV=1 - [B2R4M6_HUMAN]
A0A024RDI4	1851	203.3	6.23	1.600	Ankyrin 2, neuronal, isoform CRA_a OS=Homo sapiens GN=ANK2 PE=4 SV=1 - [A0A024RDI4_HUMAN]
Q6EVJ6	105	10.9	8.81	1.597	Peptidyl arginine deiminase type IV (Fragment) OS=Homo sapiens

					GN=PADI4 PE=4 SV=1 - [Q6EVJ6_HUMAN]
P46108	304	33.8	5.55	1.592	Adapter molecule crk OS=Homo sapiens GN=CRK PE=1 SV=2 - [CRK_HUMAN]
C9JW69	372	39.6	8.37	1.588	Regulator of chromosome condensation (Fragment) OS=Homo sapiens GN=RCC1 PE=1 SV=1 - [C9JW69_HUMAN]
P98095	1184	126.5	4.82	1.586	Fibulin-2 OS=Homo sapiens GN=FBLN2 PE=1 SV=2 - [FBLN2_HUMAN]
Q19UK3	33	3.7	8.09	1.582	Truncated coagulation factor IX (Fragment) OS=Homo sapiens GN=F9 PE=4 SV=1 - [Q19UK3_HUMAN]
F5H4Z6	171	20.0	7.84	1.581	Folate receptor beta (Fragment) OS=Homo sapiens GN=FOLR2 PE=4 SV=1 - [F5H4Z6_HUMAN]
P49913	170	19.3	9.41	1.578	Cathelicidin antimicrobial peptide OS=Homo sapiens GN=CAMP PE=1 SV=1 - [CAMP_HUMAN]
B4DSW4	157	16.4	12.25	1.578	cDNA FLJ51541, moderately similar to Transcription factor Sp8 OS=Homo sapiens PE=2 SV=1 - [B4DSW4_HUMAN]
E9PQ22	191	22.9	9.45	1.578	Uncharacterized protein C11orf65 (Fragment) OS=Homo sapiens GN=C11orf65 PE=4 SV=3 - [E9PQ22_HUMAN]
E9PC44	393	43.9	6.15	1.577	Protein transport protein Sec24D OS=Homo sapiens GN=SEC24D PE=1 SV=2 - [E9PC44_HUMAN]
B4DLX8	617	69.4	6.61	1.575	cDNA FLJ57031, highly similar to Midline-1 (EC 6.3.2.-) OS=Homo sapiens PE=2 SV=1 - [B4DLX8_HUMAN]
E9PQI8	164	17.5	11.17	1.575	U4/U6.U5 tri-snRNP-associated protein 1 OS=Homo sapiens GN=SART1 PE=1 SV=1 - [E9PQI8_HUMAN]
B4DI03	156	17.4	8.91	1.573	SEC11-like 3 (S. cerevisiae), isoform CRA_a OS=Homo sapiens GN=SEC11L3 PE=2 SV=1 - [B4DI03_HUMAN]
Q9Y281	166	18.7	7.88	1.571	Cofilin-2 OS=Homo sapiens GN=CFL2 PE=1 SV=1 - [COF2_HUMAN]
A0A087WX11	918	103.3	5.12	1.570	Folliculin-interacting protein 1 OS=Homo sapiens GN=FNIP1 PE=4 SV=1 - [A0A087WX11_HUMAN]
G3V2R9	217	23.4	6.19	1.560	Prostaglandin reductase 2 OS=Homo sapiens GN=PTGR2 PE=1 SV=1 - [G3V2R9_HUMAN]
Q9UK54	128	14.0	6.95	1.560	Hemoglobin beta subunit variant (Fragment) OS=Homo sapiens GN=HBB PE=2 SV=1 - [Q9UK54_HUMAN]
P59665	94	10.2	6.99	1.557	Neutrophil defensin 1 OS=Homo sapiens GN=DEFA1 PE=1 SV=1 - [DEF1_HUMAN]
Q4ZGM8	100	10.8	9.04	1.549	Hemoglobin alpha-2 globin mutant (Fragment) OS=Homo sapiens PE=3 SV=1 - [Q4ZGM8_HUMAN]

B4DJ12	1253	139.2	6.57	1.546	cDNA FLJ58355, highly similar to Tyrosine-protein phosphatase non-receptor type 23 (EC 3.1.3.48) OS=Homo sapiens PE=2 SV=1 - [B4DJ12_HUMAN]
A0A087WUP0	265	30.0	5.34	1.541	Annexin A8-like protein 1 OS=Homo sapiens GN=ANXA8L1 PE=4 SV=1 - [A0A087WUP0_HUMAN]
E9PAR0	99	11.2	10.36	1.540	Peptidyl-prolyl cis-trans isomerase OS=Homo sapiens GN=FKBP11 PE=1 SV=1 - [E9PAR0_HUMAN]
B2R4C9	102	11.2	9.52	1.537	cDNA, FLJ92044, highly similar to Homo sapiens death-associated protein (DAP), mRNA OS=Homo sapiens PE=2 SV=1 - [B2R4C9_HUMAN]
Q9NWH4	148	16.9	11.09	1.534	cDNA FLJ10024 fis, clone HEMBA1000636 OS=Homo sapiens PE=2 SV=1 - [Q9NWH4_HUMAN]
E3Q1J2	273	31.6	5.97	1.531	MHC class I antigen (Fragment) OS=Homo sapiens GN=HLA-B PE=3 SV=1 - [E3Q1J2_HUMAN]
Q67AK3	233	26.9	7.42	1.531	MHC class II antigen (Fragment) OS=Homo sapiens GN=HLA-DQB1 PE=4 SV=1 - [Q67AK3_HUMAN]
B4DLR0	579	61.1	5.26	1.529	cDNA FLJ55719, highly similar to Mus musculus armadillo repeat containing 5 (Armc5), mRNA OS=Homo sapiens PE=2 SV=1 - [B4DLR0_HUMAN]
Q86UY0	360	40.3	5.83	1.526	Protein BLOC1S5-TXNDC5 OS=Homo sapiens GN=TXNDC5 PE=2 SV=1 - [Q86UY0_HUMAN]
E7EQB2	696	76.6	8.02	1.526	Lactotransferrin (Fragment) OS=Homo sapiens GN=LTF PE=1 SV=1 - [E7EQB2_HUMAN]
Q9P2B2	879	98.5	6.61	1.520	Prostaglandin F2 receptor negative regulator OS=Homo sapiens GN=PTGFRN PE=1 SV=2 - [FPRP_HUMAN]
Q96P70	1041	115.9	4.81	1.517	Importin-9 OS=Homo sapiens GN=IPO9 PE=1 SV=3 - [IPO9_HUMAN]
Q5CZ93	159	19.2	9.88	1.517	Putative uncharacterized protein DKFZp686A0568 OS=Homo sapiens GN=DKFZp686A0568 PE=2 SV=1 - [Q5CZ93_HUMAN]
Q5VX52	437	50.3	8.43	1.514	Spermatogenesis-associated protein 1 OS=Homo sapiens GN=SPATA1 PE=2 SV=3 - [SPAT1_HUMAN]
P80511	92	10.6	6.25	1.513	Protein S100-A12 OS=Homo sapiens GN=S100A12 PE=1 SV=2 - [S10AC_HUMAN]
A8MVU1	366	41.8	8.84	1.512	Putative neutrophil cytosol factor 1C OS=Homo sapiens GN=NCF1C PE=5 SV=1 - [NCF1C_HUMAN]
B5BTZ6	769	87.9	6.20	1.502	Signal transducer and activator of transcription OS=Homo sapiens GN=STAT3 PE=2 SV=1 - [B5BTZ6_HUMAN]
Q15323	416	47.2	4.88	1.502	Keratin, type I cuticular Ha1 OS=Homo sapiens GN=KRT31 PE=2 SV=3 -

					[K1H1_HUMAN]
P07585	359	39.7	8.54	1.501	Decorin OS=Homo sapiens GN=DCN PE=1 SV=1 - [PGS2_HUMAN]
C9JKG1	238	26.7	6.79	1.501	Biglycan (Fragment) OS=Homo sapiens GN=BGN PE=4 SV=1 - [C9JKG1_HUMAN]
H0YA93	1400	158.1	5.82	1.501	NEDD4-binding protein 2 (Fragment) OS=Homo sapiens GN=N4BP2 PE=1 SV=1 - [H0YA93_HUMAN]
G3V295	203	22.8	8.32	0.660	Proteasome subunit alpha type OS=Homo sapiens GN=PSMA6 PE=1 SV=1 - [G3V295_HUMAN]
O96009	420	45.4	6.61	0.658	Napsin-A OS=Homo sapiens GN=NAPSA PE=1 SV=1 - [NAPSA_HUMAN]
E9PN95	56	6.3	4.96	0.626	Uteroglobin OS=Homo sapiens GN=SCGB1A1 PE=4 SV=1 - [E9PN95_HUMAN]
P07339	412	44.5	6.54	0.615	Cathepsin D OS=Homo sapiens GN=CTSD PE=1 SV=1 - [CATD_HUMAN]
A8K987	222	25.7	9.00	0.603	Glutathione S-transferase OS=Homo sapiens PE=2 SV=1 - [A8K987_HUMAN]
B2R7Z6	484	52.5	7.55	0.591	cDNA, FLJ93674 OS=Homo sapiens PE=2 SV=1 - [B2R7Z6_HUMAN]
B4E1L4	668	71.6	5.63	0.531	cDNA FLJ59081, highly similar to Mucin-5B OS=Homo sapiens PE=2 SV=1 - [B4E1L4_HUMAN]
B7Z269	**351**	**40.3**	**7.24**	**0.181**	**cDNA FLJ50754, highly similar to Voltage-dependent L-type calcium channel subunit alpha-1D OS=Homo sapiens PE=2 SV=1 - [B7Z269_HUMAN]**

Table 9:

Changes in proteins (with 1.5x cutoff) following surgery with LFV. Proteins with >2x change are in bold.

Accession	# AAs	MW [kDa]	calc. pI	LFV (Post)/ LFV (Pre)	Description
Q701L7	**513**	**56.6**	**6.74**	**14.876**	**Type II hair keratin 2 OS=Homo sapiens GN=KRTHB2 PE=2 SV=1 - [Q701L7_HUMAN]**
Q9BYT5	**123**	**12.9**	**7.81**	**14.741**	**Keratin-associated protein 2-2 OS=Homo sapiens GN=KRTAP2-2 PE=2 SV=3 - [KRA22_HUMAN]**
O76013	**467**	**52.2**	**4.94**	**7.140**	**Keratin, type I cuticular Ha6 OS=Homo sapiens GN=KRT36 PE=1 SV=1 - [KRT36_HUMAN]**
A0A087X2I6	**404**	**46.1**	**4.84**	**4.627**	**Keratin, type I cuticular Ha3-II OS=Homo sapiens GN=KRT33B PE=4 SV=1 - [A0A087X2I6_HUMAN]**
A0JNT2	**447**	**49.6**	**5.39**	**3.857**	**KRT83 protein OS=Homo sapiens GN=KRT83 PE=2 SV=1 - [A0JNT2_HUMAN]**
B7Z269	**351**	**40.3**	**7.24**	**2.379**	**cDNA FLJ50754, highly similar to Voltage-dependent L-type calcium channel subunit alpha-1D OS=Homo sapiens PE=2 SV=1 - [B7Z269_HUMAN]**
Q15323	**416**	**47.2**	**4.88**	**2.158**	**Keratin, type I cuticular Ha1 OS=Homo sapiens GN=KRT31 PE=2 SV=3 - [K1H1_HUMAN]**
Q96Q06	1357	134.3	8.73	1.840	Perilipin-4 OS=Homo sapiens GN=PLIN4 PE=2 SV=2 - [PLIN4_HUMAN]
Q05315	142	16.4	7.37	1.823	Galectin-10 OS=Homo sapiens GN=CLC PE=1 SV=3 - [LEG10_HUMAN]
H0YF46	255	28.3	5.82	1.698	SPOC domain-containing protein 1 (Fragment) OS=Homo sapiens GN=SPOCD1 PE=4 SV=1 - [H0YF46_HUMAN]
Q7Z6I6	1101	118.5	4.81	1.687	Rho GTPase-activating protein 30 OS=Homo sapiens GN=ARHGAP30 PE=1 SV=3 - [RHG30_HUMAN]
P11678	715	81.0	10.29	1.663	Eosinophil peroxidase OS=Homo sapiens GN=EPX PE=1 SV=2 - [PERE_HUMAN]
A4FU00	317	35.6	5.81	1.651	SYT2 protein (Fragment) OS=Homo sapiens GN=SYT2 PE=2 SV=1 - [A4FU00_HUMAN]

P27701	267	29.6	5.24	1.574	CD82 antigen OS=Homo sapiens GN=CD82 PE=1 SV=1 - [CD82_HUMAN]
B4DMJ5	242	27.3	4.50	1.547	cDNA FLJ53012, highly similar to Tubulin beta-7 chain OS=Homo sapiens PE=2 SV=1 - [B4DMJ5_HUMAN]
Q6P4A8	553	63.2	9.06	1.524	Phospholipase B-like 1 OS=Homo sapiens GN=PLBD1 PE=1 SV=2 - [PLBL1_HUMAN]
A0A024R637	1298	146.5	7.01	1.514	TBC1 domain family, member 4, isoform CRA_b OS=Homo sapiens GN=TBC1D4 PE=4 SV=1 - [A0A024R637_HUMAN]
M0QZ50	93	9.8	4.48	1.512	Microtubule-associated protein 1S OS=Homo sapiens GN=MAP1S PE=1 SV=1 - [M0QZ50_HUMAN]
B3KQ72	130	14.3	5.52	1.500	cDNA FLJ32987 fis, clone THYMU1000032 OS=Homo sapiens PE=2 SV=1 - [B3KQ72_HUMAN]
H6VRF8	644	66.0	8.12	0.665	Keratin 1 OS=Homo sapiens GN=KRT1 PE=3 SV=1 - [H6VRF8_HUMAN]
P35237	376	42.6	5.27	0.658	Serpin B6 OS=Homo sapiens GN=SERPINB6 PE=1 SV=3 - [SPB6_HUMAN]
D6RF35	476	53.0	5.52	0.658	Vitamin D-binding protein OS=Homo sapiens GN=GC PE=1 SV=1 - [D6RF35_HUMAN]
B7Z445	386	43.3	6.83	0.656	cDNA FLJ51492, highly similar to Arachidonate 15-lipoxygenase (EC 1.13.11.33) OS=Homo sapiens PE=2 SV=1 - [B7Z445_HUMAN]
P62851	125	13.7	10.11	0.650	40S ribosomal protein S25 OS=Homo sapiens GN=RPS25 PE=1 SV=1 - [RS25_HUMAN]
Q99549	860	97.1	6.06	0.644	M-phase phosphoprotein 8 OS=Homo sapiens GN=MPHOSPH8 PE=1 SV=2 - [MPP8_HUMAN]
Q7Z6G4	31	3.2	5.78	0.634	HBA2 (Fragment) OS=Homo sapiens GN=HBA2 PE=3 SV=1 - [Q7Z6G4_HUMAN]
K7EPK9	51	5.5	5.11	0.626	Mucin-like protein 1 (Fragment) OS=Homo sapiens GN=MUCL1 PE=4 SV=3 - [K7EPK9_HUMAN]
Q86TT1	375	41.2	6.79	0.616	Full-length cDNA clone CS0DD006YL02 of Neuroblastoma of Homo sapiens (human) OS=Homo sapiens PE=2 SV=1 - [Q86TT1_HUMAN]
B2R6F5	350	39.6	5.12	0.607	cDNA, FLJ92928, highly similar to Homo sapiens retinitis pigmentosa 2 (X-linked recessive) (RP2), mRNA OS=Homo sapiens PE=2 SV=1 - [B2R6F5_HUMAN]
P23527	126	13.9	10.32	0.605	Histone H2B type 1-O OS=Homo sapiens GN=HIST1H2BO PE=1 SV=3 - [H2B1O_HUMAN]

B3KUR3	242	28.0	5.85	0.604	cDNA FLJ40459 fis, clone TESTI2041800, highly similar to BISPHOSPHOGLYCERATE MUTASE (EC 5.4.2.4) OS=Homo sapiens PE=2 SV=1 - [B3KUR3_HUMAN]
P11277	2137	246.3	5.27	0.591	Spectrin beta chain, erythrocytic OS=Homo sapiens GN=SPTB PE=1 SV=5 - [SPTB1_HUMAN]
P02656	99	10.8	5.41	0.591	Apolipoprotein C-III OS=Homo sapiens GN=APOC3 PE=1 SV=1 - [APOC3_HUMAN]
Q9NZD4	102	11.8	5.00	0.584	Alpha-hemoglobin-stabilizing protein OS=Homo sapiens GN=AHSP PE=1 SV=1 - [AHSP_HUMAN]
G4V2I8	911	101.7	5.21	0.574	Anion exchanger-1 variant OS=Homo sapiens PE=2 SV=1 - [G4V2I8_HUMAN]
B7Z4Q8	613	68.2	7.85	0.574	cDNA FLJ52333, highly similar to Erythrocyte membrane protein band 4.2 OS=Homo sapiens PE=2 SV=1 - [B7Z4Q8_HUMAN]
P03973	132	14.3	8.75	0.570	Antileukoproteinase OS=Homo sapiens GN=SLPI PE=1 SV=2 - [SLPI_HUMAN]
P02549	2419	279.8	5.05	0.569	Spectrin alpha chain, erythrocytic 1 OS=Homo sapiens GN=SPTA1 PE=1 SV=5 - [SPTA1_HUMAN]
Q14587	947	108.3	8.87	0.566	Zinc finger protein 268 OS=Homo sapiens GN=ZNF268 PE=1 SV=2 - [ZN268_HUMAN]
P69892	147	16.1	7.20	0.553	Hemoglobin subunit gamma-2 OS=Homo sapiens GN=HBG2 PE=1 SV=2 - [HBG2_HUMAN]
P01833	764	83.2	5.74	0.549	Polymeric immunoglobulin receptor OS=Homo sapiens GN=PIGR PE=1 SV=4 - [PIGR_HUMAN]
P16157	1881	206.1	6.01	0.548	Ankyrin-1 OS=Homo sapiens GN=ANK1 PE=1 SV=3 - [ANK1_HUMAN]
Q4ZGM8	100	10.8	9.04	0.543	Hemoglobin alpha-2 globin mutant (Fragment) OS=Homo sapiens PE=3 SV=1 - [Q4ZGM8_HUMAN]
B3KVN0	416	45.8	8.60	0.534	cDNA FLJ16785 fis, clone NT2RI2015342, highly similar to Solute carrier family 2, facilitated glucose transporter member 1 OS=Homo sapiens PE=2 SV=1 - [B3KVN0_HUMAN]
Q4VB87	615	68.4	5.91	0.532	EPB41 protein (Fragment) OS=Homo sapiens GN=EPB41 PE=2 SV=1 - [Q4VB87_HUMAN]
B4DF70	183	20.1	8.78	0.527	cDNA FLJ60461, highly similar to Peroxiredoxin-2 (EC 1.11.1.15) OS=Homo sapiens PE=2 SV=1 - [B4DF70_HUMAN]
Q4TZM4	101	11.0	6.52	0.518	Hemoglobin beta chain (Fragment) OS=Homo sapiens GN=HBB PE=3 SV=1 - [Q4TZM4_HUMAN]

P00918	260	29.2	7.40	0.507	Carbonic anhydrase 2 OS=Homo sapiens GN=CA2 PE=1 SV=2 - [CAH2_HUMAN]
O75602	509	55.4	6.83	0.504	Sperm-associated antigen 6 OS=Homo sapiens GN=SPAG6 PE=2 SV=1 - [SPAG6_HUMAN]
Q6J1Z9	90	9.6	9.50	0.501	Hemoglobin alpha 1 (Fragment) OS=Homo sapiens GN=HBA1 PE=3 SV=1 - [Q6J1Z9_HUMAN]
Q86YQ1	**91**	**9.7**	**9.25**	**0.497**	**Hemoglobin alpha-2 (Fragment) OS=Homo sapiens GN=HBA2 PE=3 SV=1 - [Q86YQ1_HUMAN]**
Q13938	**189**	**21.0**	**4.89**	**0.495**	**Calcyphosin OS=Homo sapiens GN=CAPS PE=1 SV=1 - [CAYP1_HUMAN]**
E9PN95	**56**	**6.3**	**4.96**	**0.450**	**Uteroglobin OS=Homo sapiens GN=SCGB1A1 PE=4 SV=1 - [E9PN95_HUMAN]**
A8K987	**222**	**25.7**	**9.00**	**0.448**	**Glutathione S-transferase OS=Homo sapiens PE=2 SV=1 - [A8K987_HUMAN]**
P00915	**261**	**28.9**	**7.12**	**0.442**	**Carbonic anhydrase 1 OS=Homo sapiens GN=CA1 PE=1 SV=2 - [CAH1_HUMAN]**
Q6J1Z8	**42**	**4.5**	**9.38**	**0.429**	**Hemoglobin beta (Fragment) OS=Homo sapiens GN=HBB PE=3 SV=1 - [Q6J1Z8_HUMAN]**
H3BML9	**118**	**13.1**	**5.68**	**0.397**	**Myosin regulatory light chain 2, skeletal muscle isoform (Fragment) OS=Homo sapiens GN=MYLPF PE=4 SV=1 - [H3BML9_HUMAN]**
E5RGQ7	**148**	**16.8**	**8.88**	**0.388**	**Dematin (Fragment) OS=Homo sapiens GN=DMTN PE=1 SV=1 - [E5RGQ7_HUMAN]**
Q6VFQ6	**42**	**4.5**	**8.24**	**0.384**	**Hemoglobin beta chain (Fragment) OS=Homo sapiens GN=HBB PE=3 SV=1 - [Q6VFQ6_HUMAN]**
P02042	**147**	**16.0**	**8.05**	**0.383**	**Hemoglobin subunit delta OS=Homo sapiens GN=HBD PE=1 SV=2 - [HBD_HUMAN]**
Q5T619	**568**	**62.3**	**8.62**	**0.380**	**Zinc finger protein 648 OS=Homo sapiens GN=ZNF648 PE=2 SV=1 - [ZN648_HUMAN]**
Q5RHS7	**95**	**11.0**	**9.28**	**0.346**	**Protein S100-A2 OS=Homo sapiens GN=S100A2 PE=1 SV=2 - [Q5RHS7_HUMAN]**
Q8IUL9	**105**	**11.5**	**6.05**	**0.270**	**Hemoglobin beta chain variant Hb.Sinai-Bel Air (Fragment) OS=Homo sapiens GN=HBB PE=3 SV=1 - [Q8IUL9_HUMAN]**
B4E1L4	**668**	**71.6**	**5.63**	**0.257**	**cDNA FLJ59081, highly similar to Mucin-5B OS=Homo sapiens PE=2 SV=1 - [B4E1L4_HUMAN]**
B2R7Z6	**484**	**52.5**	**7.55**	**0.248**	**cDNA, FLJ93674 OS=Homo sapiens PE=2 SV=1 - [B2R7Z6_HUMAN]**

Supplemental Figure 1:

Principle component analysis (by Partek) of gene expression data, showing no significant outliers within the data.

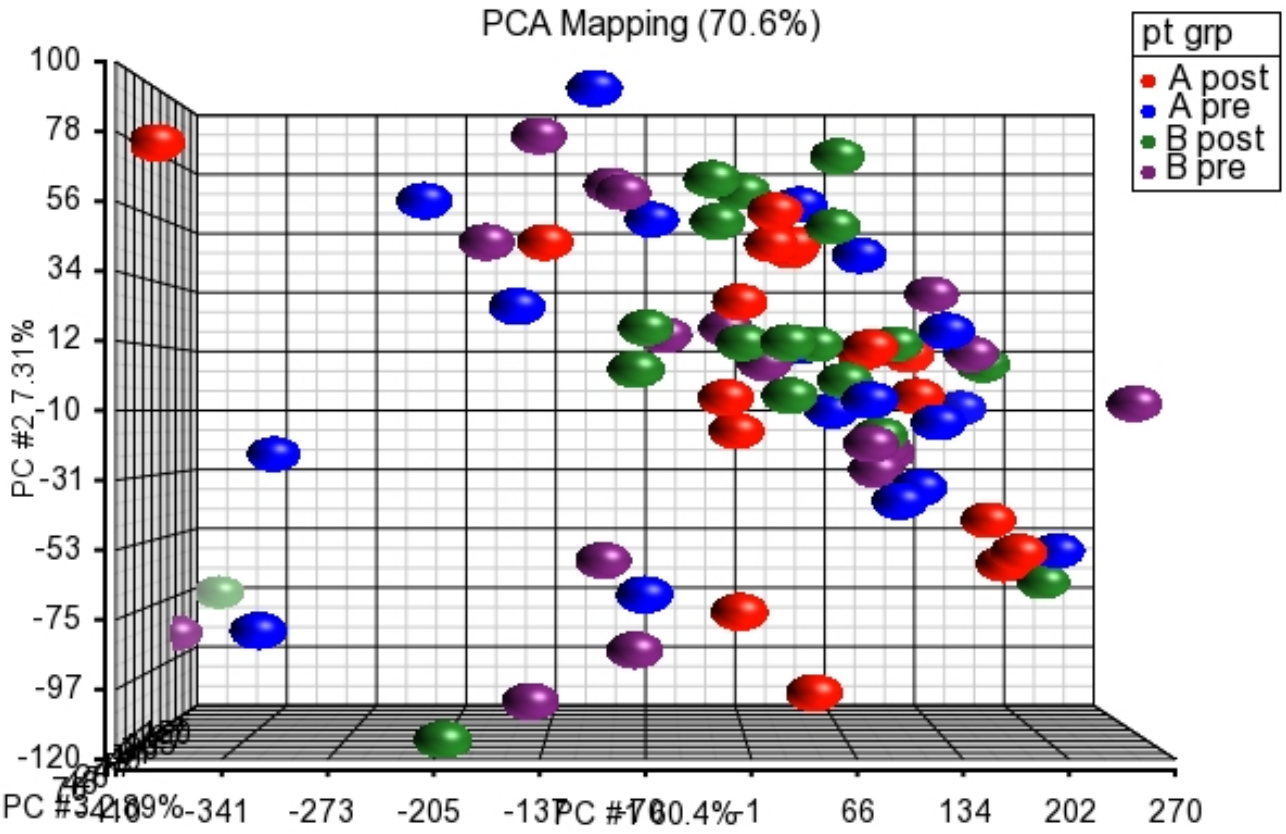

Supplemental Figure 2:

There were no significant changes in **(A)** lipid species or **(B)** lipid class (as a percentage of the total) following surgery either with standard CPB with collapsed lung or with LFV.

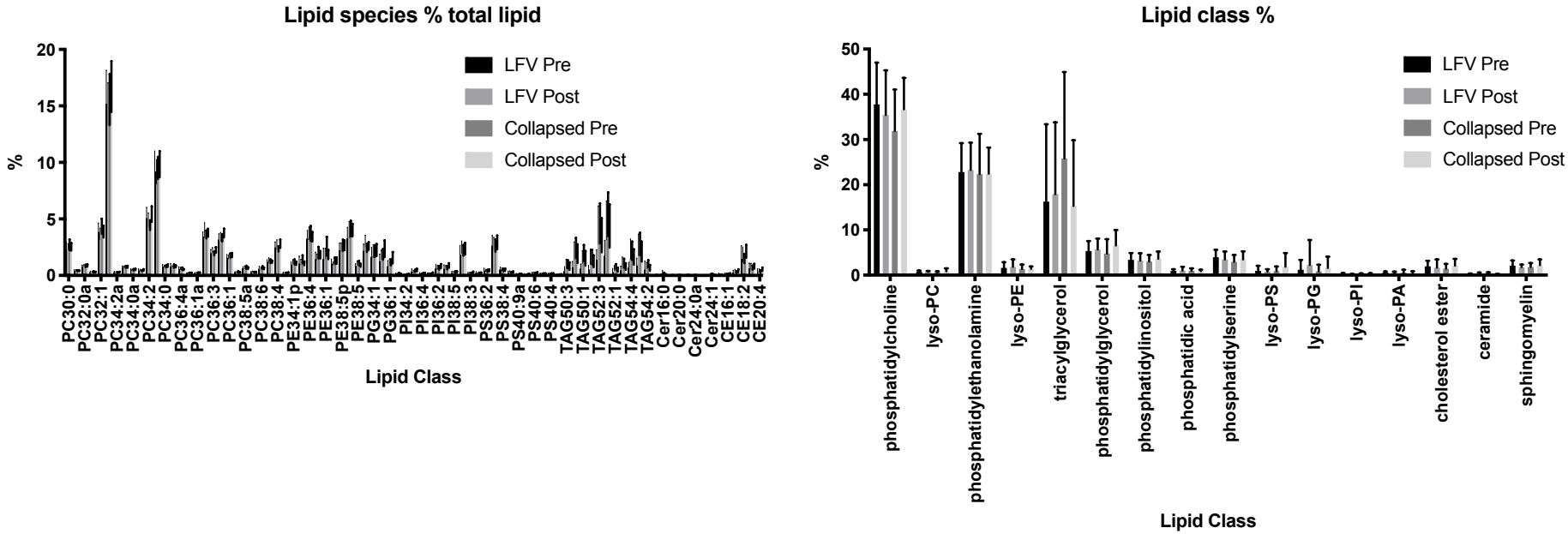

Highlights:

- Cardiopulmonary bypass surgery causes systemic and pulmonary inflammation
- Surgery increases oxidative stress and hypoxia in the lungs and free iron in the blood
- Omics suggest ischemia is the principle driver of inflammation
- Unlike animal models lung ventilation during surgery increases inflammation
- Ventilation increased ischemia, potentially through increased surgical time

Abstract

Background

Heart surgery with cardio-pulmonary bypass (CPB) is associated with lung ischemia leading to injury and inflammation. It has been suggested this is a result of the lungs being kept deflated throughout the duration of CPB. Low frequency ventilation (LFV) during CPB has been proposed to reduce lung dysfunction.

Methods

We used a semi-biased multi-omic approach to analyse lung biopsies taken before and after CPB from 37 patients undergoing coronary artery bypass surgery randomised to both lungs left collapsed or using LFV for the duration of CPB. We also examined inflammatory and oxidative stress markers from blood samples from the same patients.

Results

30 genes were induced when the lungs were left collapsed and 80 by LFV. Post-surgery 26 genes were significantly higher in the LFV vs. lungs left collapsed, including genes associated with inflammation (e.g. *IL6* and *IL8)* and hypoxia/ischemia (e.g. *HIF1A*, *IER3* and *FOS*). Relatively few changes in protein levels were detected, perhaps reflecting the early time point or the importance of post-translational modifications. However, pathway analysis of proteomic data indicated that LFV was associated with increased "cellular component morphogenesis" and a decrease in "blood circulation". Lipidomic analysis did not identify any lipids significantly altered by either intervention.

Discussion

Taken together these data indicate the keeping both lungs collapsed during CPB significantly induces lung damage, oxidative stress and inflammation. LFV during CPB increases these deleterious effects, potentially through prolonged surgery time, further decreasing blood flow to the lungs and enhancing hypoxia/ischemia.

Multi-omic analysis of the effects of low frequency ventilation during cardiopulmonary bypass surgery.

Durham AL PhD[1], Al Jaaly E MD[2], Graham R MSc[1], Brook PO MSc[1], Bae JH BSc[1], Heesom KJ PhD[3], Postle AD PhD[4], Lavender P PhD[5], Jazrawi E BSc[1], Reeves B DPhil[2], Fiorentino F PhD[2], Mumby S PhD[1], Angelini GD MD[2,6]*, Adcock IM PhD[1].

*Author for correspondence
Professor Gianni Angelini
Bristol Heart Institute
Bristol Royal Infirmary
Upper Maudlin Street
Bristol
BS2 8HW
UK
Tel: +44 (0) 117 34 23165
email: g.d.angelini@bristol.ac.uk

1. Airways Disease Section, National Heart and Lung Institute, Imperial College London, Dovehouse Street, London SW3 6LY

2. Cardiothoracic Surgery, National Heart and Lung Institute, Imperial College London, Hammersmith Hospital, London, UK

3. University of Bristol Proteomics Facility, BioMedical Sciences Building, University Walk, Bristol, UK

4. Faculty of Medicine, University of Southampton, Building 85, Life Sciences Building, Highfield Campus, Southampton, UK

5. Department of Asthma, Allergy, and Respiratory Science, King's College London, London, UK

6. Bristol Heart Institute, University of Bristol, Bristol Royal Infirmary, Level 7, Marlborough Street, Bristol, UK

7. Immunobiology, Blizard Institute, Barts and the London School of Medicine and Dentistry, Queen Mary University of London, 4 Newark St, London, UK

Short Title.
Omic analysis of lungs ventilation during open heart surgery.
Total Word Count: 3436

Multi-omic analysis of the effects of low frequency ventilation during cardiopulmonary bypass surgery.

Durham AL PhD[1], Al Jaaly E MD[2], Graham R MSc[1], Brook PO MSc[1], Bae JH BSc[1], Heesom KJ PhD[3], Postle AD PhD[4], Lavender P PhD[5], Jazrawi E BSc[1], Reeves B DPhil[2], Fiorentino F PhD[2], Mumby S PhD[1], Angelini GD MD[2,6]*, Adcock IM PhD[1].

*Author for correspondence

Professor Gianni Angelini

Bristol Heart Institute

Bristol Royal Infirmary

Upper Maudlin Street

Bristol

BS2 8HW

UK

Tel: +44 (0) 117 34 23165

email: g.d.angelini@bristol.ac.uk

1. Airways Disease Section, National Heart and Lung Institute, Imperial College London, Dovehouse Street, London SW3 6LY

2. Cardiothoracic Surgery, National Heart and Lung Institute, Imperial College London, Hammersmith Hospital, London, UK

3. University of Bristol Proteomics Facility, BioMedical Sciences Building, University Walk, Bristol, UK

4. Faculty of Medicine, University of Southampton, Building 85, Life Sciences Building, Highfield Campus, Southampton, UK

5. Department of Asthma, Allergy, and Respiratory Science, King's College London, London, UK

6. Bristol Heart Institute, University of Bristol, Bristol Royal Infirmary, Level 7, Marlborough Street, Bristol, UK

7. Immunobiology, Blizard Institute, Barts and the London School of Medicine and Dentistry, Queen Mary University of London, 4 Newark St, London, UK

Short Title.

Omic analysis of lungs ventilation during open heart surgery.

Total Word Count: 3725

Abstract

Background

Heart surgery with cardio-pulmonary bypass (CPB) is associated with lung ischemia leading to injury and inflammation. It has been suggested this is a result of the lungs being kept deflated throughout the duration of CPB. Low frequency ventilation (LFV) during CPB has been proposed to reduce lung dysfunction.

Methods

We used a semi-biased multi-omic approach to analyse lung biopsies taken before and after CPB from 37 patients undergoing coronary artery bypass surgery randomised to both lungs left collapsed or using LFV for the duration of CPB. We also examined inflammatory and oxidative stress markers from blood samples from the same patients.

Results

30 genes were induced when the lungs were left collapsed and 80 by LFV. Post-surgery 26 genes were significantly higher in the LFV vs. lungs left collapsed, including genes associated with inflammation (e.g. *IL6* and *IL8)* and hypoxia/ischemia (e.g. *HIF1A*, *IER3* and *FOS*). Relatively few changes in protein levels were detected, perhaps reflecting the early time point or the importance of post-translational modifications. However, pathway analysis of proteomic data indicated that LFV was associated with increased "cellular component morphogenesis" and a decrease in "blood circulation". Lipidomic analysis did not identify any lipids significantly altered by either intervention.

Discussion

Taken together these data indicate the keeping both lungs collapsed during CPB significantly induces lung damage, oxidative stress and inflammation. LFV during CPB increases these deleterious effects, potentially through prolonged surgery time, further decreasing blood flow to the lungs and enhancing hypoxia/ischemia.

Key Words:

Cardio-pulmonary bypass

Ventilation

Inflammation

Transcriptomics

Proteomics

1. Introduction

Cardiopulmonary bypass (CPB), which allows operation on a motionless and bloodless heart, is used in most heart surgery procedures. Recovery from cardiac surgery utilising CPB is generally good with a 30 day survival rate of 98.4% [1]. However, CPB is still associated with severe systemic inflammation and tissue damage with an accompanying mortality of 1.5% along with post-operative lung dysfunction of various degrees in up to 30% of patients [2]. The underlying mechanisms driving inflammation following CPB are yet to be fully elucidated and there are currently no strategies to effectively prevent it.

Institution of CPB is associated with significant physiological changes and insults to the lung. Ventilation is generally stopped, and lungs deflated to reduce mediastinal motions. Venous return is directed away from the right heart thereby pulmonary artery flow is dramatically reduced. Furthermore, bronchial blood flow is reduced due to haemodynamic and pulsatility changes during bypass and changes in vascular resistances. These atelectatic and ischemic changes may promote tissue hypoxia, oxidative stress and lung cellular damage [3–6]. Towards the end of CPB, full ventilation is recommenced and pulmonary blood flow is restored with potential injury by reperfusion including oxidative stress [7,8], and inflammatory cell infiltration [9]. Further oxidative stress could be triggered by free iron catalysed reactions [10,11] from iron released by haemolysis as the blood passes through the bypass circuit.

There have been various attempts made to protect the lung during CPB. Among these, it has been suggested that low frequency ventilation (LFV) during CPB may alleviate

hypoxia and ischemia of the lungs and thereby help to reduce inflammation. In contrast to previous animal trials [12], we have recently provided evidence that in patients undergoing elective coronary artery bypass grafting (CABG), the use of LFV during CPB when compared to both lungs left collapsed does not seem to reduce inflammation in lung biopsies and blood [13,14].

The low frequency ventilation technique reported in our study has been investigated previously by different groups with contrasting results. This study, for the first time, uses the simultaneous of human lung biopsy and blood samples to assess the effect of the technique. In order to establish a mechanistic link between the effects of both interventions on the lung we used a semi-biased multi-omics approach (transcriptomics, proteomics and lipidomics) to analyse lung biopsies taken at the start of surgery before CPB and at the end of surgery after lung reperfusion but before weaning from CPB from the above mentioned randomised study recently published [14]. We also analysed serial blood plasma taken before and after surgery.

2. Methods:

2.1 Study design

37 patients undergoing elective or urgent CABG with CPB and cold blood cardioplegic arrest at the Hammersmith Hospital, were recruited as part of a single-centre, parallel group, randomised, controlled trial investigating low frequency ventilation study recently published [14].

Venous blood samples were taken from the patients at induction, 10mins, 2, 6 and 24 hours post CPB.

Lung biopsies were taken both prior to and immediately after surgery. The pre-surgery biopsies were taken from the left upper lobe immediately after sternotomy with lungs ventilated for both groups. The post-surgery biopsy was taken from the left lower lobe at the end of the operation just before weaning from CPB.

This study was approved by the NRES committee London- Camden and Islington (Research Ethics Committee reference number 12/LO/0458) on 25/04/2012. Further approval was obtained from the research and development department of the Imperial College Healthcare NHS Trust. This research complied with the Helsinki Declaration. The trial is registered as ISRCTN No: 34428459. All patients involved in the study gave written and informed consent

2.2 Luminex:

Cytokines in human plasma samples, taken 24 hours post-surgery, were quantified using the Luminex Screening Human Magnetic Assay kit (R&D, Abingdon, UK).

2.3 Transcriptomics:

RNA was extracted and analysed by Affymetrix GeneChip Human Gene 1.0 ST Array (ThermoFisher) following the manufacturer's instructions.

RNA samples were also quantified using RT-qPCR. More details are available in the supplemental materials.

2.4 Proteomics:

Protein was extracted as described previously [14]. More details are available in the supplemental materials.

2.5 Heme assay:

Heme levels in the whole cell protein extracts were measured using the Heme colorimetric assay kit (BioVision, Milpitas, CA, USA) following manufacturer's instruction.

2.6 Lipidomics:

Lung tissue was processed as described previously [15,16].

More details are available in the supplemental materials.

2.7 Oxidative stress/ Anti-oxidant capacity:

We used the RedoxSys® to electrochemically measure the oxidant redox potential (ORP) and antioxidant capacity (AOC), following manufacturer's instructions (Aytu Biosciences, Englewood, CO, USA).

2.8 Statistics and Data analysis:

Gene arrays were analysed by Partek genomics Suite (Partek Inc). Gene and protein classification were tested using PANTHER Overrepresentation Test analysed against the Homo Sapiens reference list, using the PANTHER Go-SLIM Biological process annotation dataset [17]. Analysis included Bonferroni correction for multiple data.

The remaining data were analysed using Graphpad Prism 6 (Graphpad Software Inc, La Jolla, CA, USA) utilising Friedman and using Dunn's multiple comparison test unless otherwise stated. A probability value of <0.05 was considered significant.

3. Results:

Patient demographics and clinical characterisation are provided in detail in Fiorentino et al, 2019 [14].

3.1 Patient serum samples:

3.1.1 Luminex of serum cytokines:

Plasma IL-6, IL-8 and IL-10 levels increased significantly 24 hours post-surgery in both groups compared to the pre-surgery control samples. IL-6 levels increased 17-fold in lungs collapsed group and 25-fold in the LFV group (**Figure 1A**). IL-8 levels (**Figure 1B**) increased approximately 1.5-fold in both study groups, whilst IL-10 (**Figure 1C**) increased approximately 1.3x. In contrast, there was no significant change in inflammatory cytokines IL-1β and MCP-1 in the plasma of patients before CPB and 24hrs after CPB in both groups (**Figure 1D & E**).

3.1.2 Cell-Free heme:

The levels of cell free heme were measured in the blood plasma following surgery. Cell free heme was significantly higher in both groups at 10 minutes and 2 hours after surgery before returning to baseline. Cell-free heme levels in plasma were increased but not significantly in the LFV group (51.5μM vs 38.1μM, 2-way ANOVA $p=0.17$) (**Figure 2**).

3.1.3 Oxidative stress in blood:

Plasma ORP and AOC from all patients were measured following bypass. By 2-way ANOVA time after surgery was linked to significantly increased ORP ($p<0.0001$) and this was matched by a significant decline in AOC ($p<0.0001$). However, the ANOVA

did not identify any statistical significance related to intervention, indicating that CPB induced changes in ORP and AOC were not altered by LFV (p=0.44, p=0.16 respectively) (**Figure 2**).

Since LFV intervention did not effect plasma ORP or AOC we examined the combined data to increase statistical power and determine the effects of surgery. The combined data showed a significant increase in ORP within 10 minutes following surgery, which increased at all timepoints measured but appeared to plateau at 6 hours. Similarly, the decrease in AOC following surgery reached a nadir at 6 hours which was maintained (**Figure 2**).

3.2 Biopsy RNA gene expression data:

Full data set is available at https://figshare.com/articles/_/4772167. Principle component analysis (PCA) did not identify any significant outliers; therefore, no patient samples were excluded from the analysis (**Supplemental Figure 1**). There were no significant differences in gene expression between the two groups at baseline.

3.2.1 Transcriptional response to CPB with lungs collapsed:

Lungs left collapsed significantly increased the expression of 30 genes in the biopsy immediately after surgery (**Supplemental data: Table 1**). These genes include the inflammatory genes *CCL2* (encoding MCP-1) and *IL6*, which had the highest increase following surgery (6.7x and 6.6x higher than baseline respectively). Panther pathway analysis identified the "cholecystokinin receptor (CCKR) signalling map" (p=2.26E-08), the "Interleukin signalling pathway" (5.41E-05) and the "p53 pathway" (4.81E-

02) as significantly over-represented within the genes induced in the lung collapsed group (**Supplemental data: Table 2**).

3.2.2 Transcription response to CPB with LFV:

LFV significantly induced 80 genes in lung tissue after surgery (**Supplemental data: Table 3**). No genes were significantly suppressed. All CPB-induced genes were enhanced in the LFV group and up-regulated genes shared the same pathways as those induced by lungs collapsed CPB namely the "CCKR signalling map" (p= 2.14E-10), the "interleukin signaling pathway" (p=4.34E-03) and the "p53 pathway" (p=4.46E-02)(**Supplemental data: Table 4**). In addition, the "Inflammation mediated by chemokine and cytokine signaling pathway" and the "Gonadotropin-releasing hormone receptor pathway" were also enriched. Biological process analysis identified "endoderm development", "MAPK cascade", "cell death" and "response to stress" as significantly over-represented.

The 50 genes that were upregulated in the LFV group alone (i.e. not in CPB lungs collapsed group) included inflammatory genes such as *IL1B* and *CYR61*. Pathway and biological process analysis did not identify any specific pathways or processes as overrepresented in these 50 genes although raw, uncorrected p values indicated over-representation of the 'CCKR signalling map' and "Inflammation mediated by chemokine and cytokine signaling" pathways (p=2.01E-03).

3.2.3 Effect of low frequency ventilation:

Comparing gene expression biopsies from the LFV and lungs left collapsed groups taken after surgery identified statistically significant changes in 26 genes in patients

who underwent LFV compared to patients undergoing lungs collapsed CPB (**Supplemental data: Table 5**). *HLA-DRB5*, encoding the HLA class II histocompatibility antigen DRB5 was reduced in the LFV group whilst the remaining 25 genes were increased with LFV. The expression of HLA-DRB5 was not significantly altered following surgery in either groups compared to their respective pre-surgical controls.

The genes significantly increased by LFV intervention compared to lungs left collapsed included the inflammatory *IL6*, *CCL2* and *CCL8* (encoding IL-6, MCP1 and MCP2 respectively). Pathway analysis showed that LFV significantly activated the "Plasminogen activating cascade" (p=3.17E-02), "CCKR signaling map" (p=6.81E-03), and "Inflammation mediated by chemokine and cytokine signaling pathway" (p=3.30E-02)(**Supplemental data: Table 2**).

Combining both intervention groups to increase the analytical power of the effects of surgery identified 51 genes with significantly altered expression following surgery (**Supplemental data: Table 6**). Pathway analysis of this data identified the "Oxidative stress response" (p= 4.76E-02), "Interleukin signaling" (p= 5.10E-04), "CCKR signaling map" (p=9.53E-07) and "p53" (p= 8.22E-03) pathways as over-represented.

3.2.4 Validation of transcriptomic response:

We have previously examined the induction of *IL6*, *IL8* and *IL1B* gene expression in the lung biopsies by Taqman qPCR. The gene expression data following CPB showed the same increase in inflammatory gene expression in the LFV group compared to the

lungs collapsed group [14]. In addition, we demonstrated significant up-regulation of hypoxia inducible factor 1A (*HIF1A*) gene expression in the biopsies after lungs collapsed CBP, which was further enhanced in the biopsies from patients who underwent LFV (**Figure 3A**), compared to the pre-surgery control biopsies.

3.3 Biopsy Proteomic analysis:

Full data set is available at https://figshare.com/articles/_/4772167. Whole cell protein extracts from each biopsy were pooled into 4 groups: lungs left collapsed or LFV both pre and post-surgery. Tandem mass tagging (TMT) identified over 3000 distinct proteins in the pooled biopsy samples. There was minimal variation in the pre-surgery baseline levels of proteins detected. Two proteins were significantly elevated >2-fold in the lungs left collapsed group and 34 were elevated >2x in the LFV group (**Supplemental data: Table 7**) before surgery. Panther pathways analysis of these proteins did not identify any biological pathways or processes as overrepresented. Using a 1.5-fold cut-off, there were 4 significantly different proteins in the lungs collapsed group and 155 proteins more highly expressed in the LFV group. PANTHER analysis of these proteins identified "immune system process" as over-represented in the LFV group at baseline before surgery.

3.3.1 Proteomic response to CPB with lungs collapsed:

Lungs collapsed CBP resulted in 25 proteins having a >2-fold increase in expression post-surgery and 1 protein decreased >2-fold (**Supplemental data: Table 8**) relative to the same donors before surgery. The up-regulated proteins included the detoxifying enzyme glutathione S-transferase P (GSTP1), and eosinophil peroxidase. The decreased protein was identified as "cDNA FLJ50754, highly similar to voltage-

dependent L-type calcium channel subunit alpha-1D". Reducing the cut-off ratio to 1.5-fold change increased the number of differentially expressed proteins to 109 with enhanced expression and 8 proteins that were decreased. These did not reflect any pathways or processes although at the unadjusted p value level the "CCKR signalling map" and "intergrin signalling pathways" were identified as over-represented (p=4.91E-2 and p=1.33E-02 respectively).

3.3.2 Proteomic response to CPB with LFV:

CBP in the presence of LFV resulted in >2-fold upregulation of 7 proteins with keratin, both type I and II, making up 6 out of 7 of these proteins (**Supplemental data: Table 8**). Keratin is a common contaminant of proteomic experiments, so these changes may simply be an artefact, however keratin expression in the lungs has previously been reported, including its upregulation during lung repair [18] and by shear forces.[19,20] The remaining protein was "cDNA FLJ50754, highly similar to Voltage-dependent L-type calcium channel subunit alpha-1D". Whilst no pathways were identified as changed the keratin proteins were all linked to the process of "cellular component organisation or biogenesis" ($p=2.8x10^{-6}$). 15 proteins were decreased >2-fold following surgery with LFV, including 5 haemoglobin subunits (HBA2, HBB, HBD). Analysis of biological processes identified "blood circulation" as overrepresented (p>0.001).

19 proteins were increased following LFV using a 1.5-fold cut off, 7 of which were linked to the "cellular component morphogenesis" process (p>0.001). 47 proteins were decreased following surgery. The analysis did not identify any pathways

significantly altered by LFV at the protein level, however, cellular process analysis again identified "blood circulation" as overrepresented (p=0.001).

3.3.3 Comparison of LFV with lungs left collapsed:

Direct comparison of the post-bypass samples identified 4 proteins that were increased in the lungs collapsed group with >2-fold change and 9 proteins that were increased in the LFV group (**Supplemental data: Table 5**). Biological pathway and process analysis did not identify any significantly over-represented pathways/processes between these groups. 16 proteins were identified as >1.5-fold higher in lungs collapsed compared to LFV, of which 3 were also higher at baseline and therefore excluded from the analysis. Proteins increased in the lungs collapsed group included haemoglobin alpha, beta and delta. These proteins were not associated with any significant changes in biological pathways but were identified with the processes of blood circulation (p=2.27E-04) and transport (p=3.14E-05).

11 proteins were higher in the LFV group compared to lungs collapsed post-surgery but not pre-surgery. No processes or pathways were identified as significant.

3.4 Confirmation of reduced haemoglobin in biopsies following LFV:

Due to the proteomics identification of haemoglobin as downregulated in the LFV group the level of heme was measured in the protein isolated from each lung biopsy (**Figure 3B**). The amount of heme in the biopsies did not significantly change following CPB with lungs collapsed, however, it was significantly reduced following surgery with LFV.

3.5 Lipidomics:

Full data set is available at https://figshare.com/articles/_/4772167. There were no significant differences in lipid class or species between groups either before or after surgery regardless of intervention. (Data is shown in **Supplemental Figure 2**.)

4 Discussion:

Surgery with CPB is associated with acute systemic and pulmonary inflammation and can lead to pulmonary dysfunction in a significant number of patients. We confirmed previous data showing enhanced levels of inflammatory cytokines, oxidative stress, cell free heme and decreased plasma anti-oxidant capacity with CPB. We also provided evidence for the first time in transcriptomic analysis of lung biopsy in patients undergoing CABG, that CPB triggers a significant increase in hypoxic and inflammatory responses and a decrease in genes associated with blood flow. These effects were amplified in patients undergoing CPB with LFV when compared with CPB with lungs collapsed. These data provide a mechanistic link to the adverse clinical effects seen with the addition of LFV to CPB in patients undergoing CABG (14).

Analysis of the patients' plasma showed that following CPB with lungs collapsed there was a significant increase in the levels of inflammatory cytokines, oxidative stress, cell free heme and a decrease in plasma anti-oxidant capacity corresponding to the effects of CPB surgery previously reported [21]. These systemic effects were not significantly altered by CPB with LFV intervention.

LFV may increase the deleterious effects of CPB by three main mechanisms: increased surgical time, direct oxygenation of the lungs or ventilator-associated injury. The movement of the lungs during CPB with LFV may increase surgery time. The LFV group had a higher levels of cell free heme in the blood following CPB, a reflection of the longer CPB time compared to the lungs left collapsed CPB group

(87.5 minutes median (range 68-97) vs 69 minutes median (range 54-79)) (p=0.03) [14].

The increased oxygenation of the lungs during LFV may also enhance lung injury. Without the hypoxic response to reduce metabolic rates, LFV may cause a more rapid use of metabolic substrates and the build-up of by-products causing increased lung damage. Hyperoxia during surgery showed similar inflammation and stress following CPB as normoxia, although hyperoxia led to oxygen-mediated myocardial, hepatic and cerebral injury [22]. This hypothesis is unlikely as the LFV group showed increased *HIF1A* gene expression in blood indicating that the lungs were less, not more, oxygenated during LFV. However, intermittent hypoxia has been shown to be more potent at activating HIF-1α and FOS/AP-1 than continuous hypoxia [23].

Finally, LFV may cause biotrauma to the lung by repetitive alveolar collapse and hyperinflation [24].

Our data are unique because of the use of lung biopsies taken during the surgery in the on-going debate regarding relative contributions of ischaemia and reperfusion to tissue injury. The data indicate that the practice of lungs left collapsed during CPB prior to reperfusion, can trigger gene expression, inflammation and stress in the lungs. These could be the consequence of atelectasis, direct effect of lung hypoperfusion and ischemia superimposed by perfusion with activated inflammatory cells due to their activation by the CPB machine and circuit. There has been considerable debate as to the relative importance of these mechanisms in driving lung inflammation [3,4,25] but the strong correlation between increased stress, hypoxia and inflammation in the lungs

support the hypothesis that ischemia alone is enough to drive inflammation. Ischemia during surgery is associated with significant changes in inflammation (interleukin signalling pathway) and stress (CCKR and p53 pathways) in the lung.

In addition, the principle driver of increased inflammation in the LFV group appears to be increased surgery time, and hence ischemic, time, whilst reperfusion remained unchanged. As our lung biopsies were collected immediately after reperfusion it is unlikely that systemic inflammation or reperfusion injury would have been able to influence gene expression, but rather that ischemia alone is capable of significantly damaging the lungs.

Whilst the proteomic analysis of CPB identified several proteins that changed expression in the pooled samples, this did not identify any specific pathways as activated by routine CPB with lungs left collapsed. Proteomic analysis is hampered by the short timeframes in which the surgery occurs and (to overcome resource constraints) the pooling of samples from all patients in each treatment group. Whilst pooling the samples loses the ability to discern individual patient variation, this approach reduces biological variation and thereby increases the power to detect treatment differences [26]. Nevertheless, CCKR signalling and integrin signalling pathways were significantly over-represented by proteins up-regulated by CPB when assessed using a raw p value <0.05. As stated above, the CCKR signalling may be induced by hypoxic conditions and up-regulated protein levels correlated well with gene expression. The integrin signalling proteins consisted of collagen alpha-1 (I) chain, the collagen alpha-1 (XIV) chain, the adapter molecule Crk and Crk-like (CrkL) proteins. Crk and CrkL have been shown to play a key role in the activation

and transformation of fibroblasts, which are the principle produces of extracellular matrix, including collagen in response to injury. These data indicate that fibroblast activation, in response to lung injury, occurs at an early stage in CPB. This study provides valuable insight into the underlying mechanisms that drive lung inflammation during CPB. This increased understanding may lead to more effective interventions in the future.

Proteomic analysis of the LFV group showed a significant decrease in proteins representing blood circulation, such as haemoglobin, which was confirmed in the biopsy samples. These data indicate that LFV may have increased vascular resistance and further reduced pulmonary blood flow during surgery, which may increase the level of ischemia and the level of pulmonary inflammation [27]. Patients undergoing LFV did show an increase in requiring haemodynamic support following surgery compared to those undergoing CPB with lungs left collapsed, so alternatively this may reflect a reduction in blood pressure [14].

Whilst changes in lipids have been reported in response to oxidative stress, such as the accumulation of pro-inflammatory isoprostanes and oxylipins in smokers and in patients with cardiovascular disease, no significant changes in lipidomics were detected following CPB, indicating that either the timeframe of the study was too short for these changes to occur or CPB has little effect on the lipid composition of the lung. The lack of change in the proteomics and lipidomic profiles detected may also reflect the important role that post-translational modifications play in regulating

protein and lipid function. Unfortunately, examination of post-translational modifications was beyond the scope of this study.

A major limitation of the study is the timing of the sample collection. The initial pilot study was not designed to identify differences between ischemia and reperfusion and ideally lung biopsies should have been taken immediately before and after reperfusion occurred. Additionally the timing may be suboptimal for detecting changes which drive lung injury following CPB. A study by Hepponstall examining the plasma proteome following CPB found changes in C-reactive protein and hepatoglobin peaked at 12-24 hours following surgery [28]. This is reflected in the differences in results between the Luminex measure of cytokines in the plasma and the lung biopsy proteomics. In the biopsies collected immediately post-surgery there was no significant increases in the levels of inflammatory cytokines detected, which contrasted with the significant increases in the plasma samples collected 24 hours later, reflecting the several hours of transcription, translation and post-translational modification required for fully mature cytokines to be produced. However, as shown by our previous publication on LFV and CPB inflammatory signals, such as NF-κB were significantly higher immediately after surgery in the lung biopsies [14]. However, for practical reasons, later timepoints could not be directly measured in the lung.

Summary

LFV increased pulmonary, but not systemic inflammation, following CPB. Semi-biased transcriptomic and proteomic analysis of lung biopsies suggest that ischemia is the principle driver of pulmonary inflammation following CPB and that LFV,

possibly through reduced blood flow through the bronchial artery and increased surgery time, further enhances pulmonary ischemia and inflammation.

Sources of Funding

The work was supported by a project grant by the British Heart Foundation (BHF) Grant PG/13/9/29990 and the National Institute for Health Research [NIHR] Biomedical Research Centre at University Hospitals Bristol NHS Foundation Trust and the University of Bristol. The views expressed in this publication are those of the author(s) and not necessarily those of the NHS, the National Institute for Health Research or the Department of Health and Social Care.

Acknowledgements

The authors would like to thank Nandor Marczin for their help finalising the manuscript and co-supervision of JHB.

Statement of the contribution

Substantial contributions to the conception or design of the work; or the acquisition, analysis, or interpretation of data for the work: ALD, EAJ, RG, POB, JHB, KJH, ADP, PL, EJ, BR

Drafting the work or revising it critically for important intellectual content: ALD, EAJ, KJH, ADP, PL, FF, GDA, SM, IMA

Final approval of the version to be published: ALD, EAJ, FF, GDA, IMA

Agreement to be accountable for all aspects of the work in ensuring that questions related to the accuracy or integrity of any part of the work are appropriately investigated and resolved: ALD, EAJ, FF, GDA, IMA

Conflicts of interest

None declared

1

2

References:

[1] B. Bridgewater, B. Keogh, R. Kinsman, P. Walton, SCTS 6th National Adult Cardiac Surgical Database Report 2008, 2008. https://doi.org/10.1016/j.healun.2014.04.010.

[2] R.A. Bronicki, M. Hall, Cardiopulmonary Bypass-Induced Inflammatory Response: Pathophysiology and Treatment., Pediatr. Crit. Care Med. 17 (2016) S272-8. https://doi.org/10.1097/PCC.0000000000000759.

[3] C. Schlensak, T. Doenst, S. Preusser, M. Wunderlich, M. Kleinschmidt, F. Beyersdorf, Cardiopulmonary bypass reduction of bronchial blood flow: a potential mechanism for lung injury in a neonatal pig model., J. Thorac. Cardiovasc. Surg. 123 (2002) 1199–1205.

[4] C. Schlensak, T. Doenst, S. Preusser, M. Wunderlich, M. Kleinschmidt, F. Beyersdorf, Bronchial artery perfusion during cardiopulmonary bypass does not prevent ischemia of the lung in piglets: assessment of bronchial artery blood flow with fluorescent microspheres., Eur. J. Cardiothorac. Surg. 19 (2001) 322–326.

[5] P.J. Chai, J.A. Williamson, A.J. Lodge, C.W. Daggett, J.E. Scarborough, J.N. Meliones, I.M. Cheifetz, J.J. Jaggers, R.M. Ungerleider, Effects of ischemia on pulmonary dysfunction after cardiopulmonary bypass., Ann. Thorac. Surg. 67 (1999) 731–735.

[6] J.M. Dodd-o, L.E. Welsh, J.D. Salazar, P.L. Walinsky, E.A. Peck, J.G. Shake, D.J. Caparrelli, B.T. Bethea, S.M. Cattaneo, W.A. Baumgartner, D.B. Pearse, Effect of bronchial artery blood flow on cardiopulmonary bypass-induced lung injury., Am. J. Physiol. Heart Circ. Physiol. 286 (2004) H693-700.

https://doi.org/10.1152/ajpheart.00888.2003.

[7] F. Bagheri, V. Khori, A.M. Alizadeh, S. Khalighfard, S. Khodayari, H. Khodayari, Reactive oxygen species-mediated cardiac-reperfusion injury: Mechanisms and therapies., Life Sci. 165 (2016) 43–55. https://doi.org/10.1016/j.lfs.2016.09.013.

[8] E. Pantazi, M. Bejaoui, E. Folch-Puy, R. Adam, J. Rosello-Catafau, Advances in treatment strategies for ischemia reperfusion injury., Expert Opin. Pharmacother. 17 (2016) 169–179. https://doi.org/10.1517/14656566.2016.1115015.

[9] B.P. Van Putte, J. Kesecioglu, J.M.H. Hendriks, V.P. Persy, E. van Marck, P.E.Y. Van Schil, M.E. De Broe, Cellular infiltrates and injury evaluation in a rat model of warm pulmonary ischemia-reperfusion., Crit. Care. 9 (2005) R1-8. https://doi.org/10.1186/cc2992.

[10] P.B. Anning, Y. Chen, N.J. Lamb, S. Mumby, G.J. Quinlan, T.W. Evans, J.M. Gutteridge, Iron overload upregulates haem oxygenase 1 in the lung more rapidly than in other tissues., FEBS Lett. 447 (1999) 111–114.

[11] S. Mumby, T.W. Koh, J.R. Pepper, J.M. Gutteridge, Risk of iron overload is decreased in beating heart coronary artery surgery compared to conventional bypass., Biochim. Biophys. Acta. 1537 (2001) 204–210.

[12] H. Imura, M. Caputo, K. Lim, M. Ochi, M.S. Suleiman, K. Shimizu, G.D. Angelini, Pulmonary injury after cardiopulmonary bypass: Beneficial effects of low-frequency mechanical ventilation, J. Thorac. Cardiovasc. Surg. 137 (2009) 1530–1537. https://doi.org/10.1016/j.jtcvs.2008.11.014.

[13] A.B. Durukan, H.A. Gurbuz, N. Salman, E.U. Unal, H.I. Ucar, C.E.M. Yorgancioglu, Ventilation during cardiopulmonary bypass did not attenuate

inflammatory response or affect postoperative outcomes., Cardiovasc. J. Afr. 24 (2013) 224–230. https://doi.org/10.5830/CVJA-2013-041.

[14] F. Fiorentino, E. Al Jaaly, A. Durham, I. Adcock, G. Lockwood, E. Jazrawi, C. Rogers, R. Ascione, B. Reeves, G. Angelini, Low frequency ventilation during cardiopulmonary bypass for lung protection: A randomised controlled trial, J. Card. Surg. (2019). https://doi.org/10.1111/jocs.14044.

[15] E.G. Bligh, W.J. Dyer, A Rapid Method Of Total Lipid Extraction And Purification, Can. J. Biochem. Physiol. 37 (1959) 911–917. https://doi.org/10.1139/o59-099.

[16] A.D. Postle, D.C. Wilton, A.N. Hunt, G.S. Attard, Probing phospholipid dynamics by electrospray ionisation mass spectrometry, Prog. Lipid Res. 46 (2007) 200—224. https://doi.org/10.1016/j.plipres.2007.04.001.

[17] H. Mi, S. Poudel, A. Muruganujan, J.T. Casagrande, P.D. Thomas, PANTHER version 10: expanded protein families and functions, and analysis tools., Nucleic Acids Res. 44 (2016) D336-42. https://doi.org/10.1093/nar/gkv1194.

[18] M. Ficial, C. Antonaglia, M. Chilosi, M. Santagiuliana, A.-O. Tahseen, D. Confalonieri, L. Zandona, R. Bussani, M. Confalonieri, Keratin-14 expression in pneumocytes as a marker of lung regeneration/repair during diffuse alveolar damage., Am. J. Respir. Crit. Care Med. 189 (2014) 1142–1145. https://doi.org/10.1164/rccm.201312-2134LE.

[19] K.M. Ridge, L. Linz, F.W. Flitney, E.R. Kuczmarski, Y.-H. Chou, M.B. Omary, J.I. Sznajder, R.D. Goldman, Keratin 8 phosphorylation by protein kinase C delta regulates shear stress-mediated disassembly of keratin intermediate filaments in alveolar epithelial cells., J. Biol. Chem. 280 (2005) 30400–30405. https://doi.org/10.1074/jbc.M504239200.

[20] S. Sivaramakrishnan, J. V DeGiulio, L. Lorand, R.D. Goldman, K.M. Ridge, Micromechanical properties of keratin intermediate filament networks, Proc. Natl. Acad. Sci. 105 (2008) 889–894. https://doi.org/10.1073/pnas.0710728105.

[21] D. Paparella, T.M. Yau, E. Young, Cardiopulmonary bypass induced inflammation: pathophysiology and treatment. An update., Eur. J. Cardiothorac. Surg. 21 (2002) 232–244.

[22] M. Caputo, A. Mokhtari, C.A. Rogers, N. Panayiotou, Q. Chen, M.T. Ghorbel, G.D. Angelini, A.J. Parry, C. M., M. A., R. C.A., P. N., C. Q., G. M.T., A. G.D., P. A.J., The effects of normoxic versus hyperoxic cardiopulmonary bypass on oxidative stress and inflammatory response in cyanotic pediatric patients undergoing open cardiac surgery : A randomized controlled trial, J. Thorac. Cardiovasc. Surg. 138 (2010) 206–214. https://doi.org/10.1016/j.jtcvs.2008.12.028.The.

[23] J. Nanduri, G. Yuan, G.K. Kumar, G.L. Semenza, N.R. Prabhakar, Transcriptional responses to intermittent hypoxia., Respir. Physiol. Neurobiol. 164 (2008) 277–281. https://doi.org/10.1016/j.resp.2008.07.006.

[24] A.S. Slutsky, R. V Marco, Ventilator-Induced Lung Injury, N. Engl. J. Med. 369 (2013) 2126–2136. https://doi.org/10.1056/NEJMra1208707.

[25] C. Schlensak, F. Beyersdorf, Lung injury during CPB: pathomechanisms and clinical relevance, Interact. Cardiovasc. Thorac. Surg. . 4 (2005) 381–382. https://doi.org/10.1510/icvts.2005.117853.

[26] A.P. Diz, M. Truebano, D.O.F. Skibinski, The consequences of sample pooling in proteomics: an empirical study., Electrophoresis. 30 (2009) 2967–2975. https://doi.org/10.1002/elps.200900210.

[27] K.A. Dora, C.P. Stanley, E. Al Jaaly, F. Fiorentino, R. Ascione, B.C. Reeves, G.D. Angelini, Isolated Human Pulmonary Artery Structure and Function Pre- and Post-Cardiopulmonary Bypass Surgery, J. Am. Hear. Assoc. Cardiovasc. Cerebrovasc. Dis. 5 (2016) e002822. https://doi.org/10.1161/JAHA.115.002822.

[28] M. Hepponstall, V. Ignjatovic, S. Binos, C. Attard, V. Karlaftis, Y. d'Udekem, P. Monagle, I.E. Konstantinov, Cardiopulmonary bypass changes the plasma proteome in children undergoing tetralogy of Fallot repair, Perfusion. 30 (2015) 556–564. https://doi.org/10.1177/0267659114566065.

Figure Legends:

Figure 1. Cytokine levels following surgery.

Plasma was extracted from the blood of patients collected after anaesthetic induction but before the cardio-pulmonary bypass (CPB) procedure (pre-CPB), and at 24hrs post-operation (post-CPB). Patients who underwent CPB with lungs left collapsed shown in black (n=18). Patients shown in grey (n=18) received CPB with low frequency ventilation (LFV). Concentrations of **(A)** IL-6, **(B)** IL-8, **(C)** IL-10, **(D)** IL-1β and **(E)** MCP-1 in the plasma were quantified with a multiplex assay. Data was analysed Freidman Test statistical analysis with Dunn's multiple comparison post-test; **p<0.01, ***p<0.001, ****p<0.0001.

Figure 2. Measurements in blood plasma following surgery.

Plasma samples were measured at various timepoints following surgery, **(A)** cell free heme in the patients undergoing CPB with lungs left collapsed (n=18), **(B)** heme in patients undergoing CPB with LFV (n=18) **(C)** oxidation reduction potential (ORP) **(D)** anti-oxidant capacity (AOC). The control group is shown in black and the LFV group in grey. Data from both patient groups were combined to examine the effects of the CPB circuit on **(E)** ORP and **(F)** AOC. Data were analysed using Freidman Test statistical analysis with Dunn's multiple comparison post-test *p<0.05, **p<0.01, ***p<0.001, ****p<0.0001.

Figure 3. Measurements in lung biopsies following surgery.

(A) Hypoxia inducible factor 1 alpha (*HIF1A*) gene expression in lung biopsies pre- and post-surgery using either CPB with lungs left collapsed or with LFV. *HIF1A* gene expression (normalised to 18S) was significantly increased (the median gene expression doubled) in lung tissue following CPB, with (n=18) or without LFV (n=18). LFV biopsies had significantly higher levels of *HIF1A* gene expression compared to biopsies from patients who underwent CPB with lungs left collapsed. Lung biopsies were taken prior to bypass (Pre) and after surgery, immediately before reperfusion (Post). n=18 in each group of patients *$p<0.05$, **$p<0.01$ comparing groups post-surgery, Wilcoxon matched-pairs signed rank test.

(B) Total Heme in lung biopsy samples from both groups, both pre- and post-surgery. Whilst heme levels were not significantly altered in the biopsies from patients undergoing CPB with lungs left collapsed they were significantly reduced in the biopsies from patients undergoing CPB with LFV following surgery. n=18 in each group of patients *$p<0.05$, **$p<0.01$ comparing groups post-surgery, Wilcoxon matched-pairs signed rank test.

Figures:
Figure 1.

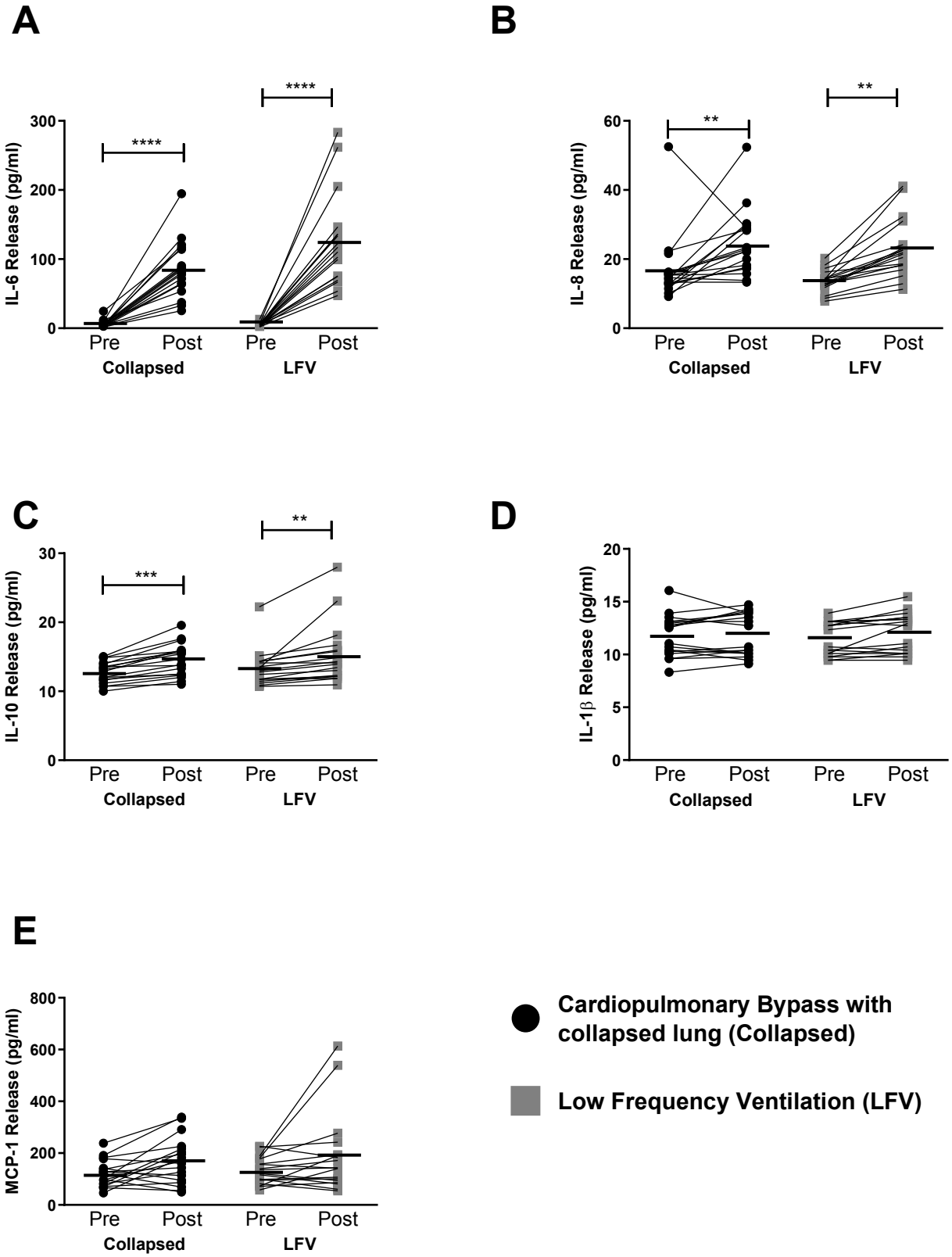

Figure 2.

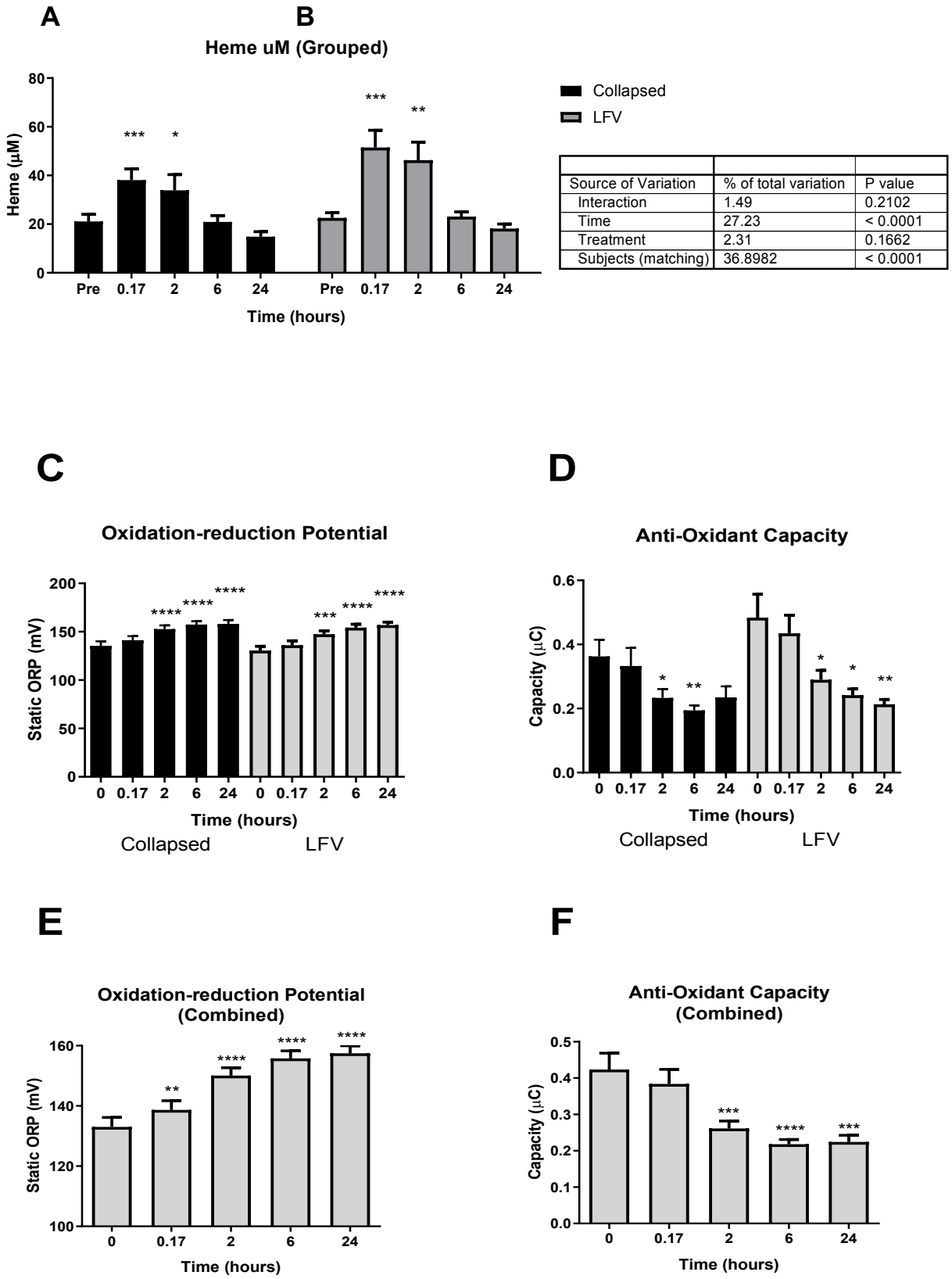

Source of Variation	% of total variation	P value
Interaction	1.49	0.2102
Time	27.23	< 0.0001
Treatment	2.31	0.1662
Subjects (matching)	36.8982	< 0.0001

Figure 3.

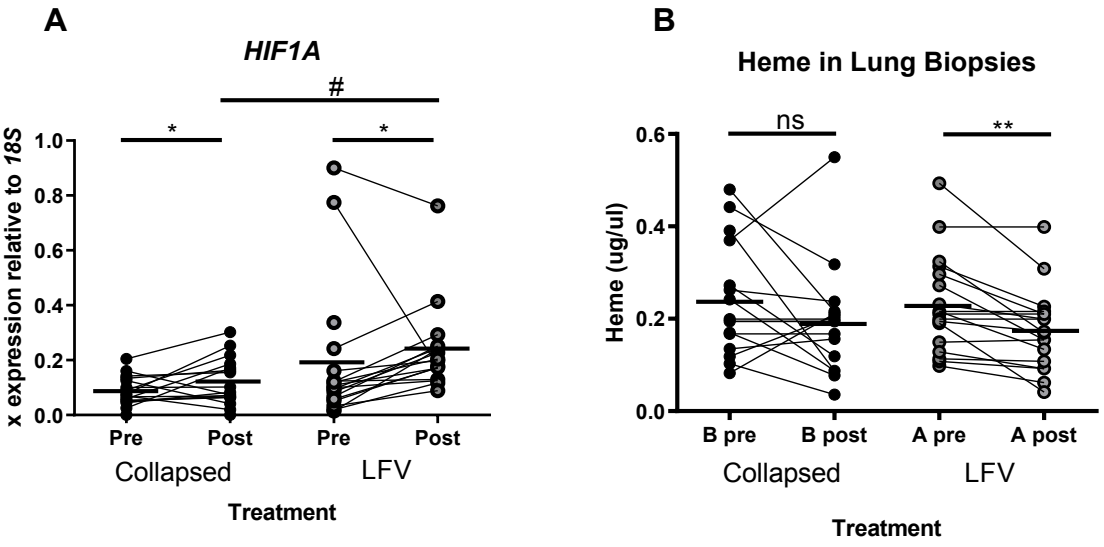
A
HIF1A
#
*
*
x expression relative to 18S
1.0
0.8
0.6
0.4
0.2
0.0
Pre
Post
Pre
Post
Collapsed
LFV
Treatment
B
Heme in Lung Biopsies
ns
**
Heme (ug/ul)
0.6
0.4
0.2
0.0
B pre
B post
A pre
A post
Collapsed
LFV
Treatment

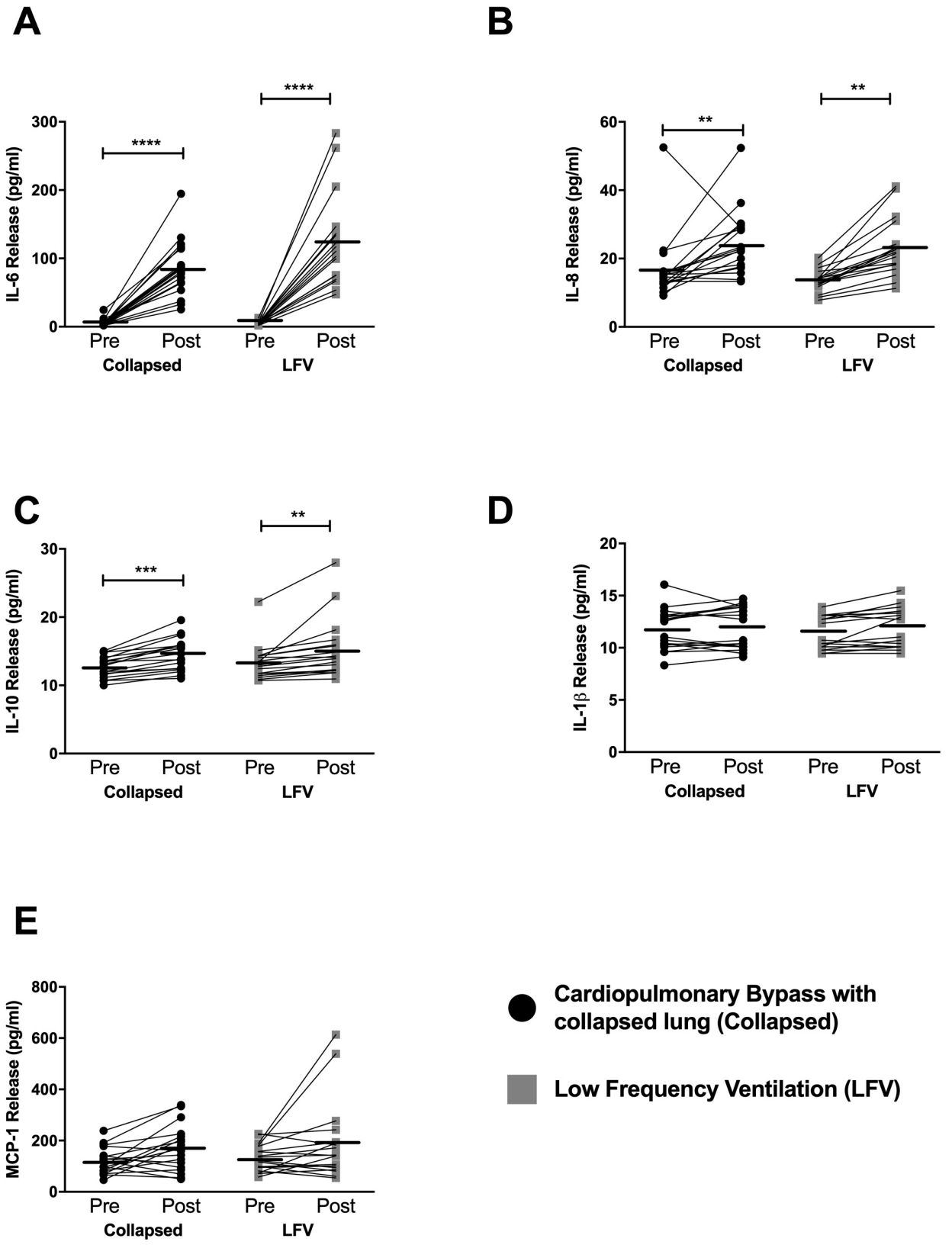
A
B
C
D
E
IL-6 Release (pg/ml)
IL-8 Release (pg/ml)
IL-10 Release (pg/ml)
IL-1β Release (pg/ml)
MCP-1 Release (pg/ml)
Pre
Post
Collapsed
LFV
Cardiopulmonary Bypass with collapsed lung (Collapsed)
Low Frequency Ventilation (LFV)

A

B

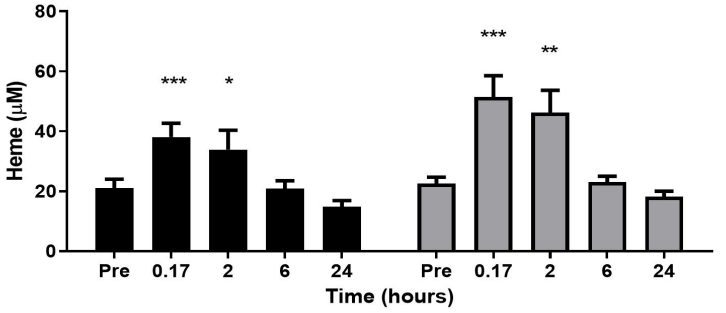

Source of Variation	% of total variation	P value
Interaction	1.489	0.4871
Time	27.23	<0.0001
Treatment	2.315	0.0218

C

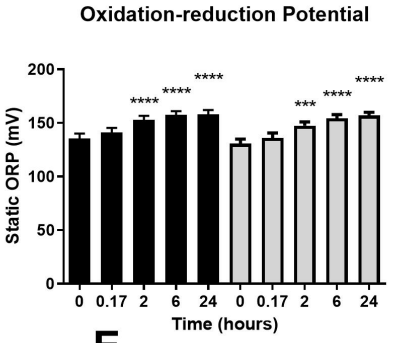

D

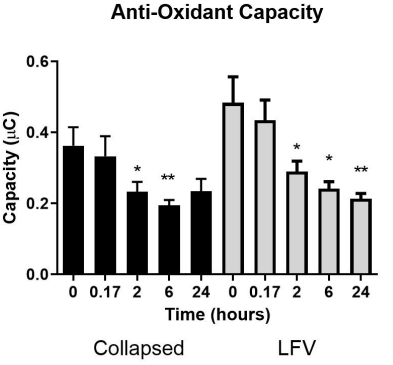

E llapsed LFV

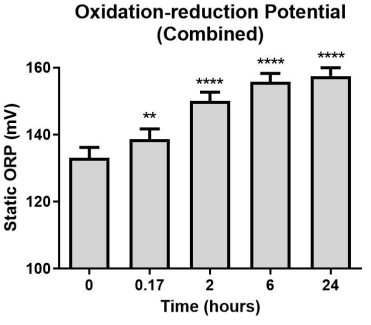

F

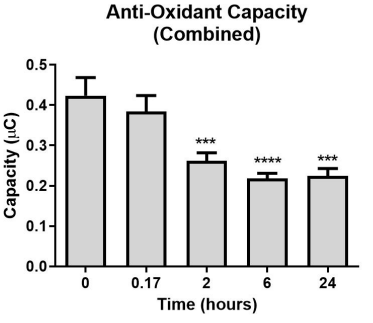

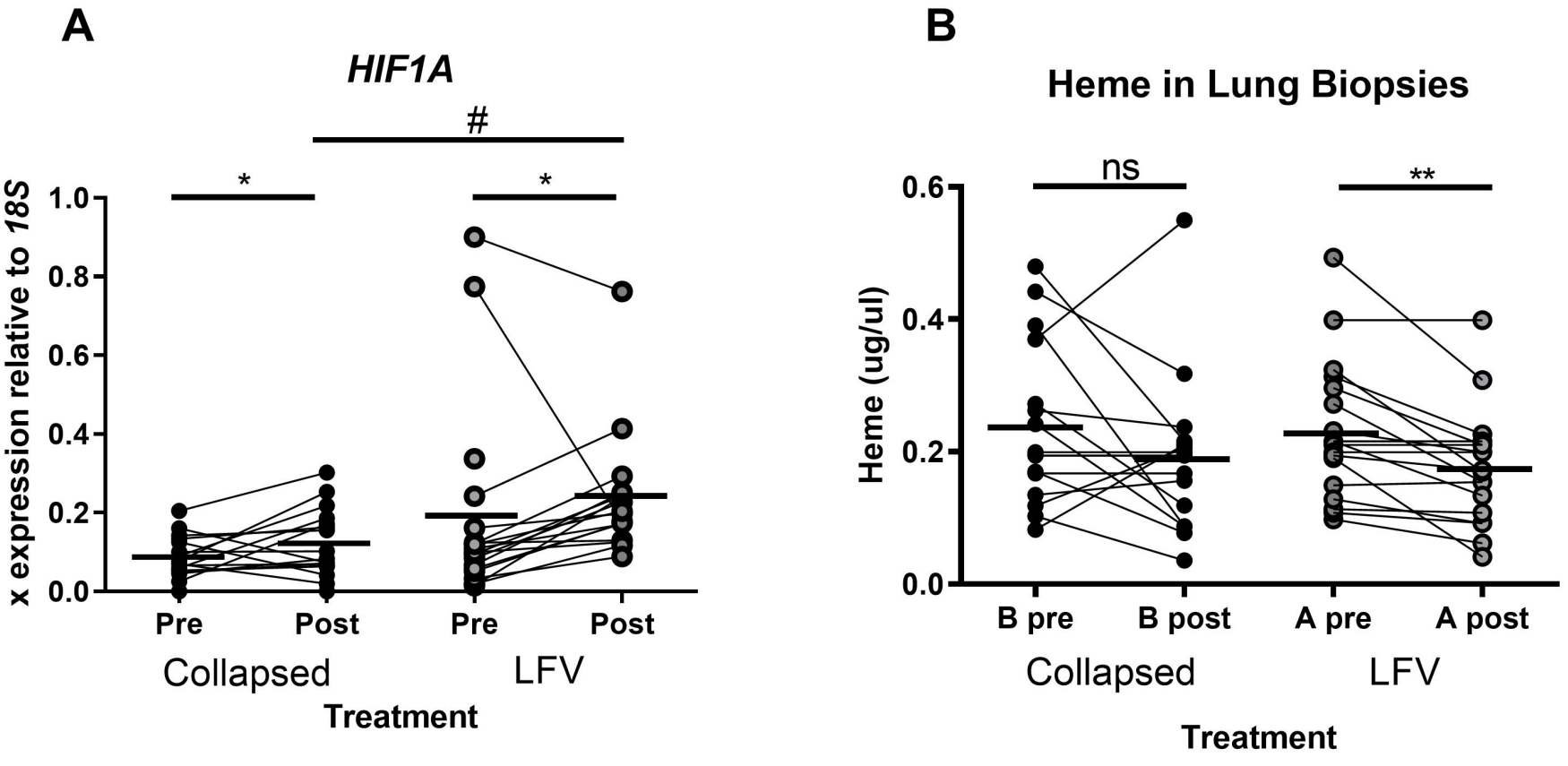
A
HIF1A
#
*
*
x expression relative to 18S
1.0
0.8
0.6
0.4
0.2
0.0
Pre
Post
Pre
Post
Collapsed
LFV
Treatment
B
Heme in Lung Biopsies
ns
**
Heme (ug/ul)
0.6
0.4
0.2
0.0
B pre
B post
A pre
A post
Collapsed
LFV
Treatment

Credit Author Statement

Andrew Durham: Conception, data curation, Investigation; Formal analysis, Methodology; Project administration; Supervision; Visualization; Roles/Writing – original draft; Writing – review & editing

Emad Al Jaaly: Methodology; Project administration; Roles/Writing – original draft;

Rebecca Graham: Investigation;

Peter Brook: Investigation;

Julie Bae: Investigation;

Kate Heesom: Investigation; Formal analysis, Roles/Writing – original draft;

Tony Postle: Investigation; Formal analysis, Roles/Writing – original draft;

Paul Lavender: Investigation; Formal analysis, Roles/Writing – original draft;

Elen Jazrawi: Investigation;

Barney Reeves: Formal analysis, Roles/Writing – original draft;

Franscesca Fiorentino: Formal analysis, Roles/Writing – original draft;

Sharon Mumby: Investigation; Supervision;

Gianni Angelini: Conception; Resources; Funding acquisition; Methodology; Project administration; Supervision; Visualization; Roles/Writing – original draft; Writing – review & editing

Ian Adcock: Conception,Methodology; Project administration; Supervision; Visualization; Roles/Writing – original draft; Writing – review & editing

Author Agreement Form – International Journal of Cardiology

Manuscript Title: **Multi-omic analysis of the effects of low frequency ventilation during cardiopulmonary bypass surgery.**

List of all Authors: **Durham AL, Al Jaaly E, Graham R, Brook PO, Bae JH, Heesom KJ, Postle AD, Lavender P, Jazrawi E, Reeves B, Fiorentino F, Mumby S, Angelini GD, Adcock IM.**

Corresponding Author: **Angelini GD**

This statement is to certify that all authors have seen and approved the manuscript being submitted, have contributed significantly to the work, attest to the validity and legitimacy of the data and its interpretation, and agree to its submission to the *International Journal of Cardiology*.

We attest that the article is the Authors' original work, has not received prior publication and is not under consideration for publication elsewhere. We adhere to the statement of ethical publishing as appears in the International of Cardiology (citable as: Shewan LG, Rosano GMC, Henein MY, Coats AJS. A statement on ethical standards in publishing scientific articles in the International Journal of Cardiology family of journals. Int. J. Cardiol. 170 (2014) 253-254 DOI:10.1016/j.ijcard.2013.11).

On behalf of all Co-Authors, the corresponding Author shall bear full responsibility for the submission. Any changes to the list of authors, including changes in order, additions or removals will require the submission of a new author agreement form approved and signed by all the original and added submitting authors.

All authors are requested to disclose any actual or potential conflict of interest including any financial, personal or other relationships with other people or organizations within three years of beginning the submitted work that could inappropriately influence, or be perceived to influence, their work. If there are no conflicts of interest, the COI should read: “The authors report no relationships that could be construed as a conflict of interest”.

Supplemental Data:

Multi-omic analysis of the effects of low frequency ventilation during cardiopulmonary bypass surgery.

Durham AL PhD[1], Al Jaaly E MD[2], Graham R MSc[1], Brook PO MSc[1], Bae JH BSc[1], Heesom KJ PhD[3], Postle AD PhD[4], Lavender P PhD[5], Jazrawi E BSc[1], Reeves B DPhil[2], Fiorentino F PhD[2], Mumby S PhD[1], Angelini GD MD[2,6], Adcock IM PhD[1].

Supplemental methods:

Transcriptomics:

For RNA extraction biopsies were placed in in RLT buffer (Qiagen) and homogenized using Precellys® ceramic beads (Cayman Chemicals, Cambridge, UK). Subsequently RNA was extracted using RNeasy extraction kit following manufacturer's instructions (Qiagen, Manchester, UK).

RNA was quantified by NanoDrop spectrophotometer (ThermoFisher, Waltham, MA, USA) and quality was checked by LabChip® spectrophotometer (Perkin Elmer). Subsequently RNA was amplified, converted to cDNA using the cDNA Ovation Pico WTA System (NuGen, San Carlos, CA, USA) and biotin labelled, using the Encore BiotinIL Module (Nugen), following the manufacturer's instructions. The cDNA was quantified and qualified, as above, and gene expression was measured using the Affymetrix GeneChip Human Gene 1.0 ST Array (ThermoFisher) following the manufacturer's instructions. Microarray data was

analysed using Partek Genomics Suite 6.6 (Partek GS, St. Louis, MI, USA) software and PANTHER gene ontology.[1]

RNA samples were also quantified using RT-qPCR. In brief the RNA concentration was determined using a NanoDrop 2000c spectrophotometer and standardised to 50ng/μL. Reverse transcription to create single stranded cDNA was performed using a high-capacity cDNA kit (Applied Biosystems, Foster City, CA, USA), following the manufacturer's instructions. qPCR was performed using a Rotor-Gene 3000 PCR machine (Corbett Research, Cambridge, UK) using a QuantiTect SYBR Green PCR kit and normalised to *18S* rRNA.

Proteomics:

Protein was extracted as described previously. In brief samples were homogenized in RIPA buffer (Sigma Aldrich, Poole, UK) containing HALT protease and phosphatase inhibitors (ThermoFisher, Paisley, UK) using Precellys® ceramic beads (Cayman Chemicals). After 30 minutes incubation at 4°C the samples were centrifuged (13,000g, 5 minutes, 4°C).

Supernatants from each group were quantified against a standard curve using the bininchoninic acid (BCA) assay (Sigma Aldrich) and equal amounts from each sample were pooled and changes in protein expression analysed using tandem mass tagging (TMT), as described previously.[2]

TMT Labelling and cation exchange chromatography

Aliquots of 100µg of each sample were digested with trypsin (2.5µg trypsin per 100µg protein; 37°C, overnight) and labelled with Tandem Mass Tag (TMT) sixplex reagents according to the manufacturer's protocol (Thermo Fisher Scientific, Loughborough, LE11 5RG, UK). After labelling, samples were pooled and a 50µg aliquot evaporated to dryness and resuspended in Buffer A (10mM KH2PO4, 25%MeCN pH3) prior to fractionation by strong cation exchange using an Ettan LC system (GE Healthcare). In brief, the sample was loaded onto a PolysulphoethylA column (100 x 2.1mm, 5µm, 200A; PolyLC Inc.) in buffer A and peptides eluted with an increasing gradient of buffer B (10mM KH2PO4, 25%MeCN 1M KCl pH3) from 0-100% over 30 minutes. The resulting fractions were evaporated to dryness, resuspended in 5% formic acid and then desalted using SepPak cartridges according to the manufacturer's instructions (Waters, Milford, Massachusetts, USA)). Eluate from the SepPak cartridge was again evaporated to dryness and resuspended in 1% formic acid prior to analysis by nano-LC MSMS using an LTQ-Orbitrap Velos Mass Spectrometer.

Nano-LC Mass Spectromerty

Cation exchange fractions were further fractionated using an Ultimate 3000 nanoHPLC system in line with an LTQ-Orbitrap Velos mass spectrometer (Thermo Scientific). In brief, peptides in 1% (vol/vol) formic acid were injected onto an Acclaim PepMap C18 nano-trap column (Thermo Scientific). After washing with 0.5% (vol/vol) acetonitrile 0.1% (vol/vol) formic acid peptides were resolved on a 250 mm × 75 µm Acclaim PepMap C18 reverse phase analytical column (Thermo Scientific) over a 150 min. organic gradient, using 7 gradient segments (1-6% solvent B over 1min., 6-15% B over 58min., 15-32%B

over 58min., 32-40%B over 5min., 40-90%B over 1min., held at 90%B for 6min and then reduced to 1%B over 1min.) with a flow rate of 300 nl min^{-1}. Solvent A was 0.1% formic acid and Solvent B was aqueous 80% acetonitrile in 0.1% formic acid. Peptides were ionized by nano-electrospray ionization at 2.0kV using a stainless-steel emitter with an internal diameter of 30 μm (Thermo Scientific) and a capillary temperature of 250°C. Tandem mass spectra were acquired using an LTQ- Orbitrap Velos mass spectrometer controlled by Xcalibur 2.1 software (Thermo Scientific) and operated in data-dependent acquisition mode. The Orbitrap was set to analyze the survey scans at 60,000 resolution (at m/z 400) in the mass range m/z 300 to 1800 and the top ten multiply charged ions in each duty cycle selected for MS/MS fragmentation using higher-energy collisional dissociation (HCD) with normalized collision energy of 45%, activation time of 0.1 ms and at a resolution of 7500 within the Orbitrap. Charge state filtering, where unassigned precursor ions were not selected for fragmentation, and dynamic exclusion (repeat count, 1; repeat duration, 30s; exclusion list size, 500) were used.

Data Analysis

The raw data files were processed and quantified using Proteome Discoverer software v1.2 (Thermo Scientific) and searched against the UniProt Human database using the SEQUEST algorithm. Peptide precursor mass tolerance was set at 10ppm, and MS/MS tolerance was set at 20mmu. Search criteria included oxidation of methionine (+15.9949) as a variable modification and carbamidomethylation of cysteine (+57.0214) and the addition of the TMT 6Plex mass tag (+229.163) to peptide N-termini and lysine as fixed modifications.

Searches were performed with full tryptic digestion and a maximum of 1 missed cleavage was allowed. The reverse database search option was enabled and all peptide data was filtered to satisfy false discovery rate (FDR) of 5%.

Lipidomics:

Lung tissue was weighed and homogenised on ice in 1.6ml of 0.9% saline together with 20µl of the anti-oxidant butylated hydroxyl toluene (BHT) (20 mg/ml in methanol), using a Heidolph Silent Crusher S. The homogenised lung samples were stored at -80^{o}C for subsequent lipid extraction. An aliquot of lung homogenate (800 µl) was lipid extracted with dichloromethane and methanol[3] after addition of internal quantification standards (PC14:0/14:0 10nmol, PE14:0/14:0 4nmol, TAG14:0/14:0/14:0 10nmol, PG14:0/14:0 2nmol, PS14:0/14:0 2nmol, PS14:0/14:0 2nmole, CE17:0 1nmol, CL14:0/14:0/14:0/14:0/14:0 1nmol) in 100µl methanol. The dichloromethane fraction was dried under nitrogen gas and the resultant extract was analysed using a Waters Xevo TQ mass spectrometer (Waters, Wythenshaw, UK). Samples were introduced to the mass spectrometer by syringe-driven direct infusion and the various lipid classes analysed by a comprehensive platform of diagnostic precursor and neutral loss scans as described previously.[4] Mass spectrometry results were initially processed by MassLynx software and subsequently quantified by dedicated Excel macro programmes.

Supplemental references:

[1] H. Mi, S. Poudel, A. Muruganujan, J.T. Casagrande, P.D. Thomas, PANTHER version 10: expanded protein families and functions, and analysis tools., Nucleic Acids Res. 44 (2016) D336-42. https://doi.org/10.1093/nar/gkv1194.

[2] S. Abdul-Ghani, K.J. Heesom, G.D. Angelini, M.-S. Suleiman, Cardiac phosphoproteomics during remote ischemic preconditioning: a role for the sarcomeric Z-disk proteins., Biomed Res. Int. 2014 (2014) 767812. https://doi.org/10.1155/2014/767812.

[3] E.G. Bligh, W.J. Dyer, A Rapid Method Of Total Lipid Extraction And Purification, Can. J. Biochem. Physiol. 37 (1959) 911–917. https://doi.org/10.1139/o59-099.

[4] A.D. Postle, D.C. Wilton, A.N. Hunt, G.S. Attard, Probing phospholipid dynamics by electrospray ionisation mass spectrometry, Prog. Lipid Res. 46 (2007) 200—224. https://doi.org/10.1016/j.plipres.2007.04.001.

Supplemental Tables:

Table 1. Differentially expressed genes in lung following CBP with lungs left collapsed.

Gene expression was measured in lung biopsies taken immediately following induction of bypass and immediately prior to the commencement of reperfusion. Data are organised by ratio of gene expression of the post: pre-surgery samples from patients undergoing CPB with lungs left collapsed.

Gene Name	*p-value*	*Ratio (Post vs. pre surgery)*
CCL2	1.56E-17	6.7442
IL6	2.66E-13	6.59224
THBS1	2.69E-10	4.99284
IER3	3.45E-14	4.95907
EGR1	1.19E-11	4.85421
ADAMTS1	9.20E-13	4.52339
NAMPT	7.02E-14	4.38552
ZFP36	8.06E-13	4.24673
MT2A	9.45E-11	4.18274
AXUD1	6.87E-12	3.93191
PTGS2	1.89E-10	3.63922
GADD45B	7.16E-11	3.41388
CDKN1A	7.22E-13	3.39603
NFIL3	4.68E-14	3.38138
MYC	6.46E-13	3.37585

IL8	2.29E-09	3.11566
PIM1	1.77E-11	3.07144
RGS2	1.27E-09	3.05557
NR4A2	4.01E-10	3.03127
SIK1	4.11E-11	2.88863
CXCL2	1.13E-10	2.87649
FOSB	1.59E-05	2.85606
RNF122	3.23E-10	2.74991
BHLHB2	7.16E-10	2.69932
DUSP5	2.27E-10	2.61988
EGR3	6.07E-11	2.59004
NR4A3	4.53E-11	2.57595
SLC2A3	8.13E-09	2.44753
MIDN	7.50E-07	2.31974
FOS	1.52E-05	2.16802

Table 2. Altered transcriptomic pathways and processes altered by lungs left collapsed and LFV.

Table showing the pathways and biological processes activated during cardio-pulmonary bypass with lungs left collapsed (collapsed) or with low-frequency ventilation (LFV) during surgery. Data shows the fold enrichment compared to the expected gene number in the sample size. P values include Bonferroni correction for multiple comparisons.

	Collapsed		LFV		LFV vs. Collapsed		Combined Collapsed and LFV groups post vs. pre surgery	
Pathway	Fold-change	Adj P value	Fold-change	Adj P value	Fold-change	Adj P value	Fold-change	Adj P value
CCKR signalling map	+ 31.28	2.26E-08	+ 19.66	2.14E-10	+ 20.20	6.81E-03	+ 20.20	9.53E-07
Interleukin signaling pathway	+ 34.52	5.41E-05	+ 14.46	4.34E-03			+ 22.29	5.10E-04
p53 pathway	+ 23.06	4.81E-02	+ 12.88	4.46E-02			+ 19.86	8.22E-03
Inflammation mediated by chemokine and cytokine signaling pathway			+ 8.69	6.60E-04	13.39	3.30E-02		

Gonadotropin-releasing hormone receptor pathway			+ 8.44	3.27E-03				
Plasminogen activating cascade					+ 97.09	3.17E-02		
Oxidative Stress Response							+ 23.41	4.76E-02
Process								
Endoderm development			+ >100	3.66E-02			+ >100	1.53E-02
MAPK cascade			+ 7.75	3.16E-02			+ 11.95	4.62E-04
Cell death			+ 65.40	3.30E-02	+ >100	2.53E-02		
Response to stress			+ 4.28	2.23E-03			5.08	5.05E-03
Localization							+ 14.21	4.52E-02

Table 3. Differentially expressed genes in lung samples in the LFV group. The expression of the same genes in the lungs left collapsed (Collapsed) group is shown for comparison (where also significantly changed).

The data shows the genes that were significantly changed post-surgery comparing the pre- and post-surgery samples from the LFV group. Data are organised by ratio of gene expression of the post: pre-surgery samples. Also shown are the p-values and ratios for the same genes in the CPB group pre- and post-surgery.

Gene	*p-value (Post LFV post vs. pre LFV)*	*Ratio (Post LFV post vs. pre LFV)*	*p-value (Collapsed post vs. Collapsed pre)*	*Ratio (Collapsed post vs. Collapsed pre)*
EGR1	1.52E-10	4.31211	1.19E-11	4.85421
CCL2	3.14E-11	3.7367	1.56E-17	6.7442
ZFP36	2.33E-10	3.39726	8.06E-13	4.24673
IER3	5.24E-10	3.36618	3.45E-14	4.95907
FOSB	1.97E-06	3.23688	1.59E-05	2.85606
IL6	4.20E-07	3.20897	2.66E-13	6.59224
AXUD1	7.36E-09	2.97975	6.87E-12	3.93191
GADD45B	8.53E-09	2.84233	7.16E-11	3.41388
RGS2	9.57E-09	2.82692	1.27E-09	3.05557
PTGS2	2.02E-07	2.71364	1.89E-10	3.63922
NAMPT	2.76E-08	2.69011	7.02E-14	4.38552

ADAMTS1	3.20E-07	2.65546	9.20E-13	4.52339
THBS1	4.31E-05	2.58619	2.69E-10	4.99284
CDKN1A	2.66E-09	2.58471	7.22E-13	3.39603
NR4A2	4.81E-08	2.54051	4.01E-10	3.03127
MT2A	1.58E-05	2.3859	9.45E-11	4.18274
MYC	3.80E-08	2.34622	6.46E-13	3.37585
SIK1	2.79E-08	2.33506	4.11E-11	2.88863
DUSP5	1.37E-08	2.3046	2.27E-10	2.61988
CYR61	0.000139197	2.28028		
BHLHB2	1.21E-07	2.26944	7.16E-10	2.69932
MT1A	0.00023541	2.21719		
FOS	9.31E-06	2.21653	1.52E-05	2.16802
SLC2A3	1.90E-07	2.20188	8.13E-09	2.44753
NFIL3	5.29E-08	2.19547	4.68E-14	3.38138
IL8	1.23E-05	2.17884	2.29E-09	3.11566
PIM1	4.81E-07	2.172	1.77E-11	3.07144
CXCL2	7.34E-07	2.13394	1.13E-10	2.87649
DUSP1	0.000566532	2.12812		
CRISPLD2	0.000119155	2.12754		
MIDN	1.03E-05	2.087	7.50E-07	2.31974
NR4A3	1.67E-07	2.02404	4.53E-11	2.57595
EGR3	2.96E-07	2.00958	6.07E-11	2.59004
SGK	0.000488729	2.00601		
RNF122	3.46E-06	2.00402	3.23E-10	2.74991
TRIB1	0.000175232	2.0034		

MTE	0.000367452	1.91892		
CHSY1	7.99E-05	1.8969		
CEBPD	9.24E-06	1.89357		
LDLR	0.00117263	1.86047		
NR4A1	1.09E-07	1.85738		
GADD45A	9.63E-08	1.82664		
ERRFI1	0.000199363	1.82399		
RASD1	0.00262772	1.81266		
LOC441019	3.63E-05	1.80627		
ELL2	0.000212275	1.80179		
FOSL2	1.06E-06	1.79105		
MIR21	0.000263131	1.76523		
JUNB	9.80E-08	1.7545		
ATP1B3	0.000288746	1.74548		
MAT2A	0.0012663	1.73094		
SLC20A1	8.56E-05	1.72167		
MT1E	3.74E-05	1.71535		
B4GALT1	0.00558024	1.69002		
NFKBIZ	1.00E-05	1.68699		
ALDH1A3	0.00342271	1.68698		
OBFC2A	0.000204148	1.65775		
SPSB1	0.0011272	1.65691		
LOC387763	1.66E-05	1.64433		
NFKBIA	0.00184104	1.63908		
IL1B	4.37E-05	1.62737		

CXCR7	0.00129761	1.62714		
RHOU	6.78E-05	1.62591		
CCL8	0.000337713	1.62543		
APOLD1	0.000140595	1.61926		
SYT4	0.0240593	1.58715		
PLAU	9.09E-05	1.56036		
UAP1	3.77E-05	1.55889		
SOD2	0.00203168	1.51347		
MT1X	0.00693741	1.50511		
C2CD4B	0.000338994	1.49971		
NNMT	0.00555558	1.49559		
SERPINB2	0.00229441	1.45598		
TIMP1	0.0251605	1.42749		
RDH10	0.000361211	1.42187		
C13orf33	0.000883785	1.3788		
TRK1	0.0259384	1.32595		
TRQ1	0.00924457	1.3179		
PTX3	0.0140338	1.29593		

Table 4. Differentially expressed proteins identified by TMT, comparing CPB with lungs left collapsed and LFV.

The proteins highlighted in bold were not changed at baseline between the two groups.

Accession	# AAs	MW [kDa]	calc. pI	Collapsed /LFV	Description
Q15423	64	7.1	8.18	3.700	Serum amyloid A protein (Fragment)
B4DIF5	**345**	**39.2**	**8.92**	**2.478**	**cDNA FLJ55687, highly similar to Cell cycle control protein 50A**
P20851	**252**	**28.3**	**5.14**	**2.283**	**C4b-binding protein beta chain**
Q8IUL9	**105**	**11.5**	**6.05**	**2.251**	**Hemoglobin beta chain variant Hb.Sinai-Bel Air (Fragment)**
Q6VFQ6	**42**	**4.5**	**8.24**	**1.766**	**Hemoglobin beta chain (Fragment)**
Q92531	**187**	**19.7**	**6.32**	**1.712**	**P35-related protein (Fragment)**
Q3MIB5	**262**	**28.7**	**5.27**	**1.617**	**INMT protein (Fragment)**
P02774	**474**	**52.9**	**5.54**	**1.608**	**Vitamin D-binding protein**
B4DWJ7	155	17.5	8.37	1.597	cDNA FLJ54968
P11686	**197**	**21.0**	**6.65**	**1.583**	**Pulmonary surfactant-associated protein C**
Q5T619	**568**	**62.3**	**8.62**	**1.573**	**Zinc finger protein 648**
E5RGQ7	**148**	**16.8**	**8.88**	**1.563**	**Dematin (Fragment)**
S6BGD6	235	24.8	7.24	1.557	IgG L chain
Q6J1Z9	**90**	**9.6**	**9.50**	**1.540**	**Hemoglobin alpha 1 (Fragment)**

P02042	**147**	**16.0**	**8.05**	**1.522**	**Hemoglobin subunit delta**
Q6J1Z8	**42**	**4.5**	**9.38**	**1.507**	**Hemoglobin beta (Fragment)**
D3DTX7	885	84.7	6.24	0.664	Collagen, type I, alpha 1, isoform CRA_a
M0QZ50	**93**	**9.8**	**4.48**	**0.663**	**Microtubule-associated protein 1S**
P01861	327	35.9	7.36	0.662	Ig gamma-4 chain C region
A0A087WTA8	**1364**	**129.1**	**9.01**	**0.658**	**Collagen alpha-2(I) chain**
O76041	**1014**	**116.4**	**7.99**	**0.654**	**Nebulette**
P08519	4548	501.0	5.88	0.652	Apolipoprotein(a)
C9JNE5	191	21.7	9.61	0.648	Myeloid leukemia factor 1 (Fragment)
H3BRW3	109	11.7	9.96	0.636	FAD-linked sulfhydryl oxidase ALR
P27701	**267**	**29.6**	**5.24**	**0.636**	**CD82 antigen**
Q9NZ09	**502**	**55.0**	**5.11**	**0.635**	**Ubiquitin-associated protein 1**
A4FU00	317	35.6	5.81	0.634	SYT2 protein (Fragment)
B4DMJ5	242	27.3	4.50	0.634	cDNA FLJ53012, highly similar to Tubulin beta-7 chain
P07451	**260**	**29.5**	**7.34**	**0.633**	**Carbonic anhydrase 3**
Q6PII6	533	58.3	4.77	0.610	TMF1 protein (Fragment)
P35908	**639**	**65.4**	**8.00**	**0.603**	**Keratin, type II cytoskeletal 2 epidermal**
P01880	384	42.2	7.93	0.591	Ig delta chain C region
A2J1N5	94	10.4	9.13	0.590	Rheumatoid factor RF-ET6 (Fragment)
P81605	110	11.3	6.54	0.586	Dermcidin
Q7Z6I6	**1101**	**118.5**	**4.81**	**0.567**	**Rho GTPase-activating protein 30 SV=3**

P13761	266	29.8	7.44	0.562	HLA class II histocompatibility antigen, DRB1-7 beta chain
A8K9A9	638	71.3	8.22	0.521	cDNA FLJ77744, highly similar to Homo sapiens kallikrein B, plasma (Fletcher factor) 1 (KLKB1), mRNA
Q96Q06	**1357**	**134.3**	**8.73**	**0.519**	**Perilipin-4**
B3KMX3	270	28.5	4.73	0.497	cDNA FLJ12857 fis, clone NT2RP2003513, highly similar to Homo sapiens paralemmin (PALM),
Q15323	416	47.2	4.88	0.436	Keratin, type I cuticular Ha1
Q30167	266	30.0	7.75	0.373	HLA class II histocompatibility antigen, DRB1-10 beta chain
B7Z269	351	40.3	7.24	0.299	cDNA FLJ50754, highly similar to Voltage-dependent L-type calcium channel subunit alpha-1D
A0JNT2	**447**	**49.6**	**5.39**	**0.240**	**KRT83 protein**
A0A087X2I6	**404**	**46.1**	**4.84**	**0.206**	**Keratin, type I cuticular Ha3-II**
O76013	467	52.2	4.94	0.144	Keratin, type I cuticular Ha6
Q701L7	513	56.6	6.74	0.073	Type II hair keratin 2
Q9BYT5	123	12.9	7.81	0.072	Keratin-associated protein 2-2

Table 5. Differentially expressed genes in lung biopsies post CBP with collapsed lungs (Collapsed) versus post CBP+LFV (LFV).

The data shows the genes that were significantly changed post-surgery comparing the LFV and CPB with lungs collapsed groups. Data are organised by ratio of gene expression in the CPB:LFV groups. Also shown are the p-values and ratios for the same genes in the CPB and LFV groups pre- and post-surgery.

Gene	*p-value Collapsed vs. LFV)*	*Ratio (Collapsed vs. LFV)*	*p-value (Collapsed post vs. Collapsed pre)*	*Ratio (Collapsed post vs. Collapsed pre)*	*p-value (LFV post vs. LFV pre)*	*Ratio (LFV post vs. LFV pre)*
HLA-DRB5	0.0311729	1.69779				
MIR21	0.00716334	0.664162	0.00026313	1.76523	3.13E-08	2.5143
PLAU	0.00027089	0.663153	9.09E-05	1.56036	3.92E-10	2.18467
NAMPT	0.00887185	0.653954	2.76E-08	2.69011	7.02E-14	4.38552
CRISPLD2	0.0245826	0.65374	0.00011915	2.12754	2.77E-08	3.19182
SPSB1	0.00543046	0.652837	0.0011272	1.65691	3.46E-08	2.51871
PIM1	0.00237397	0.643988	4.81E-07	2.172	1.77E-11	3.07144
MT2A	0.0212365	0.64331	1.58E-05	2.3859	9.45E-11	4.18274
CYR61	0.0334855	0.642119	0.00013919	2.28028	1.35E-05	2.60616
PTX3	3.35E-05	0.633302	0.0140338	1.29593	3.50E-09	2.00809
NFIL3	0.00061884	0.630321	5.29E-08	2.19547	4.68E-14	3.38138
C13ORF33	4.01E-06	0.629229	0.00088378	1.3788	9.54E-13	2.24342

PTGS2	0.00877579	0.627638	2.02E-07	2.71364	1.89E-10	3.63922
OBFC2A	0.00039958	0.619068	0.00020414	1.65775	1.34E-09	2.46718
SERPINB2	6.89E-05	0.604865	0.00229441	1.45598	4.19E-10	2.37424
FST	3.24E-07	0.604399	0.0263664	1.22358	1.07E-09	1.87432
TRK1	9.80E-05	0.598732	0.0259384	1.32595	3.25E-08	2.16599
NNMT	0.00050317	0.598371	0.00555558	1.49559	2.12E-10	2.85178
IER3	0.00213579	0.585514	5.24E-10	3.36618	3.45E-14	4.95907
TRQ1	1.05E-06	0.575413	0.00924457	1.3179	3.91E-10	2.12356
ADAMTS1	0.00128987	0.560691	3.20E-07	2.65546	9.20E-13	4.52339
CCL2	0.00088664	0.560328	3.14E-11	3.7367	1.56E-17	6.7442
CCL8	8.14E-06	0.537271	0.00033771	1.62543	2.39E-12	2.99664
ALDH1A3	0.00014072	0.498751	0.00342271	1.68698	3.40E-09	3.22296
IL6	0.00081229	0.481974	4.20E-07	3.20897	2.66E-13	6.59224
THBS1	0.00091702	0.470781	4.31E-05	2.58619	2.69E-10	4.99284

Table 6:

Genes significantly altered in the combined CPB with collapsed lungs and LFV dataset (all patients) comparing biopsies taken before and immediately post-surgery (prior to reperfusion).

Probeset ID	p-value	Fold-Change (Post vs. Pre)	Fold-Change (Post vs. Pre)
ADAMTS1	2.29E-14	3.46579	Post up vs Pre
ALDH1A3	2.06E-08	2.33175	Post up vs Pre
AXUD1	7.62E-16	3.42288	Post up vs Pre
BHLHB2	1.27E-13	2.47507	Post up vs Pre
CCL2	5.10E-20	5.02006	Post up vs Pre
CCL8	9.21E-11	2.20699	Post up vs Pre
CDKN1A	2.13E-16	2.96273	Post up vs Pre
CEBPD	1.48E-12	2.29829	Post up vs Pre
CHSY1	2.26E-09	2.15588	Post up vs Pre
CRISPLD2	6.38E-10	2.6059	Post up vs Pre
CXCL2	3.47E-13	2.47755	Post up vs Pre
CYR61	9.06E-08	2.43778	Post up vs Pre
DUSP1	7.63E-07	2.21634	Post up vs Pre
DUSP5	1.01E-14	2.45719	Post up vs Pre
EGR1	6.78E-17	4.57514	Post up vs Pre
EGR3	1.29E-13	2.28143	Post up vs Pre
ELL2	9.39E-10	2.13515	Post up vs Pre
ERRFI1	7.92E-10	2.21222	Post up vs Pre
FOS	3.79E-09	2.19214	Post up vs Pre
FOSB	9.80E-10	3.04051	Post up vs Pre
FOSL2	1.28E-13	2.11261	Post up vs Pre

GADD45A	1.46E-14	2.10184	Post up vs Pre
GADD45B	4.21E-15	3.11502	Post up vs Pre
IER3	3.18E-17	4.08572	Post up vs Pre
IL6	1.54E-14	4.59938	Post up vs Pre
IL8	1.49E-11	2.60548	Post up vs Pre
LOC441019	4.99E-12	2.27893	Post up vs Pre
MIDN	5.01E-10	2.20029	Post up vs Pre
MIR21	2.24E-09	2.10673	Post up vs Pre
MT1A	4.47E-10	2.90963	Post up vs Pre
MT2A	2.60E-12	3.15905	Post up vs Pre
MTE	1.97E-09	2.35834	Post up vs Pre
MYC	1.82E-15	2.81434	Post up vs Pre
NAMPT	2.56E-16	3.43475	Post up vs Pre
NFIL3	1.39E-15	2.72465	Post up vs Pre
NNMT	3.81E-09	2.06521	Post up vs Pre
NR4A2	3.74E-14	2.77506	Post up vs Pre
NR4A3	5.09E-14	2.28338	Post up vs Pre
OBFC2A	7.07E-10	2.02236	Post up vs Pre
PIM1	1.76E-13	2.58286	Post up vs Pre
PTGS2	2.79E-13	3.14254	Post up vs Pre
RASD1	5.52E-07	2.12328	Post up vs Pre
RGS2	2.93E-14	2.93902	Post up vs Pre
RNF122	3.02E-12	2.34752	Post up vs Pre
SGK	9.65E-07	2.07768	Post up vs Pre
SIK1	4.42E-15	2.59714	Post up vs Pre
SLC2A3	8.98E-13	2.32146	Post up vs Pre
SPSB1	9.27E-09	2.04286	Post up vs Pre

THBS1	4.71E-11	3.59339	Post up vs Pre
TRIB1	3.44E-08	2.15623	Post up vs Pre
ZFP36	1.56E-17	3.79832	Post up vs Pre

Table 7:

Data showing the proteins changed between the pooled control CPB with collapsed lung and LFV groups immediately prior to surgery, with a 1.5x change cutoff. Only 2 proteins had a greater than 2x increase in the CPB group and 34 were 2x higher in the LFV group (shown in bold).

Accession	# AAs	MW [kDa]	calc. pI	Collapsed (Pre)/ LFV (Pre)	Description
Q15423	**64**	**7.1**	**8.18**	**4.664**	**Serum amyloid A protein (Fragment) OS=Homo sapiens PE=2 SV=1 - [Q15423_HUMAN]**
B7Z269	**351**	**40.3**	**7.24**	**3.939**	**cDNA FLJ50754, highly similar to Voltage-dependent L-type calcium channel subunit alpha-1D OS=Homo sapiens PE=2 SV=1 - [B7Z269_HUMAN]**
Q6P4A8	553	63.2	9.06	1.677	Phospholipase B-like 1 OS=Homo sapiens GN=PLBD1 PE=1 SV=2 - [PLBL1_HUMAN]
O96009	420	45.4	6.61	1.507	Napsin-A OS=Homo sapiens GN=NAPSA PE=1 SV=1 - [NAPSA_HUMAN]
F2X0V0	23	2.8	7.78	0.666	Truncated CD61 (Fragment) OS=Homo sapiens GN=ITGB3 PE=4 SV=1 - [F2X0V0_HUMAN]
Q96T46	76	8.4	7.14	0.666	Hemoglobin alpha 2 (Fragment) OS=Homo sapiens GN=HBA2 PE=3 SV=1 - [Q96T46_HUMAN]
Q96P70	1041	115.9	4.81	0.665	Importin-9 OS=Homo sapiens GN=IPO9 PE=1 SV=3 - [IPO9_HUMAN]
Q86Z07	374	41.7	9.14	0.664	Guanine nucleotide binding protein-like 1 OS=Homo sapiens GN=HSR1 PE=4 SV=1 - [Q86Z07_HUMAN]
Q9NWH4	148	16.9	11.09	0.664	cDNA FLJ10024 fis, clone HEMBA1000636 OS=Homo sapiens PE=2 SV=1 - [Q9NWH4_HUMAN]
Q7Z379	478	51.6	6.52	0.664	Putative uncharacterized protein DKFZp686K04218 (Fragment) OS=Homo sapiens GN=DKFZp686K04218 PE=1 SV=1 - [Q7Z379_HUMAN]
B4E0V3	947	107.2	6.11	0.663	cDNA FLJ61519, highly similar to Leukocyte common antigen (EC 3.1.3.48) OS=Homo sapiens PE=2 SV=1 - [B4E0V3_HUMAN]
P32456	591	67.2	5.71	0.661	Interferon-induced guanylate-binding protein 2 OS=Homo sapiens GN=GBP2 PE=1 SV=3 - [GBP2_HUMAN]
Q0PNF2	2570	275.3	6.49	0.661	FEX1 OS=Homo sapiens PE=2 SV=1 - [Q0PNF2_HUMAN]

Q5VW33	215	24.2	7.09	0.660	BRO1 domain-containing protein BROX (Fragment) OS=Homo sapiens GN=BROX PE=1 SV=1 - [Q5VW33_HUMAN]
A2MYC8	104	11.0	7.28	0.659	V5-2 protein (Fragment) OS=Homo sapiens GN=V5-2 PE=1 SV=1 - [A2MYC8_HUMAN]
F8WD82	762	88.1	6.95	0.659	Sodium channel protein type 7 subunit alpha OS=Homo sapiens GN=SCN7A PE=4 SV=1 - [F8WD82_HUMAN]
B2R4C9	102	11.2	9.52	0.659	cDNA, FLJ92044, highly similar to Homo sapiens death-associated protein (DAP), mRNA OS=Homo sapiens PE=2 SV=1 - [B2R4C9_HUMAN]
A8K6V3	1217	135.5	5.21	0.659	cDNA FLJ78677, highly similar to Homo sapiens splicing factor 3b, subunit 3, 130kDa (SF3B3), mRNA OS=Homo sapiens PE=2 SV=1 - [A8K6V3_HUMAN]
S6B2A1	184	20.4	5.52	0.658	IgG L chain OS=Homo sapiens PE=2 SV=1 - [S6B2A1_HUMAN]
Q9H3P7	528	60.6	5.06	0.658	Golgi resident protein GCP60 OS=Homo sapiens GN=ACBD3 PE=1 SV=4 - [GCP60_HUMAN]
C9JIN6	264	29.8	7.84	0.657	Transporter (Fragment) OS=Homo sapiens GN=SLC6A20 PE=3 SV=1 - [C9JIN6_HUMAN]
E5RHW5	125	13.1	5.39	0.657	Pulmonary surfactant-associated protein C (Fragment) OS=Homo sapiens GN=SFTPC PE=4 SV=3 - [E5RHW5_HUMAN]
F8WAW4	140	15.6	9.13	0.656	Enoyl-CoA delta isomerase 2, mitochondrial OS=Homo sapiens GN=ECI2 PE=1 SV=1 - [F8WAW4_HUMAN]
B8ZZ75	194	21.5	6.93	0.655	Aldose 1-epimerase OS=Homo sapiens GN=GALM PE=1 SV=1 - [B8ZZ75_HUMAN]
H3BML9	118	13.1	5.68	0.655	Myosin regulatory light chain 2, skeletal muscle isoform (Fragment) OS=Homo sapiens GN=MYLPF PE=4 SV=1 - [H3BML9_HUMAN]
P16157	1881	206.1	6.01	0.655	Ankyrin-1 OS=Homo sapiens GN=ANK1 PE=1 SV=3 - [ANK1_HUMAN]
A0A087WXZ6	250	28.9	9.00	0.655	High affinity immunoglobulin gamma Fc receptor IB (Fragment) OS=Homo sapiens GN=FCGR1B PE=4 SV=1 - [A0A087WXZ6_HUMAN]
P31942	346	36.9	6.87	0.654	Heterogeneous nuclear ribonucleoprotein H3 OS=Homo sapiens GN=HNRNPH3 PE=1 SV=2 - [HNRH3_HUMAN]
P40261	264	29.6	5.74	0.654	Nicotinamide N-methyltransferase OS=Homo sapiens GN=NNMT PE=1 SV=1 - [NNMT_HUMAN]
P15529	392	43.7	6.74	0.654	Membrane cofactor protein OS=Homo sapiens GN=CD46 PE=1 SV=3 - [MCP_HUMAN]
G3XAJ6	542	58.7	5.34	0.653	Raft-linking protein, isoform CRA_c OS=Homo sapiens GN=RFTN1 PE=1 SV=1 - [G3XAJ6_HUMAN]
H7BZW6	143	16.0	9.13	0.652	Histone deacetylase complex subunit SAP18 (Fragment) OS=Homo sapiens

					GN=SAP18 PE=1 SV=2 - [H7BZW6_HUMAN]
P19397	219	24.3	7.52	0.652	Leukocyte surface antigen CD53 OS=Homo sapiens GN=CD53 PE=1 SV=1 - [CD53_HUMAN]
Q9C055	306	35.6	7.50	0.652	Inositol polyphosphate-5-phosphatase (Fragment) OS=Homo sapiens GN=INPP5A PE=4 SV=1 - [Q9C055_HUMAN]
P16402	221	22.3	11.02	0.651	Histone H1.3 OS=Homo sapiens GN=HIST1H1D PE=1 SV=2 - [H13_HUMAN]
P01023	1474	163.2	6.46	0.650	Alpha-2-macroglobulin OS=Homo sapiens GN=A2M PE=1 SV=3 - [A2MG_HUMAN]
Q19UK3	33	3.7	8.09	0.648	Truncated coagulation factor IX (Fragment) OS=Homo sapiens GN=F9 PE=4 SV=1 - [Q19UK3_HUMAN]
Q59FC4	687	75.9	6.51	0.648	Presynaptic protein SAP97 variant (Fragment) OS=Homo sapiens PE=4 SV=1 - [Q59FC4_HUMAN]
Q15661	275	30.5	7.11	0.647	Tryptase alpha/beta-1 OS=Homo sapiens GN=TPSAB1 PE=1 SV=1 - [TRYB1_HUMAN]
D3JV43	68	7.4	8.78	0.646	C-X-C motif chemokine (Fragment) OS=Homo sapiens PE=3 SV=1 - [D3JV43_HUMAN]
H0YH87	916	98.1	9.41	0.639	Ataxin-2 (Fragment) OS=Homo sapiens GN=ATXN2 PE=1 SV=1 - [H0YH87_HUMAN]
B7Z7P4	547	59.9	5.59	0.639	cDNA FLJ53627, highly similar to Antigen peptide transporter 1 OS=Homo sapiens PE=2 SV=1 - [B7Z7P4_HUMAN]
P13761	266	29.8	7.44	0.638	HLA class II histocompatibility antigen, DRB1-7 beta chain OS=Homo sapiens GN=HLA-DRB1 PE=1 SV=1 - [2B17_HUMAN]
B7Z539	645	72.1	7.68	0.637	cDNA FLJ56954, highly similar to Inter-alpha-trypsin inhibitor heavy chain H1 OS=Homo sapiens PE=2 SV=1 - [B7Z539_HUMAN]
H7C034	173	19.3	4.88	0.636	AP-1 complex subunit beta-1 (Fragment) OS=Homo sapiens GN=AP1B1 PE=1 SV=1 - [H7C034_HUMAN]
A8K2T4	843	93.3	6.51	0.636	cDNA FLJ78207, highly similar to Human complement protein component C7 mRNA OS=Homo sapiens PE=2 SV=1 - [A8K2T4_HUMAN]
Q9UL88	131	14.1	9.63	0.636	Myosin-reactive immunoglobulin heavy chain variable region (Fragment) OS=Homo sapiens PE=2 SV=1 - [Q9UL88_HUMAN]
P23381	471	53.1	6.23	0.636	Tryptophan--tRNA ligase, cytoplasmic OS=Homo sapiens GN=WARS PE=1 SV=2 - [SYWC_HUMAN]
E9PC44	393	43.9	6.15	0.635	Protein transport protein Sec24D OS=Homo sapiens GN=SEC24D PE=1 SV=2 - [E9PC44_HUMAN]
O76013	467	52.2	4.94	0.634	Keratin, type I cuticular Ha6 OS=Homo sapiens GN=KRT36 PE=1 SV=1 -

					[KRT36_HUMAN]
B4DM28	634	72.1	9.67	0.633	cDNA FLJ50575, highly similar to U4/U6 small nuclear ribonucleoprotein Prp3 OS=Homo sapiens PE=2 SV=1 - [B4DM28_HUMAN]
M0R088	681	78.1	12.06	0.633	Serine/arginine repetitive matrix protein 1 (Fragment) OS=Homo sapiens GN=SRRM1 PE=1 SV=1 - [M0R088_HUMAN]
E3Q1J2	273	31.6	5.97	0.633	MHC class I antigen (Fragment) OS=Homo sapiens GN=HLA-B PE=3 SV=1 - [E3Q1J2_HUMAN]
Q5JTB5	87	9.3	7.09	0.631	Placenta-specific protein 9 OS=Homo sapiens GN=PLAC9 PE=4 SV=1 - [Q5JTB5_HUMAN]
Q5CZ93	159	19.2	9.88	0.630	Putative uncharacterized protein DKFZp686A0568 OS=Homo sapiens GN=DKFZp686A0568 PE=2 SV=1 - [Q5CZ93_HUMAN]
P33764	101	11.7	4.78	0.628	Protein S100-A3 OS=Homo sapiens GN=S100A3 PE=1 SV=1 - [S10A3_HUMAN]
Q6GMX6	465	51.1	8.69	0.628	IGH@ protein OS=Homo sapiens GN=IGH@ PE=1 SV=1 - [Q6GMX6_HUMAN]
Q9P2B2	879	98.5	6.61	0.628	Prostaglandin F2 receptor negative regulator OS=Homo sapiens GN=PTGFRN PE=1 SV=2 - [FPRP_HUMAN]
Q15323	416	47.2	4.88	0.627	Keratin, type I cuticular Ha1 OS=Homo sapiens GN=KRT31 PE=2 SV=3 - [K1H1_HUMAN]
H0YA93	1400	158.1	5.82	0.625	NEDD4-binding protein 2 (Fragment) OS=Homo sapiens GN=N4BP2 PE=1 SV=1 - [H0YA93_HUMAN]
A5Z217	470	53.6	5.27	0.623	Mutant desmin OS=Homo sapiens PE=2 SV=1 - [A5Z217_HUMAN]
K7EMQ9	140	16.3	6.89	0.622	Eukaryotic translation initiation factor 3 subunit K (Fragment) OS=Homo sapiens GN=EIF3K PE=1 SV=1 - [K7EMQ9_HUMAN]
A0A024RAL1	2409	264.9	4.54	0.620	Chondroitin sulfate proteoglycan 2 (Versican), isoform CRA_c OS=Homo sapiens GN=CSPG2 PE=4 SV=1 - [A0A024RAL1_HUMAN]
H3BPF7	236	25.5	8.46	0.618	Lon protease homolog 2, peroxisomal (Fragment) OS=Homo sapiens GN=LONP2 PE=4 SV=3 - [H3BPF7_HUMAN]
A0A087WUP0	265	30.0	5.34	0.617	Annexin A8-like protein 1 OS=Homo sapiens GN=ANXA8L1 PE=4 SV=1 - [A0A087WUP0_HUMAN]
A0A068LKQ0	120	13.3	5.99	0.617	Ig heavy chain variable region (Fragment) OS=Homo sapiens PE=4 SV=1 - [A0A068LKQ0_HUMAN]
Q86YQ1	91	9.7	9.25	0.614	Hemoglobin alpha-2 (Fragment) OS=Homo sapiens GN=HBA2 PE=3 SV=1 - [Q86YQ1_HUMAN]
B5MBZ8	274	31.3	4.63	0.610	Protein phosphatase 1 regulatory subunit 7 OS=Homo sapiens GN=PPP1R7 PE=1 SV=1 - [B5MBZ8_HUMAN]

Q8N1G4	583	63.4	8.28	0.609	Leucine-rich repeat-containing protein 47 OS=Homo sapiens GN=LRRC47 PE=1 SV=1 - [LRC47_HUMAN]
O15078	2479	290.2	5.95	0.609	Centrosomal protein of 290 kDa OS=Homo sapiens GN=CEP290 PE=1 SV=2 - [CE290_HUMAN]
Q9BXN1	380	43.4	7.08	0.608	Asporin OS=Homo sapiens GN=ASPN PE=1 SV=2 - [ASPN_HUMAN]
C0IMJ3	781	87.2	7.94	0.604	Periostin isoform thy6 OS=Homo sapiens PE=2 SV=1 - [C0IMJ3_HUMAN]
B7ZMG8	83	9.1	4.59	0.602	Uncharacterized protein OS=Homo sapiens PE=2 SV=1 - [B7ZMG8_HUMAN]
E9PQ22	191	22.9	9.45	0.602	Uncharacterized protein C11orf65 (Fragment) OS=Homo sapiens GN=C11orf65 PE=4 SV=3 - [E9PQ22_HUMAN]
Q5CZB5	1157	125.0	4.49	0.601	Putative uncharacterized protein DKFZp686M0430 OS=Homo sapiens GN=DKFZp686M0430 PE=2 SV=1 - [Q5CZB5_HUMAN]
E9PQI8	164	17.5	11.17	0.600	U4/U6.U5 tri-snRNP-associated protein 1 OS=Homo sapiens GN=SART1 PE=1 SV=1 - [E9PQI8_HUMAN]
P19075	237	26.0	5.60	0.600	Tetraspanin-8 OS=Homo sapiens GN=TSPAN8 PE=1 SV=1 - [TSN8_HUMAN]
B4DSW4	157	16.4	12.25	0.598	cDNA FLJ51541, moderately similar to Transcription factor Sp8 OS=Homo sapiens PE=2 SV=1 - [B4DSW4_HUMAN]
P31146	461	51.0	6.68	0.597	Coronin-1A OS=Homo sapiens GN=CORO1A PE=1 SV=4 - [COR1A_HUMAN]
Q0KKI6	219	24.0	8.06	0.593	Immunoblobulin light chain (Fragment) OS=Homo sapiens PE=1 SV=1 - [Q0KKI6_HUMAN]
P01623	109	11.7	8.91	0.593	Ig kappa chain V-III region WOL OS=Homo sapiens PE=1 SV=1 - [KV305_HUMAN]
P08311	255	28.8	11.19	0.593	Cathepsin G OS=Homo sapiens GN=CTSG PE=1 SV=2 - [CATG_HUMAN]
P01598	108	11.8	8.44	0.592	Ig kappa chain V-I region EU OS=Homo sapiens PE=1 SV=1 - [KV106_HUMAN]
Q6P3R8	708	81.4	8.87	0.592	Serine/threonine-protein kinase Nek5 OS=Homo sapiens GN=NEK5 PE=1 SV=1 - [NEK5_HUMAN]
Q4QZC0	273	31.8	6.09	0.592	MHC class I antigen (Fragment) OS=Homo sapiens GN=HLA-A PE=3 SV=1 - [Q4QZC0_HUMAN]
C9JW69	372	39.6	8.37	0.591	Regulator of chromosome condensation (Fragment) OS=Homo sapiens GN=RCC1 PE=1 SV=1 - [C9JW69_HUMAN]
P10109	184	19.4	5.83	0.591	Adrenodoxin, mitochondrial OS=Homo sapiens GN=FDX1 PE=1 SV=1 - [ADX_HUMAN]
A0A075B785	1018	112.7	5.49	0.591	LisH domain and HEAT repeat-containing protein KIAA1468 OS=Homo sapiens GN=KIAA1468 PE=1 SV=2 - [A0A075B785_HUMAN]
K7ERI9	77	8.6	6.71	0.590	Truncated apolipoprotein C-I (Fragment) OS=Homo sapiens GN=APOC1 PE=4

					SV=1 - [K7ERI9_HUMAN]
P01833	764	83.2	5.74	0.589	Polymeric immunoglobulin receptor OS=Homo sapiens GN=PIGR PE=1 SV=4 - [PIGR_HUMAN]
P62854	115	13.0	11.00	0.587	40S ribosomal protein S26 OS=Homo sapiens GN=RPS26 PE=1 SV=3 - [RS26_HUMAN]
B4E1L5	555	63.8	6.37	0.585	cDNA FLJ51601, highly similar to Interferon-induced guanylate-binding protein 1 OS=Homo sapiens PE=2 SV=1 - [B4E1L5_HUMAN]
Q9HCM7	1045	110.8	9.67	0.585	Fibrosin-1-like protein OS=Homo sapiens GN=FBRSL1 PE=1 SV=4 - [FBSL_HUMAN]
P01611	108	11.6	7.28	0.581	Ig kappa chain V-I region Wes OS=Homo sapiens PE=1 SV=1 - [KV119_HUMAN]
B4DRW1	474	51.7	6.81	0.576	cDNA FLJ55805, highly similar to Keratin, type II cytoskeletal 4 OS=Homo sapiens PE=2 SV=1 - [B4DRW1_HUMAN]
J3KPM9	714	83.3	6.42	0.574	Signal transducer and activator of transcription OS=Homo sapiens GN=STAT1 PE=1 SV=1 - [J3KPM9_HUMAN]
Q8N1W1	1705	191.8	6.04	0.573	Rho guanine nucleotide exchange factor 28 OS=Homo sapiens GN=ARHGEF28 PE=1 SV=3 - [ARG28_HUMAN]
P23946	247	27.3	9.29	0.573	Chymase OS=Homo sapiens GN=CMA1 PE=1 SV=1 - [CMA1_HUMAN]
Q7L0Q8	258	28.2	8.06	0.572	Rho-related GTP-binding protein RhoU OS=Homo sapiens GN=RHOU PE=1 SV=1 - [RHOU_HUMAN]
O75443	2155	239.4	5.40	0.569	Alpha-tectorin OS=Homo sapiens GN=TECTA PE=1 SV=3 - [TECTA_HUMAN]
A0A087WZW8	233	25.6	6.01	0.569	Protein IGKV3-11 OS=Homo sapiens GN=IGKV3-11 PE=4 SV=1 - [A0A087WZW8_HUMAN]
A0A087WX11	918	103.3	5.12	0.565	Folliculin-interacting protein 1 OS=Homo sapiens GN=FNIP1 PE=4 SV=1 - [A0A087WX11_HUMAN]
Q9H029	130	14.8	5.30	0.564	GTP-binding protein SAR1b OS=Homo sapiens GN=DKFZp434B2017 PE=1 SV=1 - [Q9H029_HUMAN]
H0YD72	237	26.1	9.39	0.563	Liprin-alpha-1 (Fragment) OS=Homo sapiens GN=PPFIA1 PE=1 SV=1 - [H0YD72_HUMAN]
Q5NV82	104	11.1	7.97	0.562	V4-2 protein (Fragment) OS=Homo sapiens GN=V4-2 PE=1 SV=1 - [Q5NV82_HUMAN]
H3BRW3	109	11.7	9.96	0.562	FAD-linked sulfhydryl oxidase ALR OS=Homo sapiens GN=GFER PE=1 SV=1 - [H3BRW3_HUMAN]
P02452	1464	138.9	5.80	0.555	Collagen alpha-1(I) chain OS=Homo sapiens GN=COL1A1 PE=1 SV=5 - [CO1A1_HUMAN]

B2R9B9	120	13.0	6.37	0.551	cDNA, FLJ94321, highly similar to Homo sapiens eukaryotic translation initiation factor 4E binding protein 2 (EIF4EBP2), mRNA OS=Homo sapiens PE=2 SV=1 - [B2R9B9_HUMAN]
Q9UK54	128	14.0	6.95	0.547	Hemoglobin beta subunit variant (Fragment) OS=Homo sapiens GN=HBB PE=2 SV=1 - [Q9UK54_HUMAN]
P81605	110	11.3	6.54	0.547	Dermcidin OS=Homo sapiens GN=DCD PE=1 SV=2 - [DCD_HUMAN]
Q05707	1796	193.4	5.30	0.547	Collagen alpha-1(XIV) chain OS=Homo sapiens GN=COL14A1 PE=1 SV=3 - [COEA1_HUMAN]
C9JA05	70	8.2	8.56	0.547	Immunoglobulin J chain (Fragment) OS=Homo sapiens GN=IGJ PE=1 SV=1 - [C9JA05_HUMAN]
S6C4R7	212	22.5	8.24	0.546	IgG L chain OS=Homo sapiens PE=2 SV=1 - [S6C4R7_HUMAN]
P01861	327	35.9	7.36	0.541	Ig gamma-4 chain C region OS=Homo sapiens GN=IGHG4 PE=1 SV=1 - [IGHG4_HUMAN]
B2R7Z6	484	52.5	7.55	0.539	cDNA, FLJ93674 OS=Homo sapiens PE=2 SV=1 - [B2R7Z6_HUMAN]
Q9NZ09	502	55.0	5.11	0.532	Ubiquitin-associated protein 1 OS=Homo sapiens GN=UBAP1 PE=1 SV=1 - [UBAP1_HUMAN]
Q64FY1	1364	146.2	6.60	0.530	AKNA transcript B1 (Fragment) OS=Homo sapiens GN=AKNA PE=2 SV=1 - [Q64FY1_HUMAN]
M0QZ50	93	9.8	4.48	0.526	Microtubule-associated protein 1S OS=Homo sapiens GN=MAP1S PE=1 SV=1 - [M0QZ50_HUMAN]
B4DQY2	711	78.9	7.06	0.525	cDNA FLJ59388, highly similar to Mitochondrial inner membrane protein OS=Homo sapiens PE=2 SV=1 - [B4DQY2_HUMAN]
B4DEH8	168	19.0	9.23	0.516	Polyadenylate-binding protein 2 OS=Homo sapiens GN=PABPN1 PE=1 SV=1 - [B4DEH8_HUMAN]
D6RC64	136	15.6	10.14	0.513	SH3 domain-binding protein 2 (Fragment) OS=Homo sapiens GN=SH3BP2 PE=4 SV=1 - [D6RC64_HUMAN]
Q6N095	475	52.3	8.57	0.511	Putative uncharacterized protein DKFZp686K03196 OS=Homo sapiens GN=DKFZp686K03196 PE=1 SV=1 - [Q6N095_HUMAN]
B4DLF9	342	39.4	8.68	0.510	cDNA FLJ56988, highly similar to cGMP-dependent protein kinase 2 (EC 2.7.11.12) OS=Homo sapiens PE=2 SV=1 - [B4DLF9_HUMAN]
H0Y892	688	79.3	9.14	0.508	Zinc finger protein 782 (Fragment) OS=Homo sapiens GN=ZNF782 PE=4 SV=1 - [H0Y892_HUMAN]
Q4ZGM8	100	10.8	9.04	0.502	Hemoglobin alpha-2 globin mutant (Fragment) OS=Homo sapiens PE=3 SV=1 - [Q4ZGM8_HUMAN]
Q6N093	**417**	**46.0**	**7.59**	**0.497**	**Putative uncharacterized protein DKFZp686I04196 (Fragment) OS=Homo**

					sapiens GN=DKFZp686I04196 PE=1 SV=1 - [Q6N093_HUMAN]
A0A075B6L1	106	11.3	8.29	0.496	Ig lambda-7 chain C region (Fragment) OS=Homo sapiens GN=IGLC7 PE=4 SV=2 - [A0A075B6L1_HUMAN]
B2R941	417	48.7	9.00	0.495	cDNA, FLJ94198, highly similar to Homo sapiens carboxypeptidase A3 (mast cell) (CPA3), mRNA OS=Homo sapiens PE=2 SV=1 - [B2R941_HUMAN]
P14555	144	16.1	9.23	0.492	Phospholipase A2, membrane associated OS=Homo sapiens GN=PLA2G2A PE=1 SV=2 - [PA2GA_HUMAN]
C9JNE5	191	21.7	9.61	0.481	Myeloid leukemia factor 1 (Fragment) OS=Homo sapiens GN=MLF1 PE=4 SV=1 - [C9JNE5_HUMAN]
Q7Z3E2	898	103.6	6.27	0.478	Coiled-coil domain-containing protein 186 OS=Homo sapiens GN=CCDC186 PE=1 SV=2 - [CC186_HUMAN]
P08519	4548	501.0	5.88	0.474	Apolipoprotein(a) OS=Homo sapiens GN=LPA PE=1 SV=1 - [APOA_HUMAN]
Q7L7X3	1001	116.0	7.65	0.468	Serine/threonine-protein kinase TAO1 OS=Homo sapiens GN=TAOK1 PE=1 SV=1 - [TAOK1_HUMAN]
B2R8C8	140	15.1	5.26	0.461	Ubiquitin-like protein ATG12 OS=Homo sapiens PE=2 SV=1 - [B2R8C8_HUMAN]
B7Z962	190	19.9	10.84	0.461	cDNA FLJ52231 OS=Homo sapiens PE=2 SV=1 - [B7Z962_HUMAN]
F8W9J4	7461	847.4	5.25	0.457	Dystonin OS=Homo sapiens GN=DST PE=1 SV=1 - [F8W9J4_HUMAN]
Q5T4S7	5183	573.5	6.04	0.450	E3 ubiquitin-protein ligase UBR4 OS=Homo sapiens GN=UBR4 PE=1 SV=1 - [UBR4_HUMAN]
B0QYR0	100	11.1	5.36	0.447	BTB/POZ domain-containing protein 3 (Fragment) OS=Homo sapiens GN=BTBD3 PE=4 SV=3 - [B0QYR0_HUMAN]
Q3MI39	167	16.7	9.70	0.447	HNRPA1 protein (Fragment) OS=Homo sapiens GN=HNRPA1 PE=2 SV=1 - [Q3MI39_HUMAN]
Q701L7	513	56.6	6.74	0.430	Type II hair keratin 2 OS=Homo sapiens GN=KRTHB2 PE=2 SV=1 - [Q701L7_HUMAN]
P01880	384	42.2	7.93	0.404	Ig delta chain C region OS=Homo sapiens GN=IGHD PE=1 SV=2 - [IGHD_HUMAN]
B3KMX3	270	28.5	4.73	0.398	cDNA FLJ12857 fis, clone NT2RP2003513, highly similar to Homo sapiens paralemmin (PALM), transcript variant 2, mRNA OS=Homo sapiens PE=2 SV=1 - [B3KMX3_HUMAN]
Q9BYT5	123	12.9	7.81	0.397	Keratin-associated protein 2-2 OS=Homo sapiens GN=KRTAP2-2 PE=2 SV=3 - [KRA22_HUMAN]
P46109	303	33.8	6.74	0.388	Crk-like protein OS=Homo sapiens GN=CRKL PE=1 SV=1 - [CRKL_HUMAN]
H7BZ55	2252	248.2	5.83	0.386	Putative ciliary rootlet coiled-coil protein-like 3 protein OS=Homo sapiens PE=5

					SV=2 - [CROL3_HUMAN]
Q5RHS7	95	11.0	9.28	0.379	Protein S100-A2 OS=Homo sapiens GN=S100A2 PE=1 SV=2 - [Q5RHS7_HUMAN]
Q05D28	370	41.8	5.44	0.377	CCDC91 protein (Fragment) OS=Homo sapiens GN=CCDC91 PE=2 SV=1 - [Q05D28_HUMAN]
B3KS56	594	68.5	5.45	0.376	cDNA FLJ35559 fis, clone SPLEN2005009, highly similar to GRIP and coiled-coil domain-containing protein 1 OS=Homo sapiens PE=2 SV=1 - [B3KS56_HUMAN]
H0UI60	536	60.7	5.17	0.369	Taxilin beta, isoform CRA_a OS=Homo sapiens GN=TXLNB PE=4 SV=1 - [H0UI60_HUMAN]
Q30167	266	30.0	7.75	0.357	HLA class II histocompatibility antigen, DRB1-10 beta chain OS=Homo sapiens GN=HLA-DRB1 PE=1 SV=2 - [2B1A_HUMAN]
A4FU00	317	35.6	5.81	0.351	SYT2 protein (Fragment) OS=Homo sapiens GN=SYT2 PE=2 SV=1 - [A4FU00_HUMAN]
B4E1L4	668	71.6	5.63	0.347	cDNA FLJ59081, highly similar to Mucin-5B OS=Homo sapiens PE=2 SV=1 - [B4E1L4_HUMAN]
Q69YL0	99	10.9	12.00	0.337	Uncharacterized protein NCBP2-AS2 OS=Homo sapiens GN=NCBP2-AS2 PE=4 SV=1 - [NCAS2_HUMAN]
A8K9A9	638	71.3	8.22	0.334	cDNA FLJ77744, highly similar to Homo sapiens kallikrein B, plasma (Fletcher factor) 1 (KLKB1), mRNA OS=Homo sapiens PE=2 SV=1 - [A8K9A9_HUMAN]
A2J1N5	94	10.4	9.13	0.306	Rheumatoid factor RF-ET6 (Fragment) OS=Homo sapiens PE=2 SV=1 - [A2J1N5_HUMAN]
Q6PII6	533	58.3	4.77	0.288	TMF1 protein (Fragment) OS=Homo sapiens GN=TMF1 PE=2 SV=1 - [Q6PII6_HUMAN]
A0A087X243	69	7.4	7.08	0.286	Glutathione S-transferase P (Fragment) OS=Homo sapiens GN=GSTP1 PE=4 SV=1 - [A0A087X243_HUMAN]
O76041	1014	116.4	7.99	0.275	Nebulette OS=Homo sapiens GN=NEBL PE=1 SV=1 - [NEBL_HUMAN]
B4DMJ5	242	27.3	4.50	0.118	cDNA FLJ53012, highly similar to Tubulin beta-7 chain OS=Homo sapiens PE=2 SV=1 - [B4DMJ5_HUMAN]

Table 8:

Proteins changed post surgery in the control CPB with collapsed lung group, with a 1.5x cutoff. Proteins with a >2x change following surgery are in bold.

Accession	# AAs	MW [kDa]	calc. pI	Collapsed (Post)/ Collapsed (Pre)	Description
B4DMJ5	242	27.3	4.50	8.276	cDNA FLJ53012, highly similar to Tubulin beta-7 chain OS=Homo sapiens PE=2 SV=1 - [B4DMJ5_HUMAN]
A0A087X243	69	7.4	7.08	3.627	Glutathione S-transferase P (Fragment) OS=Homo sapiens GN=GSTP1 PE=4 SV=1 - [A0A087X243_HUMAN]
Q69YL0	99	10.9	12.00	3.266	Uncharacterized protein NCBP2-AS2 OS=Homo sapiens GN=NCBP2-AS2 PE=4 SV=1 - [NCAS2_HUMAN]
A4FU00	317	35.6	5.81	2.985	SYT2 protein (Fragment) OS=Homo sapiens GN=SYT2 PE=2 SV=1 - [A4FU00_HUMAN]
B4DIF5	345	39.2	8.92	2.960	cDNA FLJ55687, highly similar to Cell cycle control protein 50A OS=Homo sapiens PE=2 SV=1 - [B4DIF5_HUMAN]
H0UI60	536	60.7	5.17	2.740	Taxilin beta, isoform CRA_a OS=Homo sapiens GN=TXLNB PE=4 SV=1 - [H0UI60_HUMAN]
Q9BYT5	123	12.9	7.81	2.683	Keratin-associated protein 2-2 OS=Homo sapiens GN=KRTAP2-2 PE=2 SV=3 - [KRA22_HUMAN]
O76041	1014	116.4	7.99	2.555	Nebulette OS=Homo sapiens GN=NEBL PE=1 SV=1 - [NEBL_HUMAN]
F8W9J4	7461	847.4	5.25	2.521	Dystonin OS=Homo sapiens GN=DST PE=1 SV=1 - [F8W9J4_HUMAN]
Q701L7	513	56.6	6.74	2.519	Type II hair keratin 2 OS=Homo sapiens GN=KRTHB2 PE=2 SV=1 - [Q701L7_HUMAN]
Q6PII6	533	58.3	4.77	2.512	TMF1 protein (Fragment) OS=Homo sapiens GN=TMF1 PE=2 SV=1 - [Q6PII6_HUMAN]
A2J1N5	94	10.4	9.13	2.497	Rheumatoid factor RF-ET6 (Fragment) OS=Homo sapiens PE=2 SV=1 - [A2J1N5_HUMAN]
B7Z962	190	19.9	10.84	2.430	cDNA FLJ52231 OS=Homo sapiens PE=2 SV=1 - [B7Z962_HUMAN]
Q05D28	370	41.8	5.44	2.342	CCDC91 protein (Fragment) OS=Homo sapiens GN=CCDC91 PE=2 SV=1 - [Q05D28_HUMAN]
B3KS56	594	68.5	5.45	2.327	cDNA FLJ35559 fis, clone SPLEN2005009, highly similar to GRIP and coiled-

					coil domain-containing protein 1 OS=Homo sapiens PE=2 SV=1 - [B3KS56_HUMAN]
Q92531	187	19.7	6.32	2.313	P35-related protein (Fragment) OS=Homo sapiens GN=FCN1 PE=4 SV=1 - [Q92531_HUMAN]
H0Y892	688	79.3	9.14	2.291	Zinc finger protein 782 (Fragment) OS=Homo sapiens GN=ZNF782 PE=4 SV=1 - [H0Y892_HUMAN]
Q3MI39	167	16.7	9.70	2.287	HNRPA1 protein (Fragment) OS=Homo sapiens GN=HNRPA1 PE=2 SV=1 - [Q3MI39_HUMAN]
B2R8C8	140	15.1	5.26	2.263	Ubiquitin-like protein ATG12 OS=Homo sapiens PE=2 SV=1 - [B2R8C8_HUMAN]
Q7L7X3	1001	116.0	7.65	2.241	Serine/threonine-protein kinase TAO1 OS=Homo sapiens GN=TAOK1 PE=1 SV=1 - [TAOK1_HUMAN]
B3KMU4	481	54.5	5.08	2.107	cDNA FLJ12640 fis, clone NT2RM4001940, highly similar to Timeless homolog OS=Homo sapiens PE=2 SV=1 - [B3KMU4_HUMAN]
P14555	144	16.1	9.23	2.101	Phospholipase A2, membrane associated OS=Homo sapiens GN=PLA2G2A PE=1 SV=2 - [PA2GA_HUMAN]
B0QYR0	100	11.1	5.36	2.088	BTB/POZ domain-containing protein 3 (Fragment) OS=Homo sapiens GN=BTBD3 PE=4 SV=3 - [B0QYR0_HUMAN]
P11678	715	81.0	10.29	2.012	Eosinophil peroxidase OS=Homo sapiens GN=EPX PE=1 SV=2 - [PERE_HUMAN]
P46109	303	33.8	6.74	2.003	Crk-like protein OS=Homo sapiens GN=CRKL PE=1 SV=1 - [CRKL_HUMAN]
Q8NEY1	1877	202.3	8.07	1.998	Neuron navigator 1 OS=Homo sapiens GN=NAV1 PE=1 SV=2 - [NAV1_HUMAN]
Q0PNF2	2570	275.3	6.49	1.979	FEX1 OS=Homo sapiens PE=2 SV=1 - [Q0PNF2_HUMAN]
H0YF46	255	28.3	5.82	1.977	SPOC domain-containing protein 1 (Fragment) OS=Homo sapiens GN=SPOCD1 PE=4 SV=1 - [H0YF46_HUMAN]
Q8TBP3	101	11.8	9.92	1.941	TOP1MT protein (Fragment) OS=Homo sapiens GN=TOP1MT PE=2 SV=1 - [Q8TBP3_HUMAN]
Q05707	1796	193.4	5.30	1.917	Collagen alpha-1(XIV) chain OS=Homo sapiens GN=COL14A1 PE=1 SV=3 - [COEA1_HUMAN]
M0QZ50	93	9.8	4.48	1.907	Microtubule-associated protein 1S OS=Homo sapiens GN=MAP1S PE=1 SV=1 - [M0QZ50_HUMAN]
H7BZ55	2252	248.2	5.83	1.883	Putative ciliary rootlet coiled-coil protein-like 3 protein OS=Homo sapiens PE=5 SV=2 - [CROL3_HUMAN]
Q8N1W1	1705	191.8	6.04	1.874	Rho guanine nucleotide exchange factor 28 OS=Homo sapiens

					GN=ARHGEF28 PE=1 SV=3 - [ARG28_HUMAN]
P20851	252	28.3	5.14	1.835	C4b-binding protein beta chain OS=Homo sapiens GN=C4BPB PE=1 SV=1 - [C4BPB_HUMAN]
Q8N1G4	583	63.4	8.28	1.830	Leucine-rich repeat-containing protein 47 OS=Homo sapiens GN=LRRC47 PE=1 SV=1 - [LRC47_HUMAN]
D6RC64	136	15.6	10.14	1.819	SH3 domain-binding protein 2 (Fragment) OS=Homo sapiens GN=SH3BP2 PE=4 SV=1 - [D6RC64_HUMAN]
Q7L0Q8	258	28.2	8.06	1.811	Rho-related GTP-binding protein RhoU OS=Homo sapiens GN=RHOU PE=1 SV=1 - [RHOU_HUMAN]
H0YCG2	258	28.2	6.52	1.809	Lysosome-associated membrane glycoprotein 2 (Fragment) OS=Homo sapiens GN=LAMP2 PE=1 SV=1 - [H0YCG2_HUMAN]
Q05315	142	16.4	7.37	1.809	Galectin-10 OS=Homo sapiens GN=CLC PE=1 SV=3 - [LEG10_HUMAN]
Q6P3R8	708	81.4	8.87	1.805	Serine/threonine-protein kinase Nek5 OS=Homo sapiens GN=NEK5 PE=1 SV=1 - [NEK5_HUMAN]
Q5T4S7	5183	573.5	6.04	1.799	E3 ubiquitin-protein ligase UBR4 OS=Homo sapiens GN=UBR4 PE=1 SV=1 - [UBR4_HUMAN]
Q7Z3E2	898	103.6	6.27	1.778	Coiled-coil domain-containing protein 186 OS=Homo sapiens GN=CCDC186 PE=1 SV=2 - [CC186_HUMAN]
B4DLF9	342	39.4	8.68	1.768	cDNA FLJ56988, highly similar to cGMP-dependent protein kinase 2 (EC 2.7.11.12) OS=Homo sapiens PE=2 SV=1 - [B4DLF9_HUMAN]
P62854	115	13.0	11.00	1.742	40S ribosomal protein S26 OS=Homo sapiens GN=RPS26 PE=1 SV=3 - [RS26_HUMAN]
A0A024R637	1298	146.5	7.01	1.737	TBC1 domain family, member 4, isoform CRA_b OS=Homo sapiens GN=TBC1D4 PE=4 SV=1 - [A0A024R637_HUMAN]
Q9H029	130	14.8	5.30	1.735	GTP-binding protein SAR1b OS=Homo sapiens GN=DKFZp434B2017 PE=1 SV=1 - [Q9H029_HUMAN]
S6BGD6	235	24.8	7.24	1.733	IgG L chain OS=Homo sapiens PE=1 SV=1 - [S6BGD6_HUMAN]
Q30058	257	29.1	6.54	1.728	HLA-DP protein OS=Homo sapiens GN=HLA-DP PE=2 SV=1 - [Q30058_HUMAN]
H3BMN5	158	18.5	4.82	1.727	Calretinin (Fragment) OS=Homo sapiens GN=CALB2 PE=4 SV=2 - [H3BMN5_HUMAN]
P02452	1464	138.9	5.80	1.710	Collagen alpha-1(I) chain OS=Homo sapiens GN=COL1A1 PE=1 SV=5 - [CO1A1_HUMAN]
B2R9B9	120	13.0	6.37	1.705	cDNA, FLJ94321, highly similar to Homo sapiens eukaryotic translation initiation factor 4E binding protein 2 (EIF4EBP2), mRNA OS=Homo sapiens

					PE=2 SV=1 - [B2R9B9_HUMAN]
B4DVF1	785	87.3	6.96	1.702	cDNA FLJ51111, highly similar to Aldehyde oxidase (EC 1.2.3.1) (Fragment) OS=Homo sapiens PE=2 SV=1 - [B4DVF1_HUMAN]
P12724	160	18.4	10.02	1.692	Eosinophil cationic protein OS=Homo sapiens GN=RNASE3 PE=1 SV=2 - [ECP_HUMAN]
Q9BXN1	380	43.4	7.08	1.691	Asporin OS=Homo sapiens GN=ASPN PE=1 SV=2 - [ASPN_HUMAN]
Q9HCM7	1045	110.8	9.67	1.667	Fibrosin-1-like protein OS=Homo sapiens GN=FBRSL1 PE=1 SV=4 - [FBSL_HUMAN]
Q86UX7	667	75.9	6.98	1.660	Fermitin family homolog 3 OS=Homo sapiens GN=FERMT3 PE=1 SV=1 - [URP2_HUMAN]
Q4QZC0	273	31.8	6.09	1.654	MHC class I antigen (Fragment) OS=Homo sapiens GN=HLA-A PE=3 SV=1 - [Q4QZC0_HUMAN]
B2R6V9	732	83.2	6.00	1.638	cDNA, FLJ93141, highly similar to Homo sapiens coagulation factor XIII, A1 polypeptide (F13A1), mRNA OS=Homo sapiens PE=2 SV=1 - [B2R6V9_HUMAN]
P15529	392	43.7	6.74	1.634	Membrane cofactor protein OS=Homo sapiens GN=CD46 PE=1 SV=3 - [MCP_HUMAN]
H0YH87	916	98.1	9.41	1.633	Ataxin-2 (Fragment) OS=Homo sapiens GN=ATXN2 PE=1 SV=1 - [H0YH87_HUMAN]
P27487	766	88.2	6.04	1.628	Dipeptidyl peptidase 4 OS=Homo sapiens GN=DPP4 PE=1 SV=2 - [DPP4_HUMAN]
P08311	255	28.8	11.19	1.624	Cathepsin G OS=Homo sapiens GN=CTSG PE=1 SV=2 - [CATG_HUMAN]
O76013	467	52.2	4.94	1.624	Keratin, type I cuticular Ha6 OS=Homo sapiens GN=KRT36 PE=1 SV=1 - [KRT36_HUMAN]
A0A075B785	1018	112.7	5.49	1.610	LisH domain and HEAT repeat-containing protein KIAA1468 OS=Homo sapiens GN=KIAA1468 PE=1 SV=2 - [A0A075B785_HUMAN]
P31146	461	51.0	6.68	1.607	Coronin-1A OS=Homo sapiens GN=CORO1A PE=1 SV=4 - [COR1A_HUMAN]
P10109	184	19.4	5.83	1.604	Adrenodoxin, mitochondrial OS=Homo sapiens GN=FDX1 PE=1 SV=1 - [ADX_HUMAN]
O15078	2479	290.2	5.95	1.604	Centrosomal protein of 290 kDa OS=Homo sapiens GN=CEP290 PE=1 SV=2 - [CE290_HUMAN]
B2R4M6	114	13.2	6.13	1.604	Protein S100 OS=Homo sapiens PE=2 SV=1 - [B2R4M6_HUMAN]
A0A024RDI4	1851	203.3	6.23	1.600	Ankyrin 2, neuronal, isoform CRA_a OS=Homo sapiens GN=ANK2 PE=4 SV=1 - [A0A024RDI4_HUMAN]
Q6EVJ6	105	10.9	8.81	1.597	Peptidyl arginine deiminase type IV (Fragment) OS=Homo sapiens

					GN=PADI4 PE=4 SV=1 - [Q6EVJ6_HUMAN]
P46108	304	33.8	5.55	1.592	Adapter molecule crk OS=Homo sapiens GN=CRK PE=1 SV=2 - [CRK_HUMAN]
C9JW69	372	39.6	8.37	1.588	Regulator of chromosome condensation (Fragment) OS=Homo sapiens GN=RCC1 PE=1 SV=1 - [C9JW69_HUMAN]
P98095	1184	126.5	4.82	1.586	Fibulin-2 OS=Homo sapiens GN=FBLN2 PE=1 SV=2 - [FBLN2_HUMAN]
Q19UK3	33	3.7	8.09	1.582	Truncated coagulation factor IX (Fragment) OS=Homo sapiens GN=F9 PE=4 SV=1 - [Q19UK3_HUMAN]
F5H4Z6	171	20.0	7.84	1.581	Folate receptor beta (Fragment) OS=Homo sapiens GN=FOLR2 PE=4 SV=1 - [F5H4Z6_HUMAN]
P49913	170	19.3	9.41	1.578	Cathelicidin antimicrobial peptide OS=Homo sapiens GN=CAMP PE=1 SV=1 - [CAMP_HUMAN]
B4DSW4	157	16.4	12.25	1.578	cDNA FLJ51541, moderately similar to Transcription factor Sp8 OS=Homo sapiens PE=2 SV=1 - [B4DSW4_HUMAN]
E9PQ22	191	22.9	9.45	1.578	Uncharacterized protein C11orf65 (Fragment) OS=Homo sapiens GN=C11orf65 PE=4 SV=3 - [E9PQ22_HUMAN]
E9PC44	393	43.9	6.15	1.577	Protein transport protein Sec24D OS=Homo sapiens GN=SEC24D PE=1 SV=2 - [E9PC44_HUMAN]
B4DLX8	617	69.4	6.61	1.575	cDNA FLJ57031, highly similar to Midline-1 (EC 6.3.2.-) OS=Homo sapiens PE=2 SV=1 - [B4DLX8_HUMAN]
E9PQI8	164	17.5	11.17	1.575	U4/U6.U5 tri-snRNP-associated protein 1 OS=Homo sapiens GN=SART1 PE=1 SV=1 - [E9PQI8_HUMAN]
B4DI03	156	17.4	8.91	1.573	SEC11-like 3 (S. cerevisiae), isoform CRA_a OS=Homo sapiens GN=SEC11L3 PE=2 SV=1 - [B4DI03_HUMAN]
Q9Y281	166	18.7	7.88	1.571	Cofilin-2 OS=Homo sapiens GN=CFL2 PE=1 SV=1 - [COF2_HUMAN]
A0A087WX11	918	103.3	5.12	1.570	Folliculin-interacting protein 1 OS=Homo sapiens GN=FNIP1 PE=4 SV=1 - [A0A087WX11_HUMAN]
G3V2R9	217	23.4	6.19	1.560	Prostaglandin reductase 2 OS=Homo sapiens GN=PTGR2 PE=1 SV=1 - [G3V2R9_HUMAN]
Q9UK54	128	14.0	6.95	1.560	Hemoglobin beta subunit variant (Fragment) OS=Homo sapiens GN=HBB PE=2 SV=1 - [Q9UK54_HUMAN]
P59665	94	10.2	6.99	1.557	Neutrophil defensin 1 OS=Homo sapiens GN=DEFA1 PE=1 SV=1 - [DEF1_HUMAN]
Q4ZGM8	100	10.8	9.04	1.549	Hemoglobin alpha-2 globin mutant (Fragment) OS=Homo sapiens PE=3 SV=1 - [Q4ZGM8_HUMAN]

B4DJ12	1253	139.2	6.57	1.546	cDNA FLJ58355, highly similar to Tyrosine-protein phosphatase non-receptor type 23 (EC 3.1.3.48) OS=Homo sapiens PE=2 SV=1 - [B4DJ12_HUMAN]
A0A087WUP0	265	30.0	5.34	1.541	Annexin A8-like protein 1 OS=Homo sapiens GN=ANXA8L1 PE=4 SV=1 - [A0A087WUP0_HUMAN]
E9PAR0	99	11.2	10.36	1.540	Peptidyl-prolyl cis-trans isomerase OS=Homo sapiens GN=FKBP11 PE=1 SV=1 - [E9PAR0_HUMAN]
B2R4C9	102	11.2	9.52	1.537	cDNA, FLJ92044, highly similar to Homo sapiens death-associated protein (DAP), mRNA OS=Homo sapiens PE=2 SV=1 - [B2R4C9_HUMAN]
Q9NWH4	148	16.9	11.09	1.534	cDNA FLJ10024 fis, clone HEMBA1000636 OS=Homo sapiens PE=2 SV=1 - [Q9NWH4_HUMAN]
E3Q1J2	273	31.6	5.97	1.531	MHC class I antigen (Fragment) OS=Homo sapiens GN=HLA-B PE=3 SV=1 - [E3Q1J2_HUMAN]
Q67AK3	233	26.9	7.42	1.531	MHC class II antigen (Fragment) OS=Homo sapiens GN=HLA-DQB1 PE=4 SV=1 - [Q67AK3_HUMAN]
B4DLR0	579	61.1	5.26	1.529	cDNA FLJ55719, highly similar to Mus musculus armadillo repeat containing 5 (Armc5), mRNA OS=Homo sapiens PE=2 SV=1 - [B4DLR0_HUMAN]
Q86UY0	360	40.3	5.83	1.526	Protein BLOC1S5-TXNDC5 OS=Homo sapiens GN=TXNDC5 PE=2 SV=1 - [Q86UY0_HUMAN]
E7EQB2	696	76.6	8.02	1.526	Lactotransferrin (Fragment) OS=Homo sapiens GN=LTF PE=1 SV=1 - [E7EQB2_HUMAN]
Q9P2B2	879	98.5	6.61	1.520	Prostaglandin F2 receptor negative regulator OS=Homo sapiens GN=PTGFRN PE=1 SV=2 - [FPRP_HUMAN]
Q96P70	1041	115.9	4.81	1.517	Importin-9 OS=Homo sapiens GN=IPO9 PE=1 SV=3 - [IPO9_HUMAN]
Q5CZ93	159	19.2	9.88	1.517	Putative uncharacterized protein DKFZp686A0568 OS=Homo sapiens GN=DKFZp686A0568 PE=2 SV=1 - [Q5CZ93_HUMAN]
Q5VX52	437	50.3	8.43	1.514	Spermatogenesis-associated protein 1 OS=Homo sapiens GN=SPATA1 PE=2 SV=3 - [SPAT1_HUMAN]
P80511	92	10.6	6.25	1.513	Protein S100-A12 OS=Homo sapiens GN=S100A12 PE=1 SV=2 - [S10AC_HUMAN]
A8MVU1	366	41.8	8.84	1.512	Putative neutrophil cytosol factor 1C OS=Homo sapiens GN=NCF1C PE=5 SV=1 - [NCF1C_HUMAN]
B5BTZ6	769	87.9	6.20	1.502	Signal transducer and activator of transcription OS=Homo sapiens GN=STAT3 PE=2 SV=1 - [B5BTZ6_HUMAN]
Q15323	416	47.2	4.88	1.502	Keratin, type I cuticular Ha1 OS=Homo sapiens GN=KRT31 PE=2 SV=3 -

					[K1H1_HUMAN]
P07585	359	39.7	8.54	1.501	Decorin OS=Homo sapiens GN=DCN PE=1 SV=1 - [PGS2_HUMAN]
C9JKG1	238	26.7	6.79	1.501	Biglycan (Fragment) OS=Homo sapiens GN=BGN PE=4 SV=1 - [C9JKG1_HUMAN]
H0YA93	1400	158.1	5.82	1.501	NEDD4-binding protein 2 (Fragment) OS=Homo sapiens GN=N4BP2 PE=1 SV=1 - [H0YA93_HUMAN]
G3V295	203	22.8	8.32	0.660	Proteasome subunit alpha type OS=Homo sapiens GN=PSMA6 PE=1 SV=1 - [G3V295_HUMAN]
O96009	420	45.4	6.61	0.658	Napsin-A OS=Homo sapiens GN=NAPSA PE=1 SV=1 - [NAPSA_HUMAN]
E9PN95	56	6.3	4.96	0.626	Uteroglobin OS=Homo sapiens GN=SCGB1A1 PE=4 SV=1 - [E9PN95_HUMAN]
P07339	412	44.5	6.54	0.615	Cathepsin D OS=Homo sapiens GN=CTSD PE=1 SV=1 - [CATD_HUMAN]
A8K987	222	25.7	9.00	0.603	Glutathione S-transferase OS=Homo sapiens PE=2 SV=1 - [A8K987_HUMAN]
B2R7Z6	484	52.5	7.55	0.591	cDNA, FLJ93674 OS=Homo sapiens PE=2 SV=1 - [B2R7Z6_HUMAN]
B4E1L4	668	71.6	5.63	0.531	cDNA FLJ59081, highly similar to Mucin-5B OS=Homo sapiens PE=2 SV=1 - [B4E1L4_HUMAN]
B7Z269	**351**	**40.3**	**7.24**	**0.181**	**cDNA FLJ50754, highly similar to Voltage-dependent L-type calcium channel subunit alpha-1D OS=Homo sapiens PE=2 SV=1 - [B7Z269_HUMAN]**

Table 9:

Changes in proteins (with 1.5x cutoff) following surgery with LFV. Proteins with >2x change are in bold.

Accession	# AAs	MW [kDa]	calc. pI	LFV (Post)/ LFV (Pre)	Description
Q701L7	**513**	**56.6**	**6.74**	**14.876**	**Type II hair keratin 2 OS=Homo sapiens GN=KRTHB2 PE=2 SV=1 - [Q701L7_HUMAN]**
Q9BYT5	**123**	**12.9**	**7.81**	**14.741**	**Keratin-associated protein 2-2 OS=Homo sapiens GN=KRTAP2-2 PE=2 SV=3 - [KRA22_HUMAN]**
O76013	**467**	**52.2**	**4.94**	**7.140**	**Keratin, type I cuticular Ha6 OS=Homo sapiens GN=KRT36 PE=1 SV=1 - [KRT36_HUMAN]**
A0A087X2I6	**404**	**46.1**	**4.84**	**4.627**	**Keratin, type I cuticular Ha3-II OS=Homo sapiens GN=KRT33B PE=4 SV=1 - [A0A087X2I6_HUMAN]**
A0JNT2	**447**	**49.6**	**5.39**	**3.857**	**KRT83 protein OS=Homo sapiens GN=KRT83 PE=2 SV=1 - [A0JNT2_HUMAN]**
B7Z269	**351**	**40.3**	**7.24**	**2.379**	**cDNA FLJ50754, highly similar to Voltage-dependent L-type calcium channel subunit alpha-1D OS=Homo sapiens PE=2 SV=1 - [B7Z269_HUMAN]**
Q15323	**416**	**47.2**	**4.88**	**2.158**	**Keratin, type I cuticular Ha1 OS=Homo sapiens GN=KRT31 PE=2 SV=3 - [K1H1_HUMAN]**
Q96Q06	1357	134.3	8.73	1.840	Perilipin-4 OS=Homo sapiens GN=PLIN4 PE=2 SV=2 - [PLIN4_HUMAN]
Q05315	142	16.4	7.37	1.823	Galectin-10 OS=Homo sapiens GN=CLC PE=1 SV=3 - [LEG10_HUMAN]
H0YF46	255	28.3	5.82	1.698	SPOC domain-containing protein 1 (Fragment) OS=Homo sapiens GN=SPOCD1 PE=4 SV=1 - [H0YF46_HUMAN]
Q7Z6I6	1101	118.5	4.81	1.687	Rho GTPase-activating protein 30 OS=Homo sapiens GN=ARHGAP30 PE=1 SV=3 - [RHG30_HUMAN]
P11678	715	81.0	10.29	1.663	Eosinophil peroxidase OS=Homo sapiens GN=EPX PE=1 SV=2 - [PERE_HUMAN]
A4FU00	317	35.6	5.81	1.651	SYT2 protein (Fragment) OS=Homo sapiens GN=SYT2 PE=2 SV=1 - [A4FU00_HUMAN]

P27701	267	29.6	5.24	1.574	CD82 antigen OS=Homo sapiens GN=CD82 PE=1 SV=1 - [CD82_HUMAN]
B4DMJ5	242	27.3	4.50	1.547	cDNA FLJ53012, highly similar to Tubulin beta-7 chain OS=Homo sapiens PE=2 SV=1 - [B4DMJ5_HUMAN]
Q6P4A8	553	63.2	9.06	1.524	Phospholipase B-like 1 OS=Homo sapiens GN=PLBD1 PE=1 SV=2 - [PLBL1_HUMAN]
A0A024R637	1298	146.5	7.01	1.514	TBC1 domain family, member 4, isoform CRA_b OS=Homo sapiens GN=TBC1D4 PE=4 SV=1 - [A0A024R637_HUMAN]
M0QZ50	93	9.8	4.48	1.512	Microtubule-associated protein 1S OS=Homo sapiens GN=MAP1S PE=1 SV=1 - [M0QZ50_HUMAN]
B3KQ72	130	14.3	5.52	1.500	cDNA FLJ32987 fis, clone THYMU1000032 OS=Homo sapiens PE=2 SV=1 - [B3KQ72_HUMAN]
H6VRF8	644	66.0	8.12	0.665	Keratin 1 OS=Homo sapiens GN=KRT1 PE=3 SV=1 - [H6VRF8_HUMAN]
P35237	376	42.6	5.27	0.658	Serpin B6 OS=Homo sapiens GN=SERPINB6 PE=1 SV=3 - [SPB6_HUMAN]
D6RF35	476	53.0	5.52	0.658	Vitamin D-binding protein OS=Homo sapiens GN=GC PE=1 SV=1 - [D6RF35_HUMAN]
B7Z445	386	43.3	6.83	0.656	cDNA FLJ51492, highly similar to Arachidonate 15-lipoxygenase (EC 1.13.11.33) OS=Homo sapiens PE=2 SV=1 - [B7Z445_HUMAN]
P62851	125	13.7	10.11	0.650	40S ribosomal protein S25 OS=Homo sapiens GN=RPS25 PE=1 SV=1 - [RS25_HUMAN]
Q99549	860	97.1	6.06	0.644	M-phase phosphoprotein 8 OS=Homo sapiens GN=MPHOSPH8 PE=1 SV=2 - [MPP8_HUMAN]
Q7Z6G4	31	3.2	5.78	0.634	HBA2 (Fragment) OS=Homo sapiens GN=HBA2 PE=3 SV=1 - [Q7Z6G4_HUMAN]
K7EPK9	51	5.5	5.11	0.626	Mucin-like protein 1 (Fragment) OS=Homo sapiens GN=MUCL1 PE=4 SV=3 - [K7EPK9_HUMAN]
Q86TT1	375	41.2	6.79	0.616	Full-length cDNA clone CS0DD006YL02 of Neuroblastoma of Homo sapiens (human) OS=Homo sapiens PE=2 SV=1 - [Q86TT1_HUMAN]
B2R6F5	350	39.6	5.12	0.607	cDNA, FLJ92928, highly similar to Homo sapiens retinitis pigmentosa 2 (X-linked recessive) (RP2), mRNA OS=Homo sapiens PE=2 SV=1 - [B2R6F5_HUMAN]
P23527	126	13.9	10.32	0.605	Histone H2B type 1-O OS=Homo sapiens GN=HIST1H2BO PE=1 SV=3 - [H2B1O_HUMAN]

B3KUR3	242	28.0	5.85	0.604	cDNA FLJ40459 fis, clone TESTI2041800, highly similar to BISPHOSPHOGLYCERATE MUTASE (EC 5.4.2.4) OS=Homo sapiens PE=2 SV=1 - [B3KUR3_HUMAN]
P11277	2137	246.3	5.27	0.591	Spectrin beta chain, erythrocytic OS=Homo sapiens GN=SPTB PE=1 SV=5 - [SPTB1_HUMAN]
P02656	99	10.8	5.41	0.591	Apolipoprotein C-III OS=Homo sapiens GN=APOC3 PE=1 SV=1 - [APOC3_HUMAN]
Q9NZD4	102	11.8	5.00	0.584	Alpha-hemoglobin-stabilizing protein OS=Homo sapiens GN=AHSP PE=1 SV=1 - [AHSP_HUMAN]
G4V2I8	911	101.7	5.21	0.574	Anion exchanger-1 variant OS=Homo sapiens PE=2 SV=1 - [G4V2I8_HUMAN]
B7Z4Q8	613	68.2	7.85	0.574	cDNA FLJ52333, highly similar to Erythrocyte membrane protein band 4.2 OS=Homo sapiens PE=2 SV=1 - [B7Z4Q8_HUMAN]
P03973	132	14.3	8.75	0.570	Antileukoproteinase OS=Homo sapiens GN=SLPI PE=1 SV=2 - [SLPI_HUMAN]
P02549	2419	279.8	5.05	0.569	Spectrin alpha chain, erythrocytic 1 OS=Homo sapiens GN=SPTA1 PE=1 SV=5 - [SPTA1_HUMAN]
Q14587	947	108.3	8.87	0.566	Zinc finger protein 268 OS=Homo sapiens GN=ZNF268 PE=1 SV=2 - [ZN268_HUMAN]
P69892	147	16.1	7.20	0.553	Hemoglobin subunit gamma-2 OS=Homo sapiens GN=HBG2 PE=1 SV=2 - [HBG2_HUMAN]
P01833	764	83.2	5.74	0.549	Polymeric immunoglobulin receptor OS=Homo sapiens GN=PIGR PE=1 SV=4 - [PIGR_HUMAN]
P16157	1881	206.1	6.01	0.548	Ankyrin-1 OS=Homo sapiens GN=ANK1 PE=1 SV=3 - [ANK1_HUMAN]
Q4ZGM8	100	10.8	9.04	0.543	Hemoglobin alpha-2 globin mutant (Fragment) OS=Homo sapiens PE=3 SV=1 - [Q4ZGM8_HUMAN]
B3KVN0	416	45.8	8.60	0.534	cDNA FLJ16785 fis, clone NT2RI2015342, highly similar to Solute carrier family 2, facilitated glucose transporter member 1 OS=Homo sapiens PE=2 SV=1 - [B3KVN0_HUMAN]
Q4VB87	615	68.4	5.91	0.532	EPB41 protein (Fragment) OS=Homo sapiens GN=EPB41 PE=2 SV=1 - [Q4VB87_HUMAN]
B4DF70	183	20.1	8.78	0.527	cDNA FLJ60461, highly similar to Peroxiredoxin-2 (EC 1.11.1.15) OS=Homo sapiens PE=2 SV=1 - [B4DF70_HUMAN]
Q4TZM4	101	11.0	6.52	0.518	Hemoglobin beta chain (Fragment) OS=Homo sapiens GN=HBB PE=3 SV=1 - [Q4TZM4_HUMAN]

P00918	260	29.2	7.40	0.507	Carbonic anhydrase 2 OS=Homo sapiens GN=CA2 PE=1 SV=2 - [CAH2_HUMAN]
O75602	509	55.4	6.83	0.504	Sperm-associated antigen 6 OS=Homo sapiens GN=SPAG6 PE=2 SV=1 - [SPAG6_HUMAN]
Q6J1Z9	90	9.6	9.50	0.501	Hemoglobin alpha 1 (Fragment) OS=Homo sapiens GN=HBA1 PE=3 SV=1 - [Q6J1Z9_HUMAN]
Q86YQ1	**91**	**9.7**	**9.25**	**0.497**	**Hemoglobin alpha-2 (Fragment) OS=Homo sapiens GN=HBA2 PE=3 SV=1 - [Q86YQ1_HUMAN]**
Q13938	**189**	**21.0**	**4.89**	**0.495**	**Calcyphosin OS=Homo sapiens GN=CAPS PE=1 SV=1 - [CAYP1_HUMAN]**
E9PN95	**56**	**6.3**	**4.96**	**0.450**	**Uteroglobin OS=Homo sapiens GN=SCGB1A1 PE=4 SV=1 - [E9PN95_HUMAN]**
A8K987	**222**	**25.7**	**9.00**	**0.448**	**Glutathione S-transferase OS=Homo sapiens PE=2 SV=1 - [A8K987_HUMAN]**
P00915	**261**	**28.9**	**7.12**	**0.442**	**Carbonic anhydrase 1 OS=Homo sapiens GN=CA1 PE=1 SV=2 - [CAH1_HUMAN]**
Q6J1Z8	**42**	**4.5**	**9.38**	**0.429**	**Hemoglobin beta (Fragment) OS=Homo sapiens GN=HBB PE=3 SV=1 - [Q6J1Z8_HUMAN]**
H3BML9	**118**	**13.1**	**5.68**	**0.397**	**Myosin regulatory light chain 2, skeletal muscle isoform (Fragment) OS=Homo sapiens GN=MYLPF PE=4 SV=1 - [H3BML9_HUMAN]**
E5RGQ7	**148**	**16.8**	**8.88**	**0.388**	**Dematin (Fragment) OS=Homo sapiens GN=DMTN PE=1 SV=1 - [E5RGQ7_HUMAN]**
Q6VFQ6	**42**	**4.5**	**8.24**	**0.384**	**Hemoglobin beta chain (Fragment) OS=Homo sapiens GN=HBB PE=3 SV=1 - [Q6VFQ6_HUMAN]**
P02042	**147**	**16.0**	**8.05**	**0.383**	**Hemoglobin subunit delta OS=Homo sapiens GN=HBD PE=1 SV=2 - [HBD_HUMAN]**
Q5T619	**568**	**62.3**	**8.62**	**0.380**	**Zinc finger protein 648 OS=Homo sapiens GN=ZNF648 PE=2 SV=1 - [ZN648_HUMAN]**
Q5RHS7	**95**	**11.0**	**9.28**	**0.346**	**Protein S100-A2 OS=Homo sapiens GN=S100A2 PE=1 SV=2 - [Q5RHS7_HUMAN]**
Q8IUL9	**105**	**11.5**	**6.05**	**0.270**	**Hemoglobin beta chain variant Hb.Sinai-Bel Air (Fragment) OS=Homo sapiens GN=HBB PE=3 SV=1 - [Q8IUL9_HUMAN]**
B4E1L4	**668**	**71.6**	**5.63**	**0.257**	**cDNA FLJ59081, highly similar to Mucin-5B OS=Homo sapiens PE=2 SV=1 - [B4E1L4_HUMAN]**
B2R7Z6	**484**	**52.5**	**7.55**	**0.248**	**cDNA, FLJ93674 OS=Homo sapiens PE=2 SV=1 - [B2R7Z6_HUMAN]**

Supplemental Figure 1:

Principle component analysis (by Partek) of gene expression data, showing no significant outliers within the data.

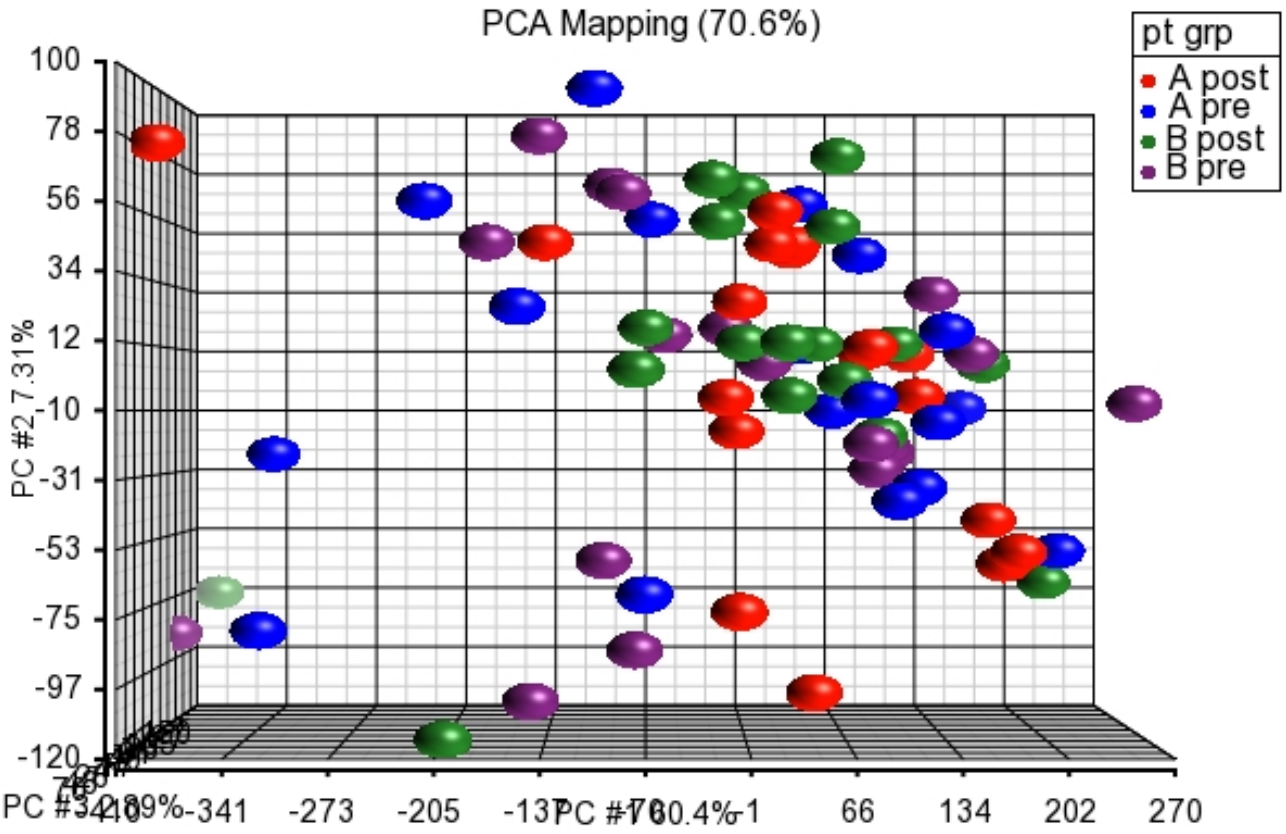

Supplemental Figure 2:

There were no significant changes in **(A)** lipid species or **(B)** lipid class (as a percentage of the total) following surgery either with standard CPB with collapsed lung or with LFV.